[American Journal of Science, Vol. 304, October/November, 2004, P. 679–751]

AN EQUATION OF STATE FOR SILICATE MELTS. II. CALIBRATION OF VOLUMETRIC PROPERTIES AT 10^5 Pa

MARK S. GHIORSO* and VICTOR C. KRESS**

ABSTRACT. Reference pressure (10^5 Pa) parameters for the silicate liquid equation of state of Ghiorso (2004a) are calibrated from literature data on measurements of densities and sound speeds. A model for the temperature- and compositionally-dependent, reference-pressure volume (density) in the system K_2O-Na_2O-CaO-MgO-FeO-NiO-CoO-Fe_2O_3-Al_2O_3-TiO_2-SiO_2 is obtained. Precision of data recovery is 0.76 percent (one root-mean-square residual). Linear mixing relations for model parameters are utilized in this calibration with the inclusion of quadratic terms between soda and titania and potash and titania to account for the effect of alkali metals on the partial molar volume of TiO_2. Liquids in the system CaO-Al_2O_3-SiO_2 with molar ratios of $CaO/SiO_2 < 0.5$ are excluded from this analysis in order to avoid the inclusion of additional non-linear terms. Iron-bearing systems are modeled by first "speciating" the liquid to obtain molecular proportions of FeO, $FeO_{1.5}$ (Fe_2O_3) and $FeO_{1.3}$ ($Fe^{2+}_{0.4}Fe^{3+}_{0.6}O_{1.3}$). Partial molar properties are extracted for all three iron oxides. This procedure is followed because (1) it affords an internally consistent means of extrapolating previously calibrated models of iron-redox equilibria in silicate melts to elevated pressure, and (2) it results in significant improvements in model recovery of density measurements on Fe-bearing systems. The model partial molar volume of $FeO_{1.3}$ is ~12 percent smaller than a linear combination of the fully oxidized and reduced endmembers. Internally consistent expressions for the reference pressure compressibility and its temperature dependence are formulated from a calibration of sound speeds in molten liquids. A model for the temperature- and compositionally-dependent sound speed in the system K_2O-Na_2O-CaO-MgO-FeO-Fe_2O_3-Al_2O_3-TiO_2-SiO_2 is obtained. Precision of data recovery is 1.7 percent. Mixing relations identical to the volume model are adopted for consistency with the inclusion of an additional quadratic composition term in soda and alumina.

INTRODUCTION

This paper is the second in a series of four that together outline the development and calibration of an equation of state (EOS) for multi-component silicate liquids. The goal of this series of papers is to propose an EOS (that is, a functional relation between volume, temperature, pressure and composition) that is applicable over the range of silicate liquid compositions that include natural magmas, and over a range of temperatures and pressures that permit calculation of densities and derived thermodynamic properties of liquids generated in the Earth's upper mantle. The first paper in this series (Ghiorso, 2004a, hereafter Part I) deals with general theoretical arguments regarding an appropriate functional form for the EOS. The third and fourth papers in the series (Ghiorso 2004b, 2004c, hereafter Parts III and IV) are concerned with calibration of model parameters at elevated pressure. In this paper the focus is on calibration of model EOS parameters at reference pressure (P_r) conditions of 10^5 Pa (that is, 1 bar or 1 atmosphere).

Because density is a fundamental physical property that is important for understanding both the thermodynamic and the dynamic behavior of a material, a great deal of attention has been focused on experimental determination of the volumetric properties of silicate melts at P_r. The first important systematic evaluation of low-pressure

*Department of Geophysical Sciences, The University of Chicago, 5734 S Ellis Avenue, Chicago, Illinois 60637; ghiorso@geosci.uchicago.edu

**Department of Earth and Space Sciences, University of Washington, Box 351310, Seattle, Washington 98195-1310; kress@u.washington.edu

density measurements on molten silicates was the seminal work of Bottinga and Weill (1970). They developed a reference pressure EOS that described the compositional dependence on the volume with *linear* mixing relations, that is the volume, V, could be expressed within experimental error as

$$V = \sum_i n_i \bar{v}_i \tag{1}$$

where $\bar{v}_i$ are the partial molar volumes and n_i are the numbers of moles of a set of linearly independent compositional variables (components). Bottinga and Weill (1970) chose simple oxides as components and noted that the $\bar{v}_i$ need only be functions of temperature. Subsequent experimental studies and reanalysis of previous work led Bottinga and others (1982) to propose more complex, non-linear mixing relations for aluminosilicate melts, but this proposal led to a controversy centering on whether the precision of the available measurements supported the additional complexity (Ghiorso and Carmichael, 1984; Bottinga and others, 1984). In the ensuing two decades, an impressive number of high quality experimental measurements of melt density have been produced (see references below). These studies have established that non-ideal volume of mixing does occur in certain simple systems, most notably CaO-Al_2O_3-SiO_2 (Courtial and Dingwell, 1995), and in mixed alkali-metal, alkali-earth titania-bearing systems (Johnson, ms, 1989; Dingwell, 1992; Liu and Lange, 2001) and possibly their ferric iron-bearing equivalents (Dingwell and Brearley, 1988). Most importantly, as a result of these studies the densities of many simple system compositions are now determined to better than 0.5 percent and the effect of oxidation state on the densities of iron-bearing melts has been explored. In addition, the last decade has seen a number of studies demonstrating how dilatometric measurements of the density of glasses can be combined with superliquidus densitometry measurements in order to extend the temperature range over which the latter can be reliably extrapolated. Simultaneous to these investigations on melt and glass density, a considerable experimental effort has been aimed at measuring the speed of sound in molten silicate systems, and from these measurements it is possible to deduce melt compressibility as a function of both temperature and composition.

The two commonly used reference pressure EOS algorithms for routine calculation of anhydrous melt density and melt compressibility of magmatic composition liquids were developed by Lange and Carmichael (1987) and Kress and Carmichael (1991), respectively. In the intervening decade since the publication of these models, experimental measurements have tripled in number and the scope of coverage, both in composition and in temperature, has expanded considerably. In this paper the work of Lange and Carmichael (1987) and Kress and Carmichael (1991) is updated by assembling a new data set of density and sound speed measurements of molten silicate liquids. These data calibrate the EOS developed in Part I and serve to anchor it to a reference pressure data set of high quality measurements. The reference pressure calibration developed in this paper will put the high-pressure parameter calibration to be undertaken in Parts III and IV on sound footing.

MODEL EQUATIONS

The EOS of Part I (eq 25) reduces to the following simple relation along the reference isobar:

$$V_{T,P_r} = V_{0,T} = V_{0,T_r} e^{\alpha(T-T_r)} \tag{2}$$

where α is the coefficient of thermal expansion. The pressure derivative of the volume evaluated at P_r is expressed as:

$$\left.\frac{\partial V}{\partial P}\right|_{T,P_r} = V_{1,T} \tag{3}$$

In Part I the V_{0,T_r} and α are taken to be independent of temperature while the temperature-dependence of $V_{1,T}$ is unspecified. The issue that must now be addressed is how to extend both of these expressions (eqs 2 and 3) to include the effect of variable composition and how to specify the temperature-dependence of $V_{1,T}$. The latter will be discussed first.

Temperature Dependence of $V_{1,T}$

The compressibility of a silicate melt $\left(\beta \equiv -\frac{1}{V}\frac{\partial V}{\partial P}\right)$ is determined experimentally from measurements of the sound speed. The relationship is given by

$$\beta = \frac{1}{\rho c^2} + \frac{TV\alpha^2}{C_P} \tag{4}$$

(for example, Rivers and Carmichael, 1987) where c is the speed of sound, ρ the density, and C_P is the isobaric heat capacity. Combining equations (2), (3) and (4) gives

$$\left.\frac{\partial V}{\partial P}\right|_{T,P_r} = V_{1,T} = -V_{0,T_r}^2\left(\frac{1}{Mc^2} + \frac{T\alpha^2}{C_P}\right)\left[e^{\alpha(T-T_r)}\right]^2 \tag{5}$$

where M is the mass. Assuming that the temperature-dependence of C_P is essentially nil for multi-component silicate liquids (no temperature-dependence to C_P could be resolved by Lange and Navrotsky, 1992), differentiation of equation (5) yields (after some minor manipulation)

$$\left.\frac{\partial^2 V}{\partial T \partial P}\right|_{T,P_r} = 2\alpha\left.\frac{\partial V}{\partial P}\right|_{T,P_r} + \frac{2V_{T,P_r}^2}{Mc^3}\frac{\partial c}{\partial T} - \frac{V_{T,P_r}^2\alpha^2}{C_P} \tag{6}$$

and this expression may be expanded using equation (2) to provide a model expression for the temperature-dependence of the cross partial derivative:

$$\left.\frac{\partial^2 V}{\partial T \partial P}\right|_{T,P_r} = \frac{\partial V_{1,T}}{\partial T} = -\left[\frac{2\alpha}{Mc^2}\left(1 - \frac{1}{c\alpha}\frac{\partial c}{\partial T}\right) + \frac{\alpha^2(1+2\alpha T)}{C_P}\right]V_{0,T_r}^2\left[e^{\alpha(T-T_r)}\right]^2 \tag{7}$$

In studies on the compressibility of silicate liquids (Kress and others, 1988; Kress and Carmichael, 1991; Webb and Dingwell, 1994; Webb and Courtial, 1996), $\left.\frac{\partial V}{\partial P}\right|_{T,P_r}$ is generally approximated as a linear function of temperature. This linear T-dependence for $\left.\frac{\partial V}{\partial P}\right|_{T,P_r}$ can be derived from equation (7) by noting that when α is small: (1) the second term within the square brackets can be neglected and (2) the exponential may be approximated by a Taylor expansion truncated to first order. Both approximations transform equation (7) to

$$\left.\frac{\partial^2 V}{\partial T \partial P}\right|_{T,P_r} \approx -\frac{2\alpha}{Mc^2}\left(1 - \frac{1}{c\alpha}\frac{\partial c}{\partial T}\right)V_{0,T_r}^2\left[1 + \alpha(T - T_r)\right]^2 \tag{8}$$

For T close to T_r, equation (8) further reduces to

$$\left.\frac{\partial^2 V}{\partial T \partial P}\right|_{T,P_r} \approx -\frac{2\alpha V_{0,T_r}^2}{Mc^2} + \frac{2V_{0,T_r}^2}{Mc^3}\frac{\partial c}{\partial T} \tag{9}$$

The temperature dependence of the sound speed in silicate melts is on the order of $c \times 10^{-4}$ m/sec (Rivers and Carmichael, 1987; Kress and Carmichael, 1991; see below) and measurements indicate that for a given bulk composition $\frac{\partial c}{\partial T}$ may be treated as a constant. These experimental observations imply that a reasonable approximation to equation (9) is

$$\left.\frac{\partial^2 V}{\partial T \partial P}\right|_{T,P_r} \approx -\frac{2\alpha V_{0,T_r}^2}{Mc_{T_r}^2} + \frac{2V_{0,T_r}^2}{Mc_{T_r}^3}\frac{\partial c}{\partial T} \tag{10}$$

where c is taken at the reference temperature and the right-hand side in this approximation is a *constant*. Equation (10) provides the theoretical justification for the model expressions adopted by Kress and Carmichael (1991; and subsequent workers): if the right-hand-side of equation (10) is constant, then integration results in a model expression of the form $\frac{\partial V}{\partial P} = k_0 + k_1(T - T_r)$, specifically

$$\frac{\partial V}{\partial P} = \left.\frac{\partial V}{\partial P}\right|_{T_r,P_r} + \frac{2V_{0,T_r}^2}{Mc_{T_r}^2}\left(-\alpha + \frac{1}{c_{T_r}}\frac{\partial c}{\partial T}\right)(T - T_r). \tag{11}$$

However, it is important to realize that under the same set of assumptions employed in deriving equation (10), equation (5) reduces to $\left.\frac{\partial V}{\partial P}\right|_{T_r,P_r} \approx \frac{-V_{0,T_r}^2}{Mc_{T_r}^2}$, which allows equation (11) to be written in an alternate form

$$\frac{\partial V}{\partial P} = \left.\frac{\partial V}{\partial P}\right|_{T_r,P_r} + 2\left.\frac{\partial V}{\partial P}\right|_{T_r,P_r}\left(\alpha - \frac{1}{c_{T_r}}\frac{\partial c}{\partial T}\right)(T - T_r) \tag{11'}$$

Equation (11′) reveals that if values of $\left.\frac{\partial V}{\partial P}\right|_{T,P_r}$ are *derived from sound speed measurements* and are then fitted to a model expression of the form $\left.\frac{\partial V}{\partial P}\right|_{T,P_r} = k_0 + k_1(T - T_r)$, the model parameters k_0 and k_1 *cannot be independent*. In practice, k_1, which is identically $\left.\frac{\partial^2 V}{\partial T \partial P}\right|_{T_r,P_r}$, is largely dominated by the thermal expansion contribution (Rivers and Carmichael, 1987), which can be seen by inserting typical values[1] for M, c, $\frac{\partial c}{\partial T}$, $V|_{T,P_r}$, α, $\left.\frac{\partial V}{\partial P}\right|_{T,P_r}$, and C_P into the right-hand-side of equation (6). The $2\alpha\left.\frac{\partial V}{\partial P}\right|_{T,P_r}$ term in (6) contributes ~80 percent of the value of $\left.\frac{\partial^2 V}{\partial T \partial P}\right|_{T,P_r}$. So, not only are the

[1]For example, $M \approx 60\ \frac{g}{mol}$, $c \approx 4 \times 10^5\ \frac{cm}{s}$, $\frac{\partial c}{\partial T} \approx -10\ \frac{cm}{s - K'}$ $V|_{T,P_r} \approx 30\ \frac{cm^3}{mol}$, $\alpha \approx 1 \times 10^{-4} K^{-1}$, $\left.\frac{\partial V}{\partial P}\right|_{T,P_r} \approx -2 \times 10^{-4}\ \frac{cm^3}{mol - bar}$, $C_P \approx 100\ \frac{J}{mol - K}$.

parameters k_0 and k_1 correlated, but the value of k_1 is largely determined by assumed volumetric properties and not the sound speed measurements. To first convert the sound speed data to $\left.\frac{\partial V}{\partial P}\right|_{T,P_r}$ and then extract model values for k_0 and k_1 on the assumption that they are independent quantities, discards information that is known regarding the temperature dependence of $\left.\frac{\partial V}{\partial P}\right|_{T,P_r}$. This indirect analysis of the sound speed data should be avoided, and it is proposed here to calibrate directly the speed of sound as a function of temperature, and subsequently utilize modeled estimates of the sound speed and equation (5) to calculate $\left.\frac{\partial V}{\partial P}\right|_{T,P_r}$ at specified T. The clear advantage of this approach is that the dependence of sound speed on temperature can be quantified from primary experimental observations without obscuring the measured quantity with contributions from temperature-dependent volumetric properties.

Mixing rules for V_{0,T_r}, $\left.\frac{\partial V_{T,P_r}}{\partial T}\right|_{T_r}$, and c

Turning now to the compositional dependence of the reference pressure model parameters, the approach to be adopted (and to be carried forward into Parts III and IV) is to consider simple mixing relations for the constituent quantities, V_{0,T_r}, $\left.\frac{\partial V_{T,P_r}}{\partial \mathrm{T}}\right|_{T_r}$, C_P, M, and c, combining these as specified in equations (2) and (5) to form $V_{0,T}$ and $V_{1,T}$. The volume and its temperature derivative, the heat capacity and the mass are extensive thermodynamic quantities. They may be written in partial molar form as

$$V_{0,T_r} = \sum_i n_i \bar{v}_{i,T_r} \tag{12}$$

$$\left.\frac{\partial V_{T,P_r}}{\partial T}\right|_{T_r} = \sum_i n_i \frac{\partial \bar{v}_i}{\partial T} \tag{13}$$

$$C_P = \sum_i n_i \bar{c}_{P,i} \tag{14}$$

$$M = \sum_i n_i MW_i \tag{15}$$

where the n_i are the number of moles of the i^{th} thermodynamic component and the bar denotes the appropriate partial molar quantity. MW_i is the molecular weight of the i^{th} component. The usual choice of components is the constituent oxides. Substituting the definition of the thermal coefficient of expansion (Part I),

$$\alpha = \frac{1}{V_{0,T_r}} \left.\frac{\partial V_{T,P_r}}{\partial T}\right|_{T_r}$$

along with equations (12) and (13) into equation (2), gives the mixing relation for volume

TABLE 1

Parameters for computation of oxidized and reduced iron species

		CaO-FeO-Fe_2O_3-SiO_2 Kress and Carmichael (1989)	Na_2O-FeO-Fe_2O_3-SiO_2 This paper; data from Lange and Carmichael (1989)	Other Fe-bearing Kress and Carmichael (1991)
ΔH^o	(kJ/mol)	−145.9	−202.6 ± 4.2	−106.2
ΔS^o	(J/K-mol)	−64.6	−96.2 ± 1.8	−55.1
ΔC_P^o	(J/K-mol)			31.86
ΔW_{SiO_2}	(kJ/mol)	46.5	8.4 ± 1.9	
$\Delta W_{Al_2O_3}$	(kJ/mol)			39.86
ΔW_{CaO}	(kJ/mol)	−45.9		−62.52
ΔW_{Na_2O}	(kJ/mol)		−25.4 ± 4.3	−102.0
ΔW_{K_2O}	(kJ/mol)			−119.0

$T_o = 1673$ K, $K_2 = 0.4$, $y = 0.3$; Kress and Carmichael, 1989, 1991; this work.

$$V_{T,P_r} = V_{0,T} = V_{0,T_r} e^{\alpha(T-T_r)} = \left(\sum_i n_i \bar{v}_{i,T_r}\right) \exp\left[\frac{\left(\sum_i n_i \dfrac{\partial \bar{v}_i}{\partial T}\right)}{\sum_i n_i \bar{v}_{i,T_r}} (T - T_r)\right] \tag{16}$$

By analogy with the extensive quantities, the following mixing relation is proposed for sound speed

$$c = \sum_i X_i \bar{c}_i \tag{17}$$

where the X_i are component mole fractions and the $\bar{c}_i$ are the temperature- and possibly composition-dependent "partial molar" sound speeds (that is, the sound speed contribution attributable to each component in the solution).

Equations (5) and (12) through (17) are formal statements of the mixing relations for the proposed EOS in the reference-pressure limit. It should be noted that no assumption has yet been made regarding the ideal or non-ideal nature of these solutions. The intensive partial molar quantities (the barred quantities) under the summation signs in equations (12) through (17) may be functions of composition, in which case the mixing is non-linear and the solution non-ideal, or they may be constants, in which case the mixing is both linear and ideal. Analysis of experimental data sets dictates the complexity of the final model.

CALIBRATION OF DENSITIES AT 10^5 PA

A data set of experimental measurements of densities of silicate liquids is assembled and sources are summarized in table 1. Details of the chemical systems investigated and temperatures and results of each experimental datum are reported in the Appendix in table A1. As a starting point for this compilation, the data set used by Lange and Carmichael (1987) is adopted, which represents determinations of melt density performed using the double bob Archemedian technique on well characterized molten silicate liquids in both simple and complex chemical systems. To these data, similar measurements on liquids performed subsequent to 1987 are added and

determinations of the density of supercooled liquids at the glass transition temperature as reported by Lange (1996, 1997), Gottsmann and Dingwell (2000), and Toplis and Richet (2000) are included. Other literature estimates of supercooled liquid densities (Webb and others, 1992; Knoche and others 1992a, 1992b, 1994, 1995) are not included in the calibration data set. In these studies low temperature dilatometric measurements on glass are extrapolated to supercooled liquid conditions using differential scanning calorimetry measurements of heat capacity. The assumption is that the thermal and volumetric relaxation behavior of the glass is identical (Webb and others, 1992). This assumption of the correlation of relaxation behaviors is problematic (see discussion in Lange, 1996, 1997) and adoption of volume estimates based on this method raises the potential for introducing systematic errors into the calibration. The liquid density data set of table A1 is expanded in size by roughly a factor of three over that considered by Lange and Carmichael (1987). More importantly, the scope of coverage in critical chemical systems like CaO-MgO-Al_2O_3-SiO_2 is greatly expanded over the previous data set.

In terms of precision of density determinations, the data set splits naturally into Fe-absent systems and Fe-bearing systems, the former measurements being notably more precise (Lange and Carmichael, 1987). Measurements in Fe-bearing systems are subject to greater error because of the increased experimental difficulty of containing Fe-bearing melts and the added complication of determining quantitatively the proportion of reduced and oxidized iron in the liquid under experimental conditions. These issues are discussed extensively by Lange and Carmichael (1987, 1990).

In order to construct a data set to parameterize their model equation for melt density in the system Na_2O-K_2O-CaO-MgO-FeO-Fe_2O_3-Al_2O_3-TiO_2-SiO_2, Lange and Carmichael (1987) chose to proceed from the observation that for the chemical systems included in their calibration data set, density is a linear function of temperature over the range of measurement. From these relations they calculate densities (molar volumes) at a fixed grid of temperatures: 1573, 1673, 1773, and 1873 K for each bulk composition in the data set. Lange and Carmichael (1987) then regress each "isothermal" data set against an expression for the volume of mixing. Analyzing the parameters of these regressions they obtained an estimate of the temperature dependence of the partial molar volume of each oxide component and a value at the reference temperature. Lange and Carmichael (1987) deduce that an ideal mixing model (that is the parameters $\bar{v}_{i,T_r}$ in equation 12 are functions only of T) is perfectly adequate for liquids with $X_{CaO} < 0.5$ and low concentrations of the mole fraction product of soda and titania. They find evidence of non-ideality in liquids with significant concentrations of both Na_2O and TiO_2. Temperature dependence of their model parameters is found to be linear over the range 1573 to 1873 K.

The procedures of Lange and Carmichael (1987) will be revised in two important ways. First, as the Fe-bearing data appear to contain more intrinsic experimental uncertainty, only model parameters related to Fe-oxide components are extracted from these data. All other model parameters are entirely determined from the Fe-absent data set. Second, rather than artificially constructing isothermal "data sets" from the experimental observations and fitting these "data sets" independently, the model is constrained directly from the experimental observations at the reported temperatures, extracting the temperature dependence of the model parameters simultaneously with a reference temperature intercept term. The construction of artificial isothermal "data sets" has the potential to impose correlation within the regression problem, thereby skewing values of model parameters obtained during the fit. This potential pitfall will be avoided by the analysis scheme adopted here.

The aim of this paper is to calibrate parameters for a liquid EOS that is applicable to magmatic composition melts and is, within the more restricted composition space of these liquids, as simple a formulation as is permitted by the available data. Keeping these objectives in mind, the calibration data set will be restricted to liquids with mole fraction of $SiO_2 > 0.5$ in the system $CaO\text{-}Al_2O_3\text{-}SiO_2$. This restriction is done to avoid the well-documented nonlinearity in liquid volume that develops in this system at lower silica contents (Ghiorso and Carmichael, 1984; Lange and Carmichael, 1987; Courtial and Dingwell, 1995). Courtial and Dingwell (1995) model this non-ideality with a quadratic interaction term between CaO and SiO_2, but their model does not reproduce density measurements in Ca- and Al-rich melts in this system; a more complex non-linear model appears to be necessary and will be avoided here. In contrast to the system $CaO\text{-}Al_2O_3\text{-}SiO_2$, and despite ample evidence of non-linear behavior, studies of the densities of alkali metal-titanate melts (Johnson, ms, 1989; Dingwell, 1992; Liu and Lange, 2001) are included. In the case of these systems the non-ideal behavior can be modeled very well with Na-Ti and K-Ti binary interaction terms (Johnson, ms, 1989) and inclusion of these non-linear effects has minimal impact on derived melt properties for natural composition liquids.

The proportion of oxidized to reduced iron must be calculated at the experimental temperature and oxygen fugacity conditions for Fe-bearing melts. The studies of Kress and Carmichael (1989, the system $CaO\text{-}FeO\text{-}Fe_2O_3\text{-}SiO_2$), Lange and Carmichael (1989, the system $Na_2O\text{-}FeO\text{-}Fe_2O_3\text{-}SiO_2$), and Kress and Carmichael (1991, all other Fe-bearing systems), provide data and models for estimating this quantity over a broad range of bulk compositions, temperatures and oxygen fugacities. Kress and Carmichael (1989) develop a method of calculation involving homogeneous equilibria among Fe-bearing melt "species" that is adopted in this study. Their method is motivated by the experimental observation that the simple oxidation-reaction

$$\mathrm{FeO}^{melt} + \frac{1}{4}\,\mathrm{O}_2 = \mathrm{FeO}_{1.5}^{melt} \tag{18}$$

fails to completely characterize the oxidized to reduced iron ratio in silicate melts. From the law of mass action, this equilibria implies the relation

$$\ln \frac{X_{\mathrm{FeO}_{1.5}}^{melt}}{X_{\mathrm{FeO}}^{melt}} = \frac{1}{4}\ln f_{\mathrm{O}_2} + non - ideal - terms \tag{19}$$

but, Kress and Carmichael (1989) obtain an empirical value of 0.203 ± 0.001, and Kress and Carmichael (1991) determine a value of 0.196 ± 0.001 for the oxygen coefficient preceding the logarithmic term in equation (19). These experimental observations prompted Kress and Carmichael (1989) to propose that a homogeneous equilibrium between reduced, intermediate and oxidized melt species

$$(1 - 2y)\mathrm{FeO}^{melt} + 2y\,\mathrm{FeO}_{1.5}^{melt} = \mathrm{FeO}_{1+y}^{melt} \tag{20}$$

governs the macroscopic variation of ferric and ferrous iron abundances. They derive the following relation

$$\frac{X_{\mathrm{FeO}_{1.5}}^{bulk}}{X_{\mathrm{FeO}}^{bulk}} = \frac{X_{\mathrm{FeO}_{1.5}}^{melt} + 2yX_{\mathrm{FeO}_{1+y}}^{melt}}{X_{\mathrm{FeO}}^{melt} + (1-2y)X_{\mathrm{FeO}_{1+y}}^{melt}} = \frac{K_{\mathrm{D1}} f_{\mathrm{O}_2}^{1/4} + 2yK_2K_{\mathrm{D1}}^{2y} f_{\mathrm{O}_2}^{y/2}}{1 + (1-2y)K_2K_{\mathrm{D1}}^{2y} f_{\mathrm{O}_2}^{y/2}} \tag{21}$$

where the left-hand-side of this expression is the *bulk* or analytically determine ferric-ferrous ratio of the melt—which is equivalent to the indicated ratio of concentrations of *melt* species. The distribution coefficient, K_{D1}, is given by

$$K_{\mathrm{D1}} = \frac{X^{melt}_{\mathrm{FeO_{1.5}}}}{X^{melt}_{\mathrm{FeO}}} = \exp\left\{ -\frac{\Delta H^o}{RT} + \frac{\Delta S^o}{R} - \frac{\Delta C^o_P}{R}\left[1 - \frac{T_o}{T} - \ln\left(\frac{T}{T_o}\right)\right] - \frac{1}{RT}\sum_i \Delta W_i X_i \right\} \quad (22)$$

and K_2 is the equilibrium constant for reaction (20):

$$K_2 = \frac{a^{melt}_{\mathrm{FeO_{1+y}}}}{(a^{melt}_{\mathrm{FeO}})^{1-2y}(a^{melt}_{\mathrm{FeO_{1.5}}})^{2y}} \equiv \frac{X^{melt}_{\mathrm{FeO_{1+y}}}}{(X^{melt}_{\mathrm{FeO}})^{1-2y}(X^{melt}_{\mathrm{FeO_{1.5}}})^{2y}} \quad (23)$$

The parameters in equation (20) correspond either to thermodynamic properties of the oxidation-reduction reaction (18) (ΔH^o, ΔS^o, ΔC^o_P), or to interaction terms (ΔW_i) relating the influence of bulk composition (X_i) on the ferric/ferrous ratio of the melt. Kress and Carmichael (1989, 1991) fit the parameters of their homogeneous speciation model and the results are reproduced in table 1. Measurements obtained by Lange and Carmichael (1989) on liquids in the system Na_2O-Fe_2O_3-FeO-SiO_2 are fitted to the speciation model of Kress and Carmichael (1989) and these results are reported in the same table. Note that for all of the systems studied experimentally, the optimal value for y is 0.3, which implies that homogeneous equilibrium between the Fe-species FeO, $FeO_{1.5}$, and $FeO_{1.3}$ (or $Fe^{2+}_{0.4}Fe^{3+}_{0.6}O_{1.3}$) define oxidation-reduction relations in the melt. One of the primary advantages of the Kress and Carmichael (1989) "speciation" approach is that by casting the calculation of the redox state of Fe as a condition of homogeneous equilibrium between Fe-bearing melt species, the resulting equilibrium species distribution corresponds to the minimum of the Gibbs free energy of the system. Forward application of their model can therefore be achieved by standard techniques of computational thermodynamics and there is never an inconsistency between ferric/ferrous ratio derived by energy minimization and that implied by some empirical calibration equation.

For all the Fe-bearing liquids in the data set of melt densities, the concentrations of FeO, $FeO_{1.3}$ and $FeO_{1.5}$ are calculated at the temperature and oxygen fugacity conditions of the experiment by solving simultaneously equations (21) through (23). Partial molar volumes are obtained for all three melt species as part of the data analysis. With the exception of some of the experiments performed by Hara and others (1988) and those experiments of Shiraishi and others (1978) on Fe_2SiO_4-composition liquids held in Fe-capsules under reducing conditions, all other Fe-bearing experiments in the density data set were performed in air.

A model corresponding to equation (16) is fitted with parameter coefficients $\bar{v}_{i,T_r}$ and $\dfrac{\partial \bar{v}_i}{\partial T}$ taken to be constants for all Fe-bearing melt species and for all other oxide components *except* TiO_2. Recognizing that densities in the alkali oxide-titania systems exhibit non-linear mixing behavior (see above), the partial molar volume of TiO_2 is parameterized as

$$\bar{v}_{\mathrm{TiO_2},T_r} = \bar{v}_{\mathrm{ref\text{-}TiO_2},T_r} + X_{\mathrm{Na_2O}}\bar{v}_{\mathrm{Na_2O\text{-}TiO_2},T_r} + X_{\mathrm{K_2O}}\bar{v}_{\mathrm{K_2O\text{-}TiO_2},T_r} \quad (24)$$

$$\frac{\partial \bar{v}_{\mathrm{TiO_2},T_r}}{\partial T} = \frac{\partial \bar{v}_{\mathrm{ref\text{-}TiO_2},T_r}}{\partial T} + X_{\mathrm{Na_2O}}\frac{\partial \bar{v}_{\mathrm{Na_2O\text{-}TiO_2},T_r}}{\partial T} + X_{\mathrm{K_2O}}\frac{\partial \bar{v}_{\mathrm{K_2O\text{-}TiO_2},T_r}}{\partial T} \quad (25)$$

where the volumetric terms on the right-hand-sides of equations (24) and (25) are taken as constant. A three stage fitting procedure is employed. Initially, parameters are extracted for the Fe-absent dataset, then fixing these parameters, coefficients for NiO and CoO are extracted from the data set of Courtial and others (1999) and finally, parameters for the Fe-bearing systems are regressed. At each stage the intrinsic correlation of the independent variables is examined using techniques adapted from

singular value analysis (Press and others, 1992). The regression problem is found at each stage to be "full rank," which means that there is sufficient variation of composition and temperature in the data set to determine uniquely all of the model parameters.

Assessment of the Fe-bearing systems revealed an incompatibility between *some of the measurements* of Dingwell and Brearley (1988) performed on liquids in the system CaO-Fe_2O_3-FeO-SiO_2 and the remainder of measurements in Fe-bearing systems, including others in the same subsystem. This incompatibility indicated the possibility of a compositional dependence to the partial molar properties of one or more of the Fe-melt species. Further investigation revealed that simple modification of the partial molar volume terms to include compositional dependence did not improve the fit. Most importantly, it is found that inclusion of all the measurements of Dingwell and Brearley (1988) induce systematic offsets in model residuals for the Na_2O-Fe_2O_3-FeO-SiO_2 liquids and natural composition melts. In order to avoid introducing this bias into the model all the measurements of densities of liquids in the system CaO-Fe_2O_3-FeO-SiO_2 are eliminated from the calibration data set. This procedure makes the average error of fit to the Fe-bearing and Fe-absent data sets statistically equivalent. Regression statistics summarizing the quality of the model are provided in table 2 and model parameters are reported in table 3. Individual residuals on each datum are tabulated in the Appendix (table A1) and are plotted in figure 1.

Analysis of model residuals for calibrants in the Fe-absent data set reveals no correlation with either silica content of the liquid or with temperature (figs. 1A, 1D, 1G). The root-mean-square (r.m.s.)[2] error of residuals for these data is 0.69 percent. For comparison, Lange and Carmichael maintain that the relative precision of individual measurements is between 0.14 percent and 0.33 percent, but these estimates are smaller than the error resulting from comparing duplicate experiments. The larger relative errors associated with the model fit must also reflect inter-laboratory systematic error and analytical uncertainties associated with reported compositions of experimental materials.

Model residuals for Fe-bearing liquids used in the calibration data set show no systematic correlation with temperature (fig. 1E), but it can be seen in figure 1H that results from different investigators in the system Na_2O-Fe_2O_3-FeO-SiO_2 show systematic inter-laboratory trends. Nevertheless, the r.m.s. error is 0.73 percent for this data subset and is statistically equivalent to the Fe-absent systems.

Model residuals for liquids in the system CaO-Fe_2O_3-FeO-SiO_2 are examined in figures (1C), (1F) and (1I). These liquids were not used in the calibration data set. Although the temperature dependence of these density data are reasonably well accounted for by the model (fig. 1F), there are systematics to the residuals that are best illustrated in figure 1I. Liquid compositions that fall along a pseudobinary, defined by a constant molar ratio of CaO to SiO_2 equal to one, fit the model well for $X_{Fe_2O_3}^{totalFe} < 0.5$. Compositions with higher CaO/SiO_2 ratios tend to have positive model residuals, which corresponds to a predicted melt density smaller than that measured. Compositions "4", "5", "9", and "A" of Dingwell and Brearley (1988) that cluster near the compositional midpoint of the system, have large and positive residuals. Sample "3" of Dingwell and Brearley (1988) is consistent with results presented by Hara and others (1988) on a similar composition, but sample "A" is not. Compositions studied by Mo and others (1982) are systematically offset from results obtained by Dingwell and Brearley (1988) on nearly identical compositions (their "1"). Sample "7" of Dingwell and Brearley (1988), which is very silica depleted, is predicted to be significantly

[2]The square root of the sum-of-squares of model residuals divided by the square root of the number of data points. This number is expressed here as a percentage of the *average* liquid volume.

TABLE 2

Statistics of volume regression

Source	System	Num. of Exp.	r.m.s	Ave. V (cc)	% error
All Data*	Table A-1	600	0.233	24.40	0.96
All Data except CFS*	**Optimized System**	**520**	**0.184**	**24.36**	**0.76**
Bockris and others (1955)	Na_2O-SiO_2, K_2O-SiO_2	32	0.081	28.81	0.28
Courtial and Dingwell (1995)	CaO-Al_2O_3-SiO_2	34	0.121	24.82	0.49
Courtial and Dingwell (1999)	MgO-Al_2O_3-SiO_2 CaO-MgO-Al_2O_3-SiO_2	32	0.185	23.16	0.80
Dingwell (1992)	CaO-TiO_2-SiO_2 Na_2O-TiO_2-SiO_2	42	0.194	24.49	0.79
Dingwell and others (1988)	Na_2O-SiO_2	3	0.082	27.34	0.30
Gottsman and Dingwell (2000)	$CaMgSi_2O_6$	4	0.061	19.65	0.31
Gottsmann and Dingwell (2002)	$CaAl_2Si_2O_8$-$CaMgSi_2O_6$	6	0.084	24.16	0.35
Johnson (1989)	CaO-, MgO-, Na_2O-, K_2O-TiO_2-SiO_2	36	0.274	28.11	0.97
Knoche and others (1992a)	$CaAl_2Si_2O_8$-$CaMgSi_2O_6$	11	0.256	23.26	1.10
Knoche and others (1992b)	$NaAlSi_3O_8$	1	(-.06)**	29.02	0.21
Lange and Carmichael (1987); Lange (1997)	CaO, MgO, Na_2O, K_2O, Al_2O_3, TiO_2, + SiO_2	82	0.116	24.70	0.47
Liu and Lange (2001)	Na_2O-TiO_2-SiO_2 K_2O-TiO_2-SiO_2	63	0.230	28.56	0.81
Stein and others (1986); Lange (1996)	Na_2O-SiO_2 Na_2O-Al_2O_3-SiO_2	32	0.112	27.99	0.40
Toplis and Richet (2000)	$CaAl_2Si_2O_8$-$CaMgSi_2O_6$	3	0.396	22.08	1.79
Webb and others (1992)	$Na_2Si_3O_7$	9	0.086	27.05	0.32
Fe-absent Data		**380**	**0.176**	**25.99**	**0.69**
Courtial and others (1999)	CoO-Na_2O-SiO_2 NiO-Na_2O-SiO_2	31	0.148	25.54	0.58
Courtial and others (1997)	CaO-MgO-FeO-Fe_2O_3-Al_2O_3-SiO_2	14	0.127	20.75	0.61
Dingwell and others (1988)	Na_2O-FeO-Fe_2O_3-SiO_2	33	0.249	28.86	0.86
Johnson (ms, 1989)	K_2O-FeO-Fe_2O_3-TiO_2-SiO_2, K_2O-Na_2O-CaO-MgO-FeO-Fe_2O_3-Al_2O_3-TiO_2-SiO_2	5	0.237	26.76	0.89
Lange and Carmichael (1987)	Na_2O-FeO-Fe_2O_3-SiO_2, K_2O-Na_2O-CaO-MgO-FeO-Fe_2O_3-Al_2O_3-TiO_2-SiO_2	12	0.258	25.69	1.00
Mo and others (1982)	Na_2O-FeO-Fe_2O_3-SiO_2, K_2O-Na_2O-CaO-MgO-FeO-Fe_2O_3-Al_2O_3-TiO_2-SiO_2	64	0.161	25.47	0.63
Shiraishi and others (1978)	Fe_2SiO_4	2	0.007	18.09	0.04
Fe-bearing Data		**130**	**0.196**	**26.86**	**0.73**
Dingwell and Brearley (1988)	CaO-FeO-Fe_2O_3-SiO_2	28	0.641	24.28	2.64
Hara and others (1988)	CaO-FeO-Fe_2O_3-SiO_2	29	0.313	25.49	1.23
Mo and others (1982)	CaO-FeO-Fe_2O_3-SiO_2	23	0.149	23.88	0.62
CFS Data		**80**	**0.431**	**24.60**	**1.75**

*Systems NiO-Na_2O-SiO_2 and CoO-Na_2O-SiO_2 from Courtial and others (1999) excluded.
**Deviate from one experiment.

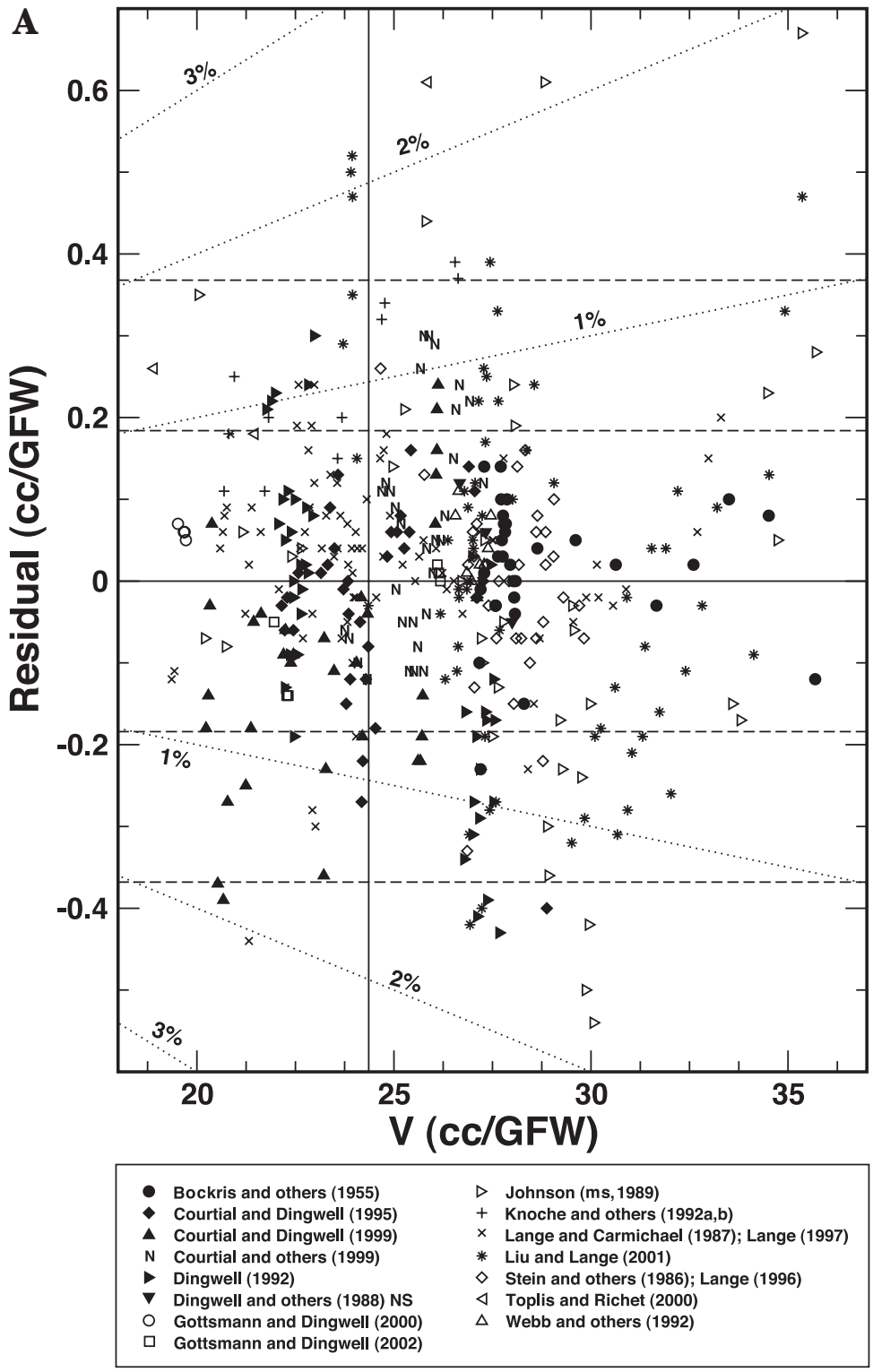

Fig. 1. Residuals for the calibration of equation (16) to the data set on melt volumes plotted as a function of (1A, 1B, and 1C) volume, (1D, 1E, and 1F) temperature, and (1G, 1H, and 1I) mole fraction of

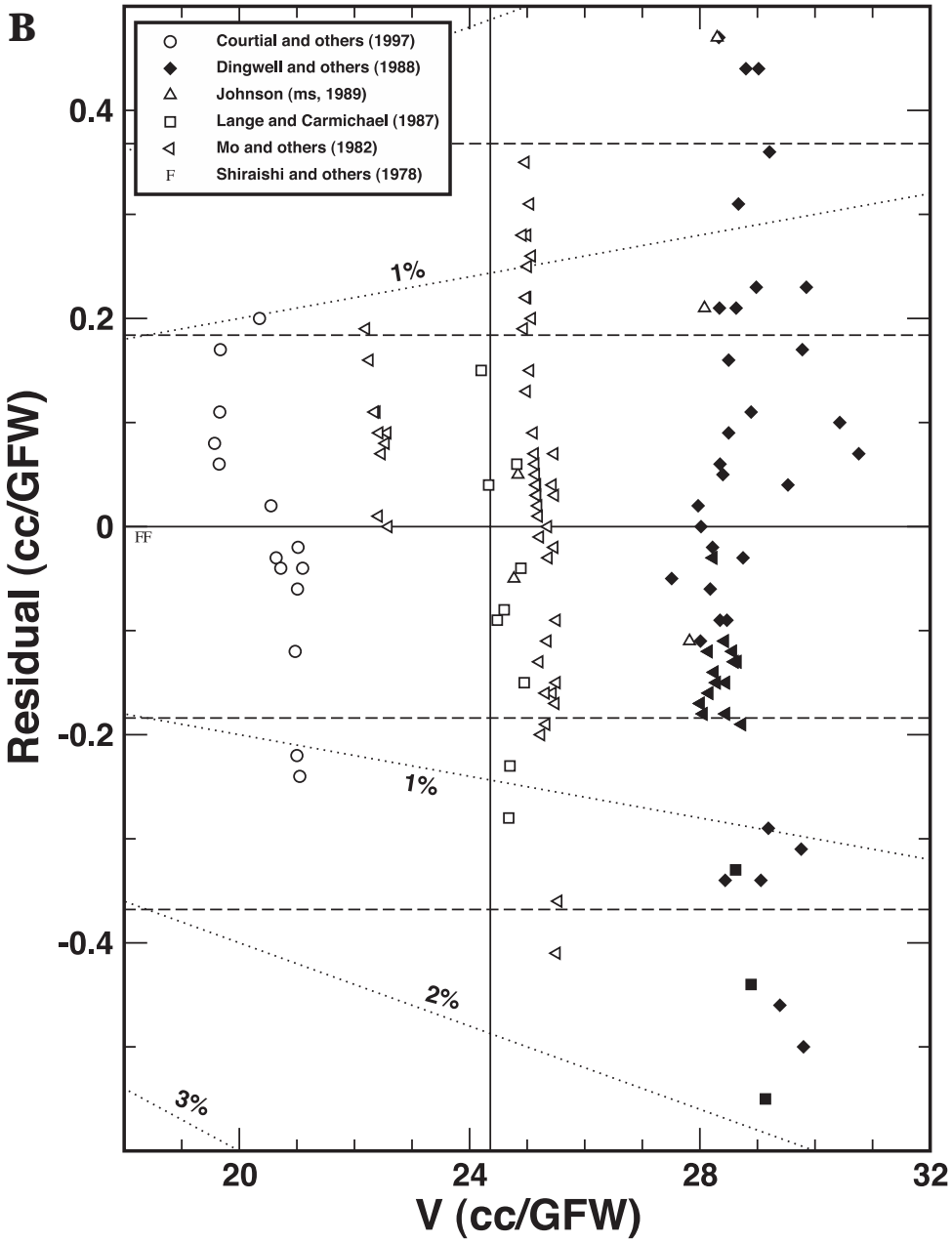

Fig. 1 (*continued*) SiO_2. Residuals plotted in figures (1A), (1D) and (1G) correspond to Fe-absent data utilized in the model calibration. Residuals plotted in figures (1B), (1E), and (1H) correspond to Fe-bearing data utilized in model calibration, where the filled symbols indicate data from bulk compositions in the system Na_2O-Fe_2O_3-FeO-SiO_2. Residuals plotted in figures (1C), (1F) and (1I) correspond to bulk compositions in the system CaO-Fe_2O_3-FeO-SiO_2 (*sensu stricto*). These data were not utilized in developing the model calibration; numbers correspond to individual compositions identified in table A2. In figure (1I) an inset shows bulk compositions plotted in a weight percent ternary diagram; the pseudobinary lines indicate *equimolar* ratios of oxides. The horizontal solid lines on all the figures are zero residual reference lines. The vertical solids lines on figures (1A), (1B) and (1C) denote the average volume of the calibration data set. The dotted lines on all figures give contours in relative error (% residual/average) while the dashed lines correspond to ± 1, ± 2, *et cetera*, root mean square (r.m.s) deviations for the fit to the calibration data set.

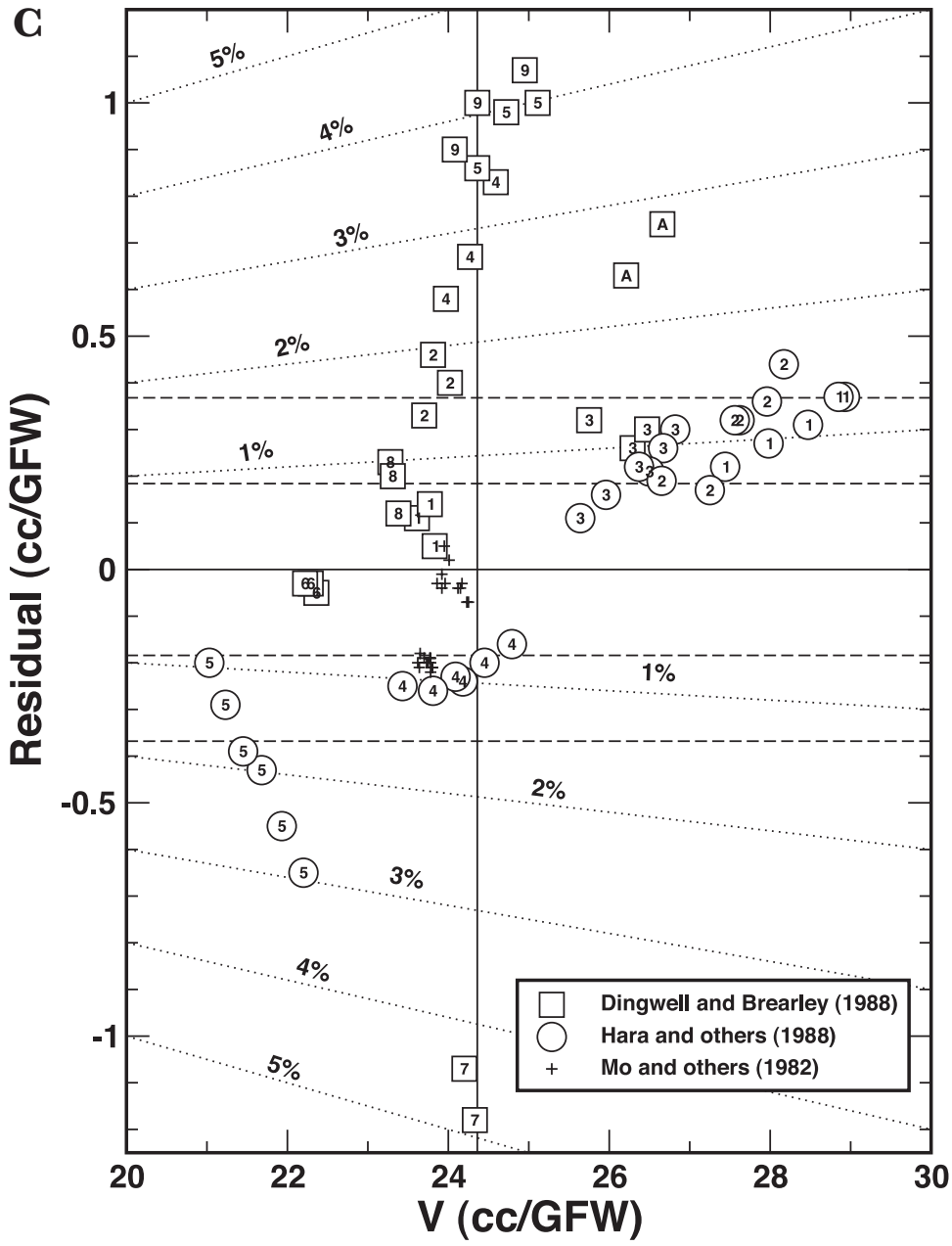

Fig. 1 (*continued*)

denser than measurements indicate, but their sample "3" and samples "1" and "2" of Hara and others (1988) show an opposite result. All of these measurements in the CaO-Fe_2O_3-FeO-SiO_2 system were performed in air with the exception of experiments "4" and "5" of Hara and others (1988) which were run under f_{O_2} ~2 and 3.5 log units below air. Experiments "3", "4" and "5" of Hara and others (1988) represent the same

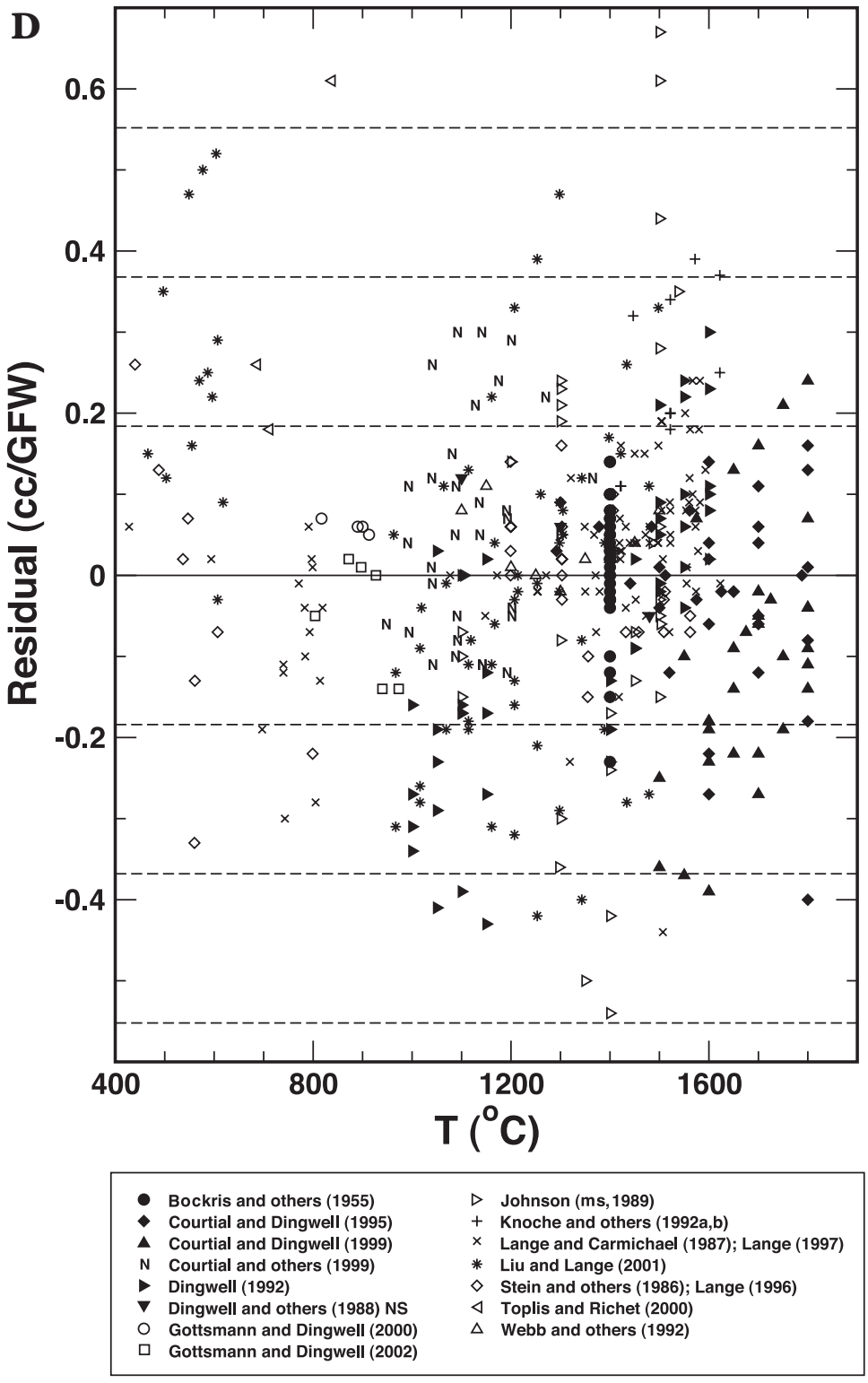

Fig. 1 (*continued*)

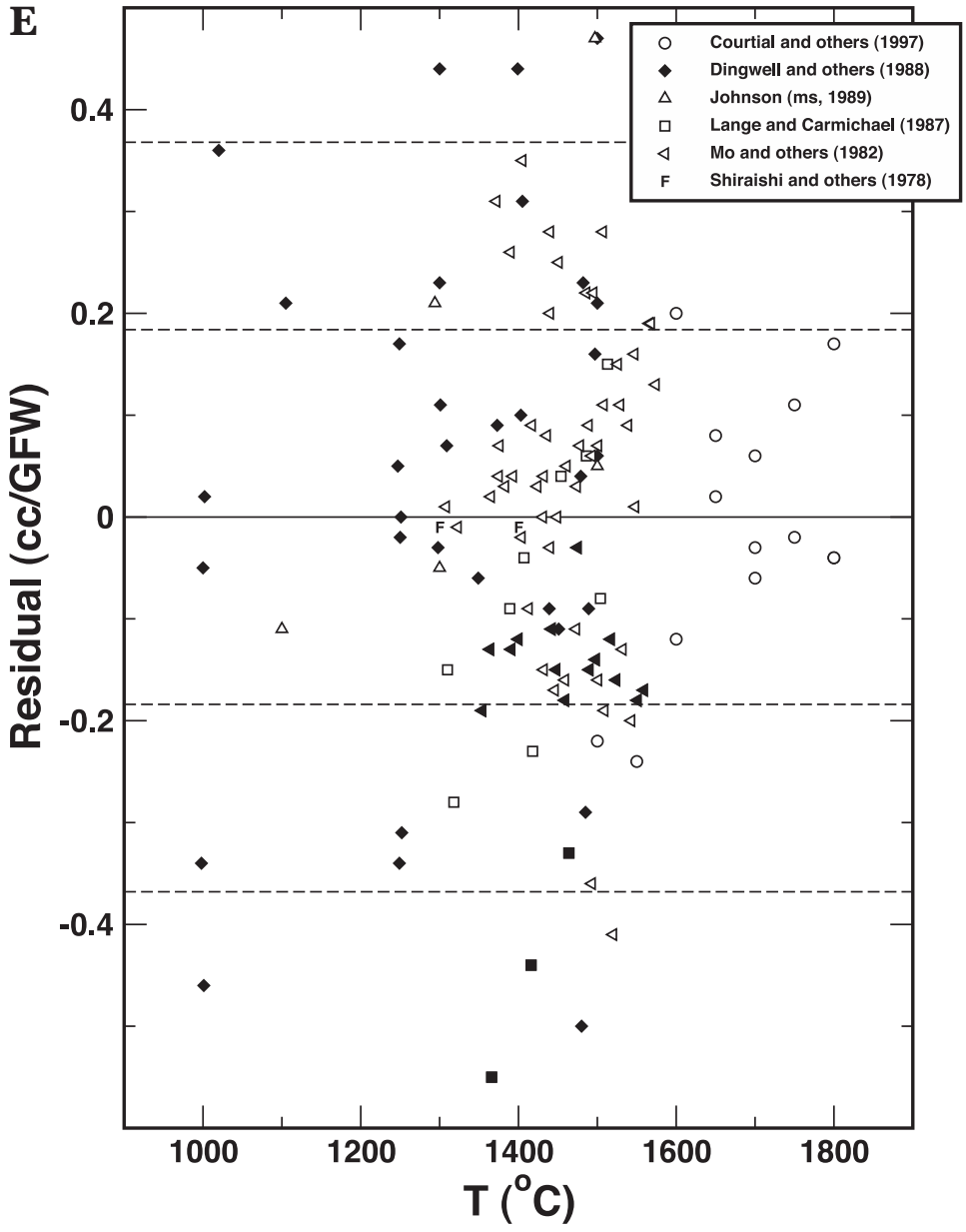

Fig. 1 (*continued*)

bulk composition. These authors interpret the scatter of residuals in "5" as potentially due to liquid immiscibility in the system under reducing conditions, but comparing residuals for their samples "3" and "4," there is a hint of some systematic dependence on oxygen fugacity. Hara and others (1988) concluded that unlike the CaO-Fe_2O_3 binary, which they found to exhibit linear mixing relations for the volume, significant nonlinear effects are seen in the ternary. In constrast, Dingwell and Brearley (1988) model their data with strongly positive interactions of CaO and Fe_2O_3 and weakly

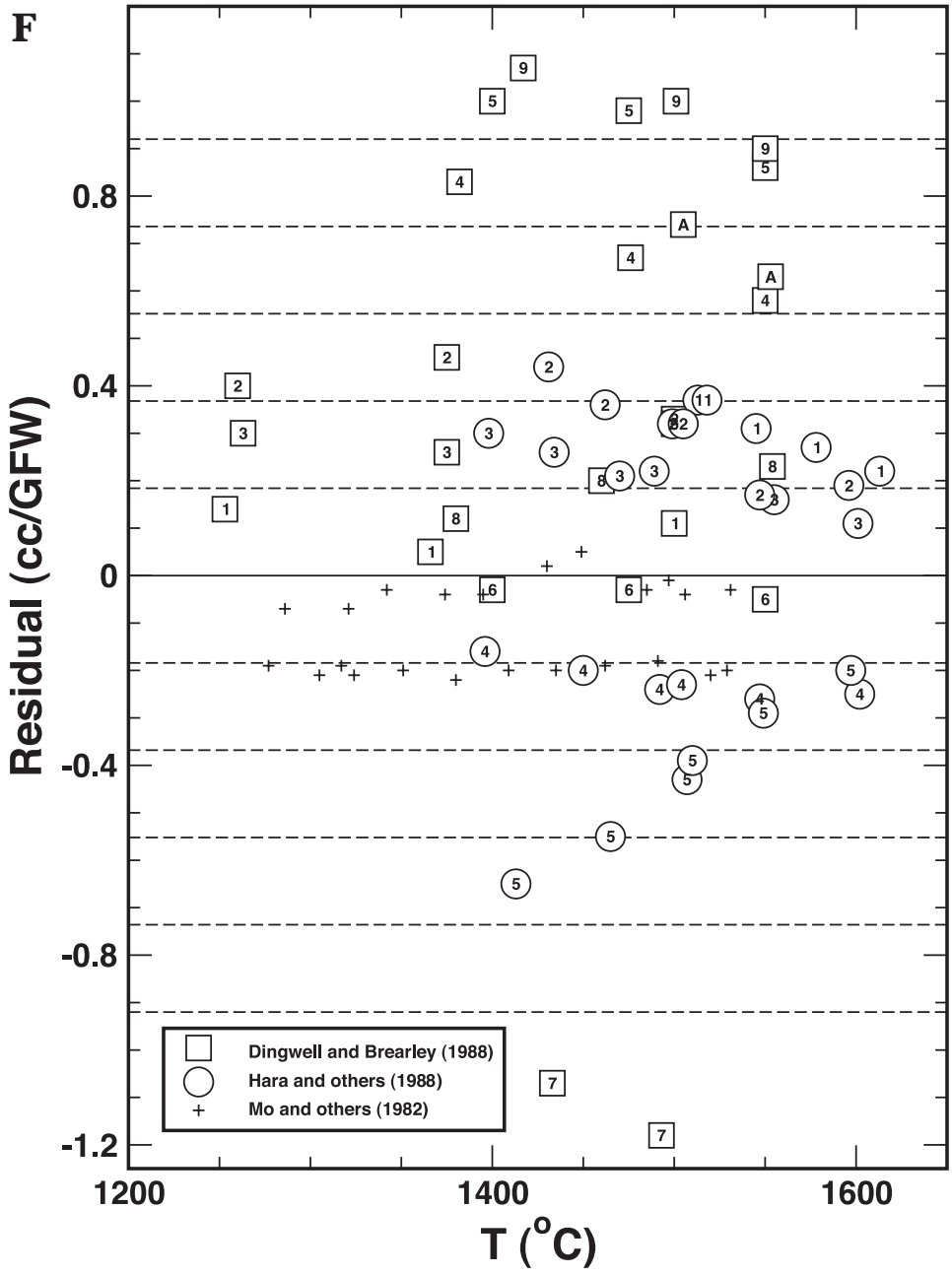

Fig. 1 (*continued*)

negative CaO-SiO_2 interactions, but the residual pattern displayed in figure 1I does not support this analysis. Kress and Carmichael (1989) were able to fit a linear mixing model to the data of Dingwell and Brearley (1988) (with $SiO_2 > 20$ wt %) and the two compositions from Mo and others (1982), but their value for the partial molar volume of Fe_2O_3 is smaller by ~5 cc/mol than the model value obtained in this analysis.

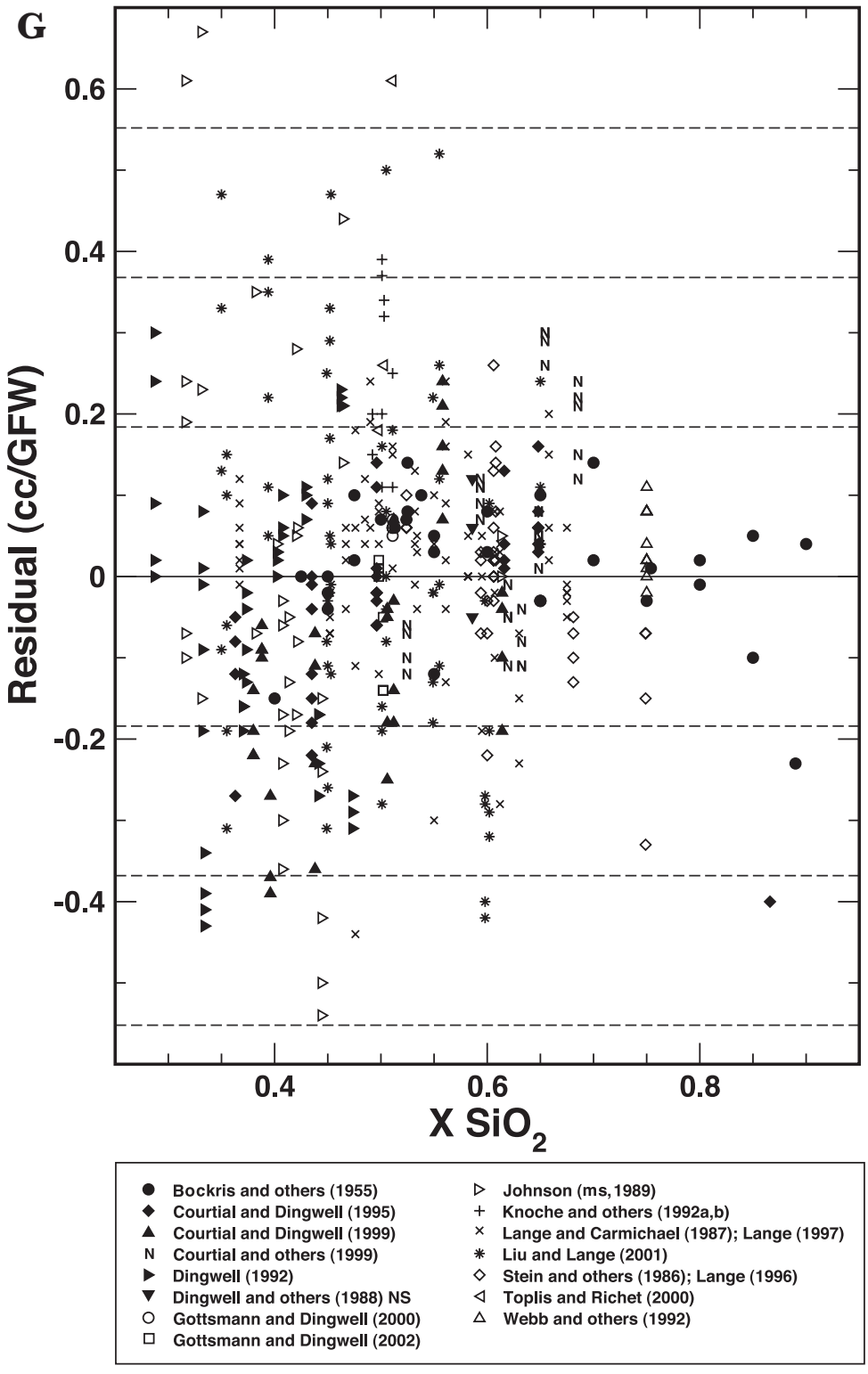

Fig. 1 (*continued*)

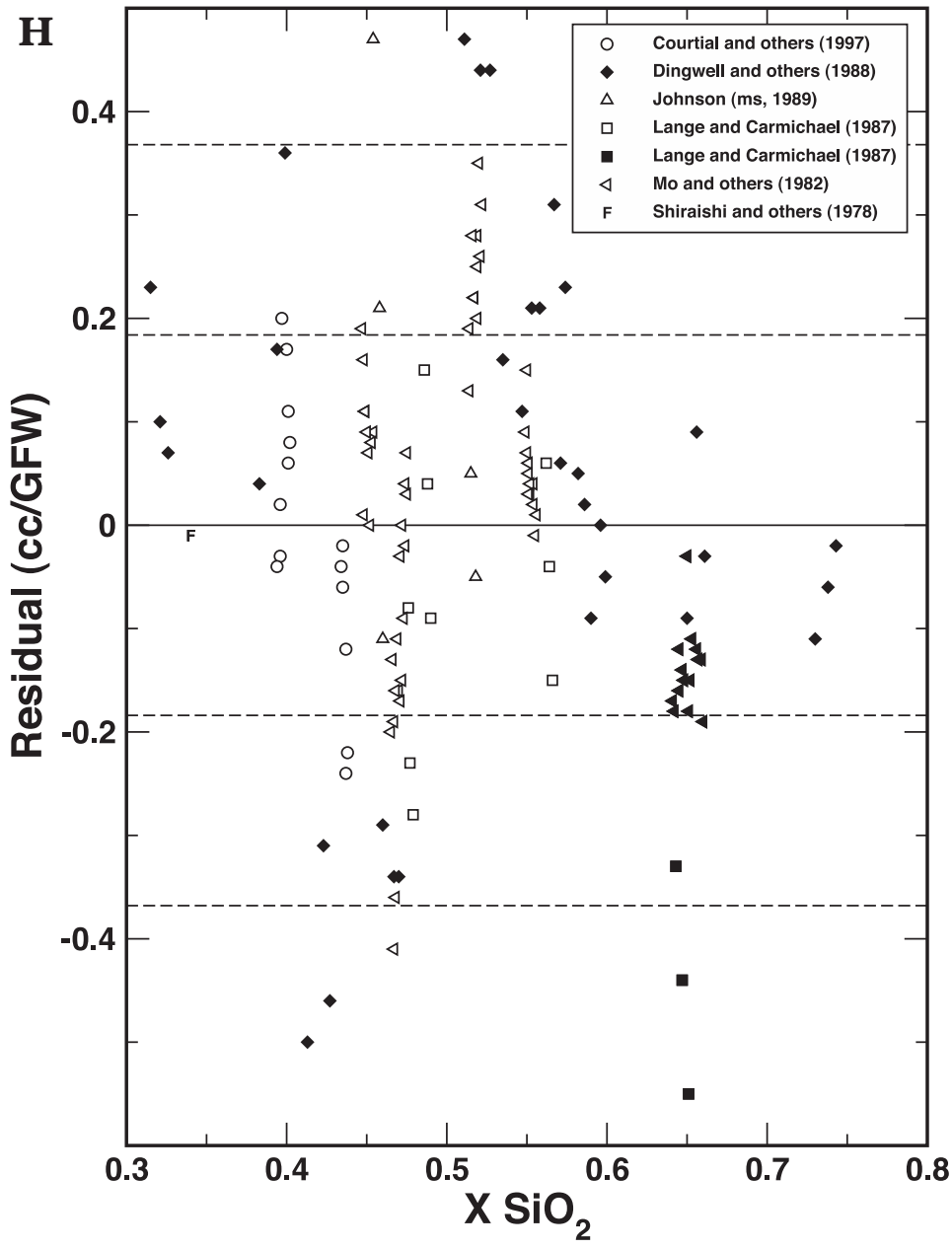

Fig. 1 (*continued*)

Although it is clear from figure 1I that there are nonlinearities in the volume mixing properties in the CaO-Fe_2O_3-FeO-SiO_2 system, it is not at all obvious how these might be accounted for in a model expression. "Binary" CaO-(FeO, $FeO_{1.3}$, Fe_2O_3) terms are unsupported by the data of Hara and others (1988). The system CaO-SiO_2 is very nearly ideal except at $X_{CaO} > 0.6$ (Courtial and Dingwell, 1995) and at higher CaO contents exhibits *positive* deviations from ideality. Interaction terms on the SiO_2-(FeO,

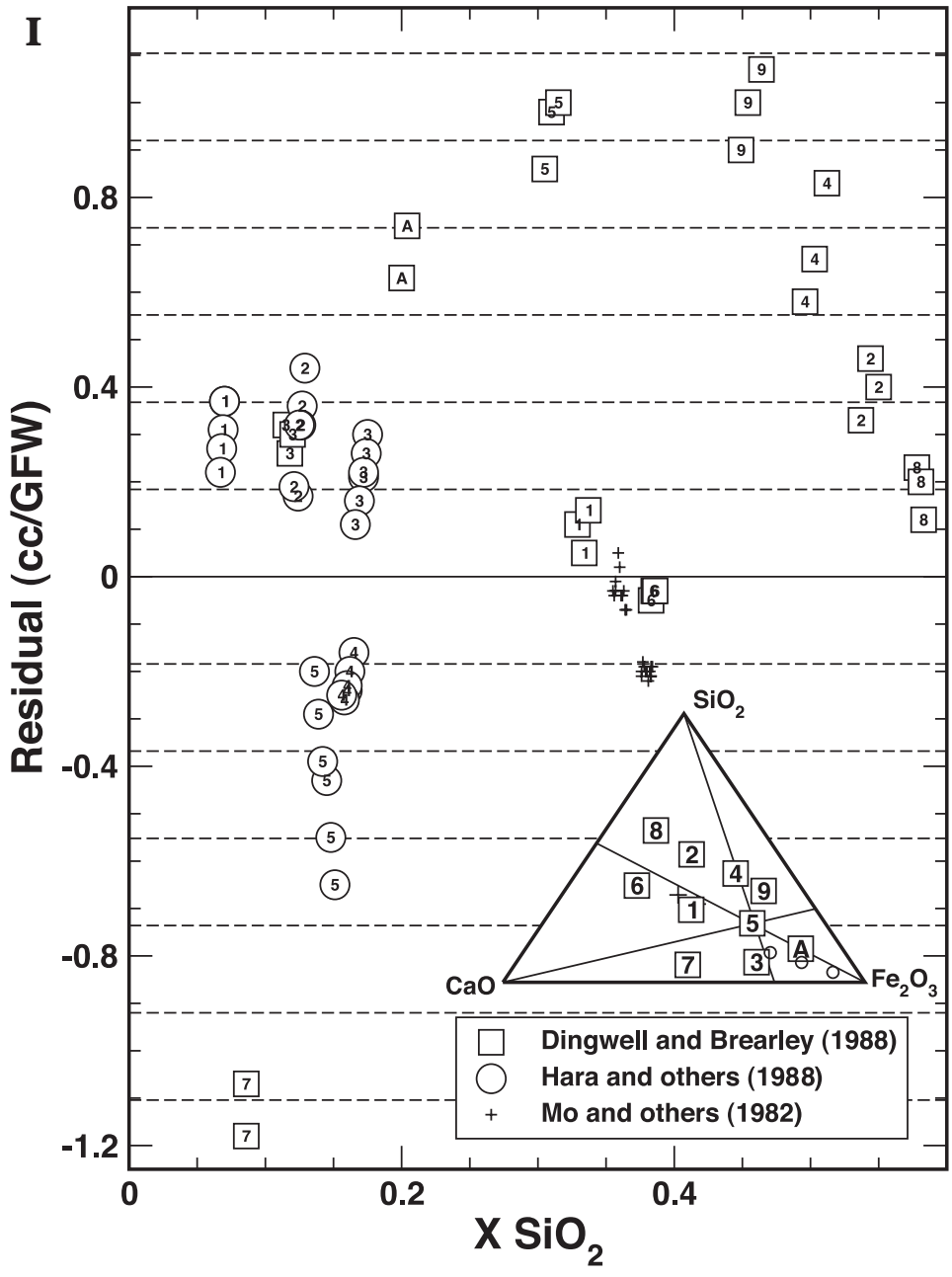

Fig. 1 (*continued*)

$FeO_{1.3}$, Fe_2O_3) join are unwarranted, in that they would impact the model results on the other Fe-bearing systems (fig. 1H) which are adequately represented by a linear model. Ternary interactions might be the answer, but the model residuals in figure 1I are not systematic about the compositional midpoint of the system. At present there is no obvious resolution to the dilemma of misfits in the system CaO-Fe_2O_3-FeO-SiO_2. The model presented here should only be used with caution for liquids in this system.

TABLE 3

Volume model parameters

Oxide	$V_{1673\,K}\left(\frac{cc}{mol}\right)$	$\frac{\partial V}{\partial T}\times 10^3\left(\frac{cc}{K-mol}\right)$
SiO_2	26.710	1.007
TiO_2	23.448	6.807
Al_2O_3	37.616	-0.649
Fe_2O_3	42.677	5.536
$FeO_{1.3}$	16.139	3.820
FeO	13.895	1.532
MgO	12.015	2.887
CaO	16.671	3.143
Na_2O	29.117	6.077
K_2O	46.401	10.432
NiO	10.568	1.068
CoO	15.080	0.406
$Na_2O{\times}TiO_2$	20.476	9.699
$Na_2O{\times}TiO_2$	27.387	4.240

In table 4 results from the proposed model and that of Lange and Carmichael (1987) are examined by comparing the calculated root-mean-square (r.m.s.) residuals from each model and each data subset. Differences in r.m.s. are evaluated in terms of an *F*-statistic and the significance level of that *F* is reported. Violation of the null hypothesis (that is statistically equivalent fits obtained from the two model approaches) is indicated by a significance level smaller than 0.05. Only the first five data sets identified in the table were considered by Lange and Carmichael (1987). Notably, the proposed model recovers the Fe-absent data of Lange & Carmichael (1987) less accurately and conversely the data of Mo and others (1982), Stein and others (1986), and Bockris and others (1955) with greater accuracy. Overall, the proposed model is significantly better in recovering the data set for both the Fe-absent and Fe-bearing subsets (table 4).

A table of values of model dependent partial molar volumes of oxide components at 10^5 Pa and over a range of temperatures is presented in table 5. These values are provided for convenience to give a sense of the magnitudes and temperature variations of the inferred endmember properties, but should not be used to calculate model volumes for mixtures; such calculations require the use of equation (16). Nevertheless, the values tabulated highlight that the partial molar expansivities of the oxides are positive with the exception of Al_2O_3. The negative thermal expansion of alumina can be interpreted as a shift in the oxygen coordination number of Al to higher values at elevated temperature. The same feature was seen for Si coordination number shifts in the example thermodynamic model for SiO_2 liquid developed in Part I. If this interpretation is correct then it highlights the likely possibility that the parameter values obtained in this modeling exercise mix vibrational effects with those that may be attributed to configurational changes associated with the compositional and temperature dependence of the coordination number of melt cations. The possible mixing of vibrational and configurational effects is an unfortunate confusion of contributions and the model would be more robust if configurational effects could be modeled independently (Part I). But, in lieu of extensive spectroscopic data or molecular dynamics simulations for the range of compositions spanned by this model, the

TABLE 4

Comparison of Model results with Lange and Carmichael (1987)

Reference	Model r.m.s	L&C (1987) r.m.s	No. of Obsv.	F	Significance level
Lange and Carmichael (1987); Lange (1997)	0.116	0.117	82	1.02	0.47
Lange and Carmichael (1987)	0.258	0.162	12	2.52	0.06
Mo and others (1982)	0.161	0.328	64	4.14	**<< 0.01**
Mo and others (1982) CFS	0.149	0.243	23	2.68	**0.01**
Stein and others (1986); Lange (1996)	0.112	0.154	32	1.89	0.04
Bockris and others (1955)	0.081	0.099	32	1.48	**0.01**
Courtial and Dingwell (1995)	0.121	0.159	34	1.73	0.06
Courtial and Dingwell (1999)	0.185	0.346	32	3.47	**<< 0.01**
Courtial and others (1997)	0.127	0.191	14	2.27	0.07
Dingwell (1992)	0.194	0.195	42	1.00	0.50
Dingwell and Brearley (1988)	0.641	0.528	28	1.47	0.16
Dingwell and others (1988)	0.082	0.071	3	1.34	0.41
Dingwell and others (1988)	0.249	0.495	33	3.97	**<< 0.01**
Gottsman and Dingwell (2000)	0.061	0.299	4	24.13	**< 0.01**
Gottsmann and Dingwell (2002)	0.084	0.131	6	2.46	0.15
Hara and others (1988)	0.313	1.402	29	20.05	**<< 0.01**
Johnson (ms, 1989)	0.274	1.334	36	23.79	**<< 0.01**
Johnson (ms, 1989)	0.237	0.293	5	1.52	0.33
Knoche and others (1992a)	0.256	0.202	11	1.61	0.22
Knoche and others (1992b)	(–.062)	(–.102)	1	-	-
Liu and Lange (2001)	0.230	1.314	63	32.57	**<< 0.01**
Shiraishi and others (1978)	0.007	0.031	2	18.59	0.05
Toplis and Richet (2000)	0.396	0.448	3	1.28	0.42
Webb and others (1992)	0.086	0.036	9	1.87	0.18
Fe-absent data set	0.176	0.210	390	1.36	**0.001**
All data	0.233	0.672	600	8.28	**$< 10^{-125}$**

preferred approach is simply not possible. The issue is especially important when using the reference pressure volume parameters calibrated here with the EOS model at high pressures and temperatures. The problem will be examined in detail in the context of such applications in Parts III and IV.

The Volume of $CaMgSi_2O_6$ Liquid

Before turning to calibration of sound speed measurements, it is instructive to examine model predictions and experimental results on liquids of nominally diopside composition. There are two reasons for this examination. First, this composition is well studied by a number of authors and a comparison of model results to experimental measurements allows the evaluation of interlaboratory reproducibility. Second, the

TABLE 5

Molar volume estimates for oxide components

	1000°C	1100°C	1200°C	1300°C	1400°C	1500°C	1600°C	1700°C	1800°C	1900°C	2000°C
SiO_2	26.31	26.41	26.51	26.61	26.71	26.81	26.91	27.01	27.12	27.22	27.32
TiO_2	20.88	21.49	22.13	22.78	23.45	24.14	24.85	25.58	26.33	27.11	27.91
Al_2O_3	37.88	37.81	37.75	37.68	37.62	37.55	37.49	37.42	37.36	37.29	37.23
Fe_2O_3	40.52	41.05	41.58	42.13	42.68	43.23	43.80	44.37	44.95	45.54	46.13
$FeO_{1.3}$	14.68	15.03	15.39	15.76	16.14	16.53	16.92	17.33	17.74	18.17	18.60
FeO	13.30	13.44	13.59	13.74	13.90	14.05	14.20	14.36	14.52	14.68	14.85
MgO	10.91	11.18	11.45	11.73	12.02	12.31	12.61	12.91	13.23	13.55	13.88
CaO	15.46	15.75	16.05	16.36	16.67	16.99	17.31	17.64	17.98	18.32	18.67
Na_2O	26.78	27.35	27.93	28.52	29.12	29.73	30.36	31.00	31.65	32.32	33.00
K_2O	42.41	43.38	44.36	45.37	46.40	47.46	48.54	49.64	50.77	51.92	53.10
NiO	10.15	10.25	10.36	10.46	10.57	10.68	10.78	10.89	11.00	11.12	11.23
CoO	14.92	14.96	15.00	15.04	15.08	15.12	15.16	15.20	15.24	15.28	15.33

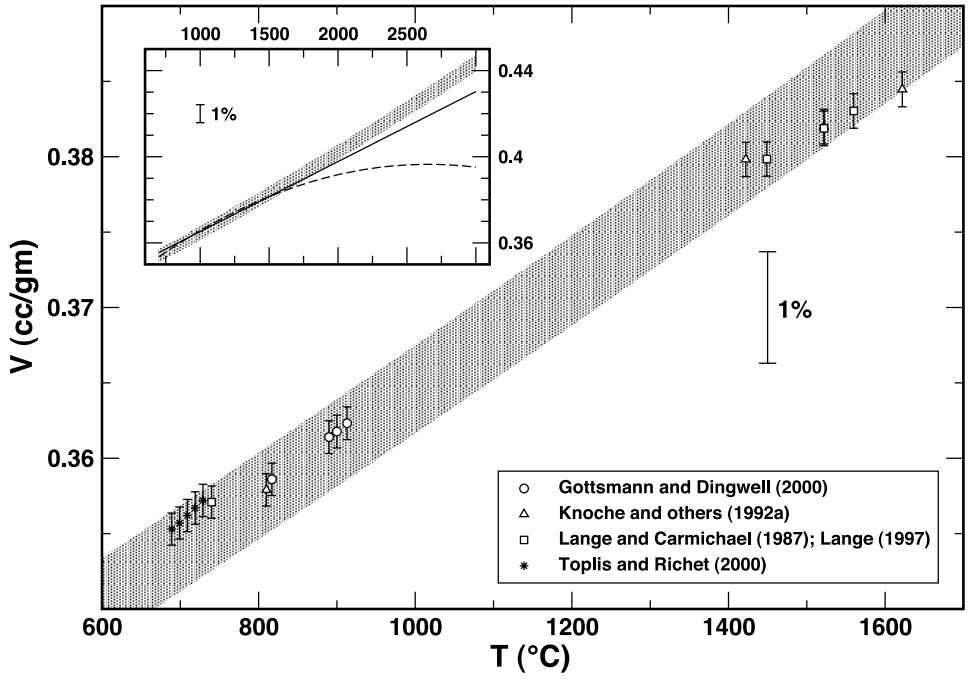

Fig. 2. Comparison of volumetric measurements on liquids ($T > 1400$ °C) and glasses ($T < 950$ °C) of nominal composition $CaMgSi_2O_6$ ("diopside") compared with model estimates. Data points are plotted with an error bracket reflecting the likely minimum error in the *accuracy* of the measurement; a value of 0.3 percent, as suggested by Lange (2002). (A) The shaded band gives a model estimate of volume ± 0.76 percent (one root-mean-square error of the model regression). Inset shows extrapolated values to 3000 °C calculated using models proposed in this paper (shaded band), Lange (1997) (solid line), and Gottsmann and Dingwell (2000) (dashed curve).

temperature dependence of the molar volume of diopside liquid has been the subject of some controversy and the model developed here can inform that debate via an analysis of uncertainty due to compositional variability of experimental materials.

In figure 2 data are plotted on the specific volume (cc/gm) of "diopside"-composition liquids and glasses taken from glass dilatometric studies by Knoche and others (1992a), Lange (1997), Gottsmann and Dingwell (2000), and Toplis and Richet (2000) and double-bob Archimedian densimetric measurements on liquids by Knoche and others (1992a) and Lange and Carmichael (1987). The error bars on these data points are those suggested by Lange (2002) and represent the likely minimal error in the *accuracy* of the determination. This error estimate is taken to be 0.3 percent. The shaded band in figure 2A represents the calculated model value for stoichiometric $CaMgSi_2O_6$ liquid plus or minus the r.m.s. model error (± 0.76%, table 2). None of these data are significant outliers in the model calibration. Gottsmann and Dingwell (2000) argue that the high-temperature densimetric data in combination with their low temperature glass measurements and those of Knoche and others (1992a) and Lange (1997), imply that there is a strong non-linear temperature dependence to the specific volume. They model a second order polynomial in temperature to these data. The figure inset shows their model as the dashed curve. Lange (2002) argues that this data set can be adequately represented by a line of constant slope. Her model (Lange, 1997) is shown by the solid line in the inset to figure 2A. Dingwell and Gottsmann (2002) dispute Lange's analysis. In our model, the choice of making the thermal

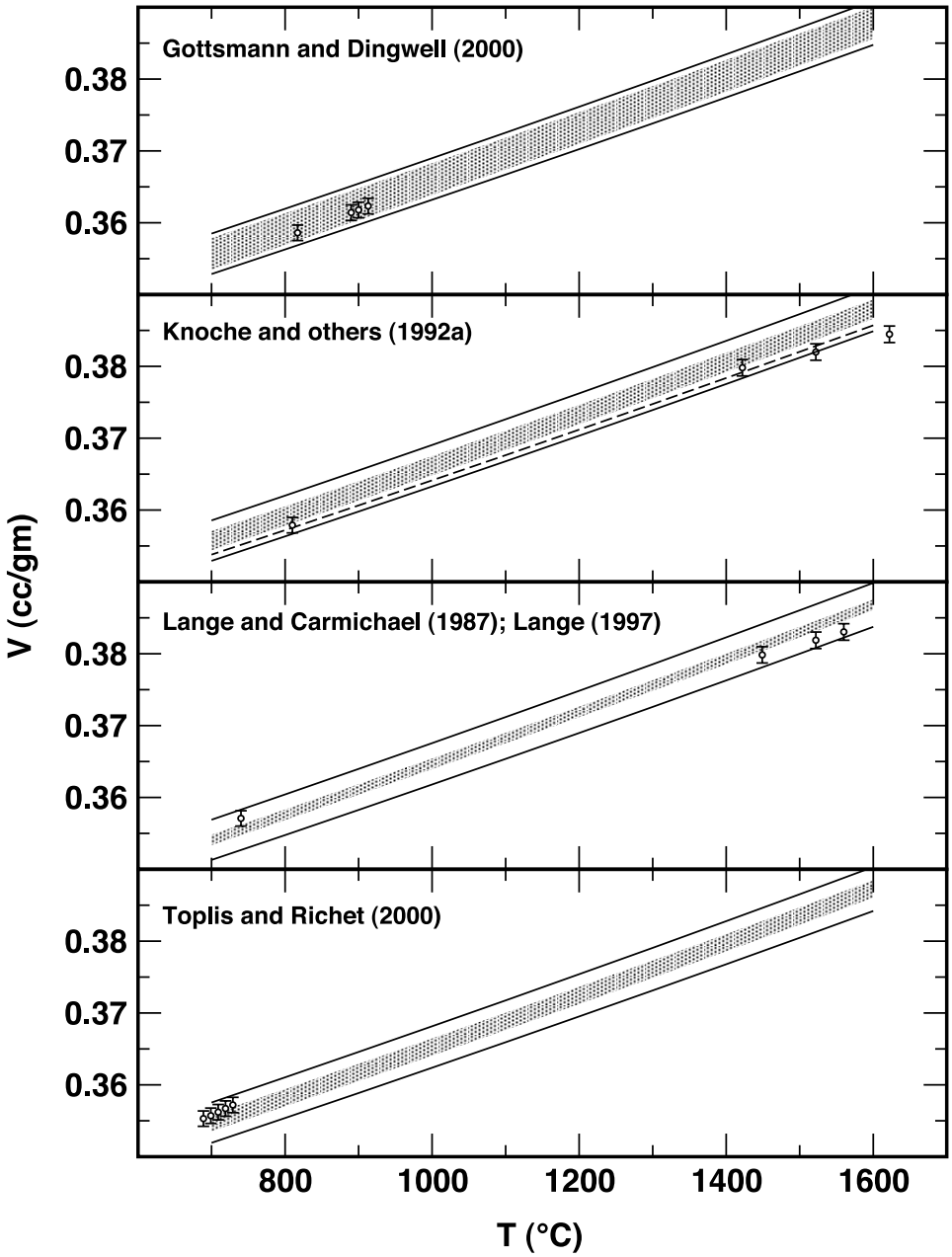

Fig. 2 (*continued*). (B) Solid curves bracket volumes (± 0.76%) of stoichiometric $CaMgSi_2O_6$ calculated from the model expression developed in this paper. Shaded bands correspond to calculations for the reported compositions of nominal $CaMgSi_2O_6$ given by the authors; *the width of the band is derived only from the reported uncertainty of the analysis.* The dashed curve is calculated from the original analysis reported by Knoche and others (1992a), where no estimate of uncertainty was given; the shaded band is calculated from a reanalysis of their composition by Gottsmann and Dingwell (2000).

coefficient of expansion a constant is motivated as a compromise to insure that results can be extrapolated outside of the temperature range of bracketed experiments. In the case of $CaMgSi_2O_6$ liquid, the model value for α is sufficiently small that over the temperature range being considered the variation of volume with temperature is effectively linear. Consequently, our extrapolated model value for volume differs from that of Lange (1997) by only 1 percent at 3000° C, whereas the volume obtained from Gottsmann and Dingwell's (2000) model is 5 percent lower (fig. 2A). Regardless of the detailed arguments regarding the precision and accuracy of these measurements that validate or invalidate either model of temperature dependence, these data illustrate that the intended use of the model can and should dictate the complexity of its structure. The simplest representations of the data are probably best adopted if the intent is to extrapolate beyond the range of available experimental data—the straight line extrapolation is probably a better estimate of the volume of diopside liquid at 3000°C than the parabolic extrapolation. This point is especially relevant if attention is directed to uncertainties in derived volumes due to uncertainties in compositions of experimental materials.

The glass and liquid compositions studied by the authors whose data are plotted in figure 2A do not correspond to stoichiometric $CaMgSi_2O_6$. There are departures from stoichiometry due to preparation procedures and techniques of synthesis. In addition, there are varying degrees of uncertainty in composition associated with the techniques used to analyze experimental materials. An attempt to address the consequences of these compositional effects is made in figure 2B. Data points are plotted from each author along with a shaded band that corresponds to the *reported uncertainty in composition* propagated through the model calibrated here to yield an implied uncertainty in specific volume. Each band is centered on the composition of "diopside" given by each author. The uncertainty in volume implied by the width of the band is solely due to reported analytical uncertainty, and data points may be displaced according to the band half-width. Non-stoichiometry of experimental materials can be assessed by noting the asymmetry of the band within the solid lines, which provide a reference bracket for model predictions of stoichiometric diopside. In the case of Knoche and others (1992a), the dashed line corresponds to the original reported analysis (given without error estimates) and the shaded band to a reanalysis of this glass by Dingwell and Gottsmann (2000). Note that Lange and Carmichael (1987) analyzed their experimental materials using wet chemical techniques, whereas the other authors utilized microprobe methods. No attempt has been made to assess systematic errors in glass standards that influence results of the mircroprobe technique. It is clear from figure 2B that analytical error associated with the glass analyses of Gotttsmann and Dingwell (2000) is comparable to the r.m.s. error of the model calibration. This uncertainty due to analytical error is approximately 4 times the estimated precision reported by these authors and over twice the minimal uncertainty in accuracy suggested by Lange (2002) for these measurements. The propagated analytical error is larger than the precision of analysis in all cases except that of Lange (Lange and Carmichael, 1987; Lange, 1997). This fact is a testament to careful wet chemical analysis of experimental materials. Two points should be gleaned from this discussion of propagated analytical error. The first is that analytical uncertainty alone brings into question the conclusion that a second order polynomial is required to describe the temperature dependence of the specific volume of diopside liquid. The second, and more important point, is that this analysis of the effect of compositional uncertainty required application of a multicomponent model to fully understand the sources of error and robustness of any conclusions. Finally, both points underscore that a multicomponent calibration of melt volume (or density) cannot be more precise than

the experimental measurements utilized in calibration. A major source of that uncertainty for the model calibrated here is compositional in origin.

CALIBRATION OF SOUND SPEED MEASUREMENTS

A data set of experimental measurements of sound speeds in silicate liquids is assembled and summarized in table 6. Details of the chemical systems investigated and temperatures and results for each experimental datum are reported in the Appendix (table A2). As a starting point for this compilation, the data set used by Kress and Carmichael (1991) is adopted to which have been added more recent work on CaO-Al_2O_3-SiO_2 (Webb and Courtial, 1996) and TiO_2-bearing systems (Webb and Dingwell, 1994). Only relaxed sound speeds are considered for inclusion in the data set. These are selected according to criteria described in Kress and Carmichael (1991). Taking a cue from results of the volume regression, parameters of the sound speed mixing relation (eq 17) are treated as functions of temperature with cross-composition terms to accommodate alkali-titania interactions in order to maintain consistency with the volume model. These considerations give the regression model:

$$c\big|_{T,P_r} = \sum_i X_i \left[\bar{c}_i\Big|_{1673K} + \frac{\partial \bar{c}_i}{\partial T}(T - 1673) \right] + X_{Na_2O} X_{TiO_2} \bar{c}_{Na-Ti} + X_{K_2O} X_{TiO_2} \bar{c}_{Na-Ti} \quad (26)$$

Note that the summation is over all oxide components and all Fe-bearing melt species in the liquid; the Fe-bearing liquids of Kress and Carmichael (1991) are processed to calculate abundances of FeO, $FeO_{1.3}$, and $FeO_{1.5}$, in an exactly analogous manner to the treatment of the density data set. The variance of temperature in the calibration data set is insufficient to resolve the temperature-dependence of the quadratic composition terms. Calibration of the parameters in equation (26) to the sound speed data generates a fit with a relative error of about 5 percent, which is considerably larger than the experimental uncertainty of ~2 percent (Kress and Carmichael, 1991). Given that Kress and Carmichael (1991) found that their model for the compositional dependence of $\partial V/\partial P$ required the addition of cross-composition terms involving the product of Na_2O and Al_2O_3 mole fractions, equation (26) is modified to

$$c\big|_{T,P_r} = \sum_i X_i \left[\bar{c}_i\Big|_{1673K} + \frac{\partial \bar{c}_i}{\partial T}(T - 1673) \right] + X_{Na_2O} X_{Al_2O_3} \bar{c}_{Na-Al} + X_{Na_2O} X_{TiO_2} \bar{c}_{Na-Ti} + X_{K_2O} X_{TiO_2} \bar{c}_{Na-Ti} \quad (27)$$

A final regression calibration with equation (27) returns a relative error of 1.7 percent. Model residuals to equation (27) were further analyzed under the suspicion that terms involving K_2O-Al_2O_3 and CaO-Al_2O_3 interactions would be warranted. While there is some hint that such terms may be important, the spectrum of melt compositions in the data set are too restrictive to determine statistically meaningful coefficients. The preferred model for sound speed is calculated from equation (27). Parameters are listed in table 7. Statistical aspects of the fit are summarized in table 6. As with the volume regression described above, techniques of singular value decomposition were used to access cross-correlation of model parameters. All parameters are determined to be statistically meaningful.

The model expression reproduces the sound speed data set with an overall relative precision of 1.7 percent (table 6). Residuals for each datum are reported in the Appendix and are plotted in figure 3. No patterns involving systematic deviation of subsets of the data are discernible from figure 3. For convenience, values of sound speed oxide coefficients are tabulated as a function of temperature in table 8.

TABLE 6

Statistics for regression of sound speed data set

Data Source	**No. of cases**	**Ave. c** $\left(\frac{m}{\text{sec}}\right)$	**r.m.s. error**	**% error**	**Ave.** $\frac{\partial V}{\partial P}$ $\left(\frac{cc}{GPa}\right)$	**r.m.s. error [c]**	**% error [c]**	**r.m.s. error** $[\frac{\partial V}{\partial P}]$	**% error** $[\frac{\partial V}{\partial P}]$
Rivers (ms, 1986) Rivers and Carmichael (1987)	86	2714	44.23	1.63%	-1.33	0.053	4.00%	0.077	5.77%
Bockris and Kojonen (1960)	5	2275	44.55	1.96%	-3.15	0.122	3.87%	0.163	5.18%
Baidov and Kunin (1968)	9	2646	90.21	3.41%	-2.10	0.189	8.98%	0.213	10.13%
Sokolov and others (1971)	2	2900	77.92	2.69%	-1.33	0.071	5.34%	0.079	5.89%
Kress and others (1988)	56	2684	62.17	2.32%	-1.85	0.081	4.38%	0.079	4.29%
Kress and Carmichael (1991)	75	2599	56.45	2.32%	-1.62	0.068	4.19%	0.044	2.73%
Webb and Courtial (1996)	112	3182	32.42	1.02%	-0.962	0.018	1.85%	0.044	4.58%
Webb and Dingwell (1994)	58	2508	35.77	1.43%	-1.10	0.054	4.89%	0.107	4.91%
Total	**403**	**2783**	**47.54**	**1.71%**	**-1.52**	**0.062**	**4.11%**	**0.078**	**5.13%**

TABLE 7

Model parameters for sound speed analysis

	$c\big\vert_{1673K}\left(\frac{m}{\text{sec}}\right)$	$\frac{\partial c}{\partial T}\times 10^3\left(\frac{m}{K-\text{sec}}\right)$
SiO_2	2321.75	399.34
TiO_2	1693.60	811.99
Al_2O_3	2738.35	503.94
Fe_2O_3	1364.53	386.08
$FeO_{1.3}$	1955.96	104.17
FeO	2399.53	-107.26
MnO	2399.53	-107.26
MgO	3349.96	275.64
CaO	3967.42	-205.26
Na_2O	3080.69	-2167.57
K_2O	1682.35	-2344.06
Na_2O-Al_2O_3	5800.72	
Na_2O-TiO_2	-1325.21	
K_2O-TiO_2	-994.34	

Values of sound speed calculated for each experimental datum from the model equation are combined with results obtained in the previous section to compute a model $\partial V/\partial P$ (eq 5). For this purpose the liquid heat capacity calibration of Lange and Navrotsky (1992) is used. Taking the measured sound speed for each datum and utilizing the same procedure and ancillary volume data, an internally consistent estimate of $\partial V/\partial P$ is obtained that may be compared to that derived from the model calibration. The *difference* between this $\partial V/\partial P$ and the estimate from the sound speed model is reported in the Appendix (table A2) and plotted against derived values of $\partial V/\partial P$ in figure 4. Table 6 summarizes statistics associated with prediction of $\partial V/\partial P$ from the sound speed model (entries in columns labeled with [c]). The overall relative error in model results is 4.1 percent. As this relative error is larger than the relative error in the sound speed regression, it might be surmised that uncertainties in volume and expansivity terms contribute to and overwhelm the errors in modeled sound speed. That is not the case. A first order error propagation analysis (Bevington, 1969) of equation (5) gives the following formula

$$s^2_{\partial V/\partial P} \approx 4V^2_{0,T_r}\left(\frac{1}{Mc^2}+\frac{T\alpha^2}{C_P}\right)^2 s^2_{V_{0,T_r}} + \left(\frac{2V^2_{0,T_r}}{Mc^3}\right)^2 s^2_c + \left(\frac{2V^2_{0,T_r}T\alpha}{C_P}\right)^2 s^2_\alpha \qquad (28)$$

Inserting typical values[3] into this expression one obtains 3.9 percent as an estimate of the relative error in modeled $\partial V/\partial P$, which is essentially identical to the 4.1 percent reported in table 6. The majority of error arises from the second term in the expression, which is related to uncertainty in the modeled sound speed, and accounts for about 70 percent of the total propagated uncertainty in $\partial V/\partial P$.

[3]For example, $M \approx 60\,\frac{g}{mol}$, $c \approx 2.8\times10^5\,\frac{cm}{s}$ (table 6), $V\big\vert_{T,P_r} \approx 25\,\frac{cm^3}{mol}$ (table 1), $\alpha \approx 5\times10^{-5}K^{-1}$, $C_P \approx 100\,\frac{J}{mol-K}$, $T = 1673K$, $s_{V_{0,T_r}} = 0.24\,\frac{cm^3}{mol}$ (table 2), $s_c \approx 4700\,\frac{cm}{s}$ (table 6), $s_\alpha \approx 1\times10^{-5}K^{-1}$.

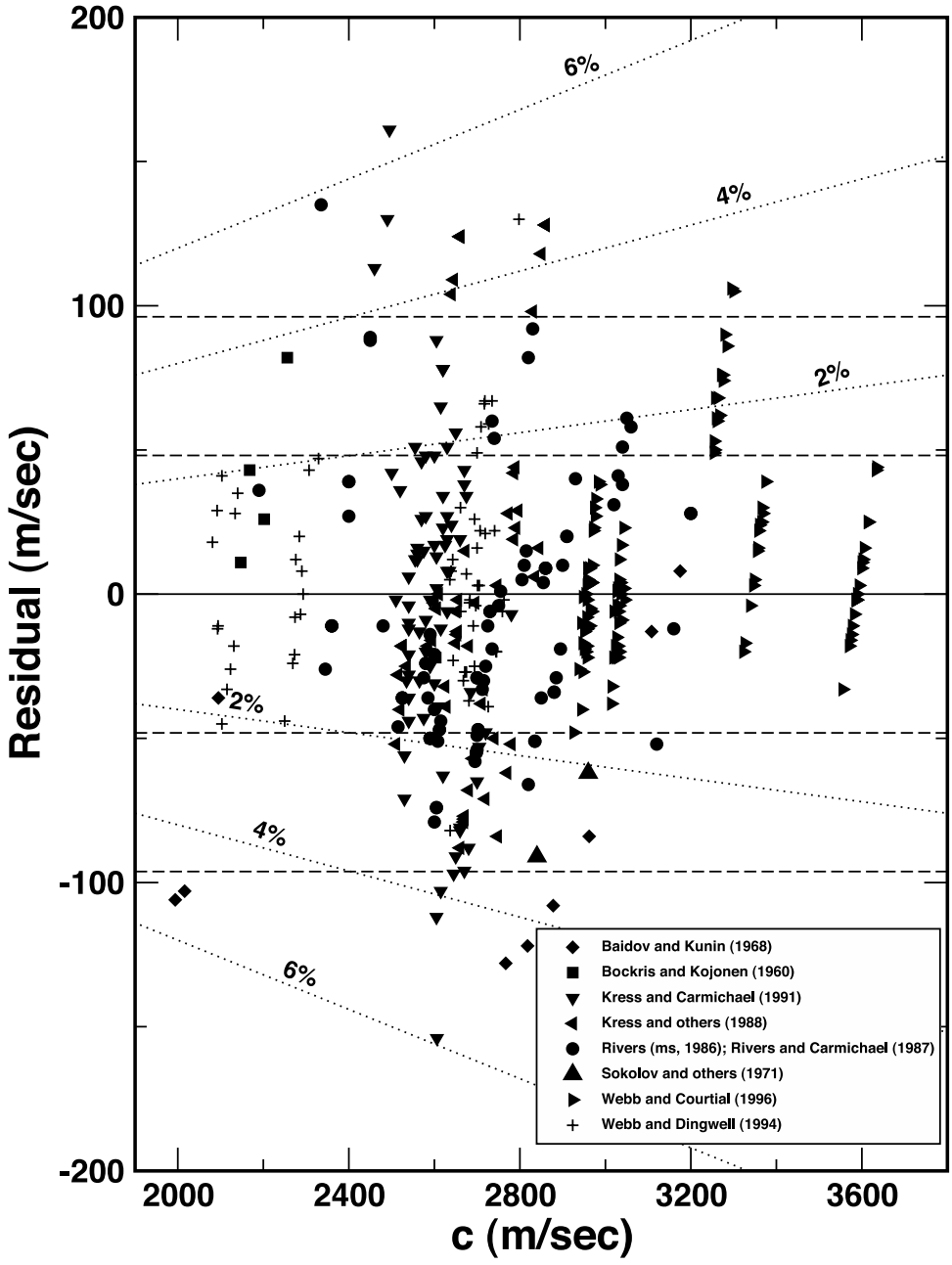

Fig. 3. Residuals of the sound speed regression (eq 19) plotted against the measured sound speed. The dotted lines give contours in relative error (% residual/average); the dashed lines correspond to ±1, ±2 root mean square deviation. The solid line is a reference for zero residuals.

TABLE 8

Model values of c (m/sec) as a function of temperature

	1000 °C	1100 °C	1200 °C	1300 °C	1400 °C	1500 °C	1600 °C	1700 °C	1800 °C	1900 °C	2000 °C
SiO_2	2162	2202	2242	2282	2322	2362	2402	2442	2481	2521	2561
TiO_2	1369	1450	1531	1612	1694	1775	1856	1937	2018	2100	2181
Al_2O_3	2537	2587	2638	2688	2738	2789	2839	2890	2940	2990	3041
Fe_2O_3	1210	1249	1287	1326	1365	1403	1442	1480	1519	1558	1596
$FeO_{1.3}$	1914	1925	1935	1946	1956	1966	1977	1987	1998	2008	2018
FeO	2442	2432	2421	2410	2400	2389	2378	2367	2357	2346	2335
MnO	2442	2432	2421	2410	2400	2389	2378	2367	2357	2346	2335
MgO	3240	3267	3295	3322	3350	3378	3405	3433	3460	3488	3515
CaO	4050	4029	4008	3988	3967	3947	3926	3906	3885	3865	3844
Na_2O	3948	3731	3514	3297	3081	2864	2647	2430	2214	1997	1780
K_2O	2620	2386	2151	1917	1682	1448	1214	979.1	744.7	510.3	275.9

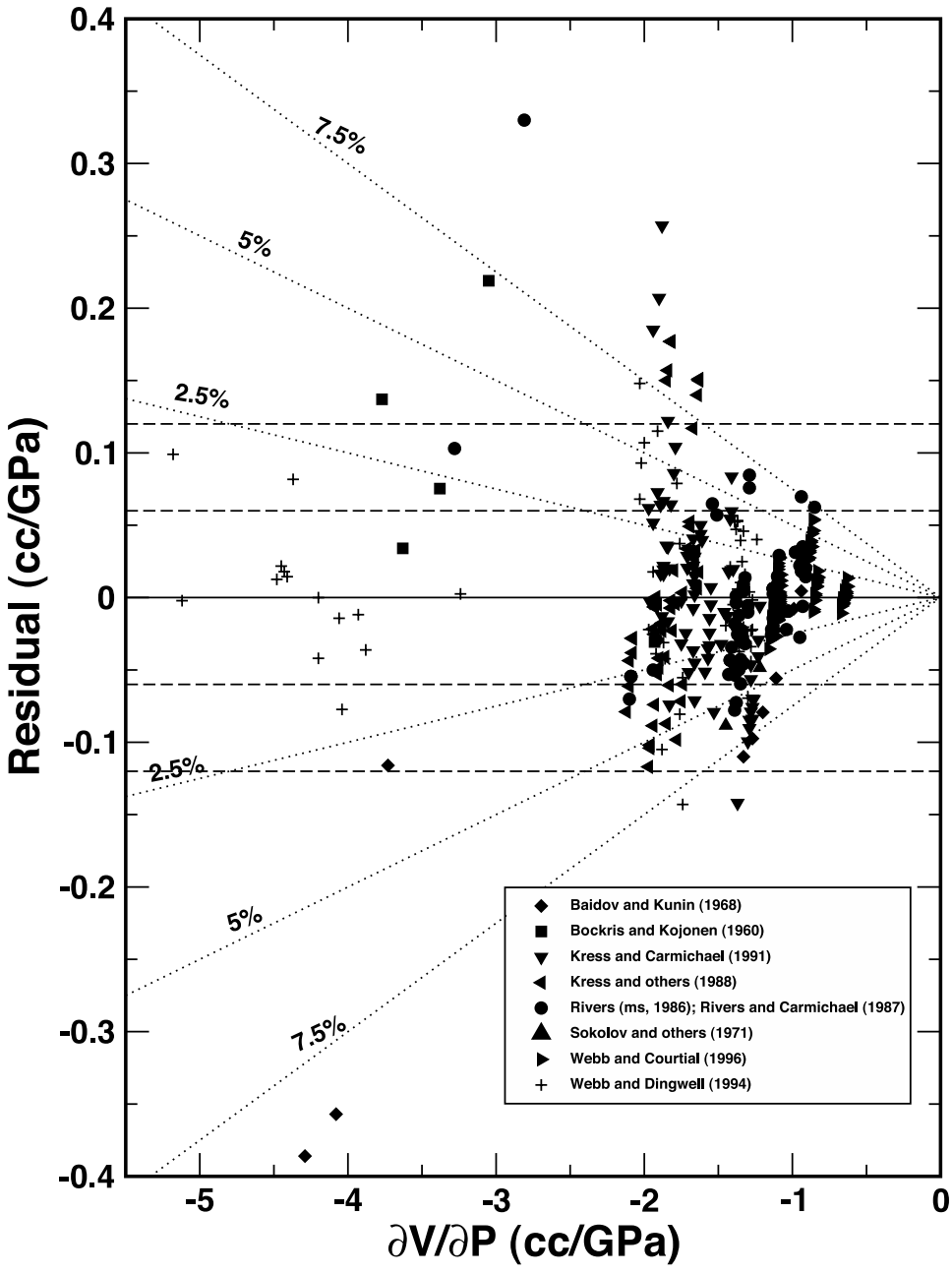

Fig. 4. Residuals of modeled values of $\partial V/\partial P$ calculated from the sound speed regression (eqs 19 and 5) plotted against values of $\partial V/\partial P$ calculated from the measured sound speed. The dotted lines give contours in relative error (% residual/average); the dashed lines correspond to ± 1, ± 2 root mean square deviation. The solid line is a reference for zero residuals.

Before examining some of the features of the sound speed-$\partial V/\partial P$ model it is instructive to access the usefulness of a more direct model equation for $\partial V/\partial P$ of the form

$$\left.\frac{\partial V}{\partial P}\right|_{T,P_r} = \sum_i n_i \left[\left.\frac{\partial \bar{v}_i}{\partial P}\right|_{1673K} + \frac{\partial^2 \bar{v}_i}{\partial T \partial P}(T-1673)\right] + (\sum_i n_i)\left(X_{Na_2O}X_{Al_2O_3}\frac{\partial \bar{v}_{Na-Al}}{\partial P} + X_{Na_2O}X_{TiO_2}\frac{\partial \bar{v}_{Na-Ti}}{\partial P} + X_{K_2O}X_{TiO_2}\frac{\partial \bar{v}_{K-Ti}}{\partial P}\right) \quad (29)$$

which is easier to manipulate and has been used previously (Kress and Carmichael, 1991; minus the alkali metal oxide-titania interaction terms). Values for model coefficients in equation (21) are obtained by regression of $\partial V/\partial P$ calculated from the sound speed dataset. In performing this analysis it is found that the uncertainty in derived values for the $\frac{\partial^2 \bar{v}_i}{\partial T \partial P}$ coefficients is so large that it makes little sense to treat them as independent parameters of the model. This problem is addressed by fixing the values of these coefficients according to equation (10), which accounts for 80 percent of the temperature variation of $\partial V/\partial P$ as discussed above, and which renders these parameters as functions of the other $\left(\left.\frac{\partial \bar{v}_i}{\partial P}\right|_{1673K}\right)$ more statistically significant terms. The result of this regression is a model equation for $\partial V/\partial P$ of poorer quality than the sound speed based model. Residuals for the two models are compared in figure 5. Statistics summarizing the quality of fit are reported in table 6. The relative error for the entire dataset (5.1%) is 25 percent higher for the direct $\partial V/\partial P$ model over that of the sound speed model. Note that the data subsets of Webb and Courtial (1996) and Baidov and Kunin (1968) are very poorly reproduced by the direct $\partial V/\partial P$ model, suggesting that the functional form of equation (29) is lacking some essential features that are necessary to accommodate these data sets. The deficiency is probably related to the fact that while $\partial V/\partial P$ is a simple function of composition in equation (29), the sound speed model implies a high degree of nonlinearity. This nonlinear behavior results from the combination of a series of essentially linear models for sound speed, heat capacity, volume, *et cetera*, via equation (5) to generate a predictive expression for $\partial V/\partial P$. Our analysis demonstrating that equation (29) cannot reproduce the experimental database with a precision comparable to the sound speed model suggests that by focusing on the latter, some important features of the compositional variation of $\partial V/\partial P$ in silicate melts have been captured indirectly. To explore this issue further, the compositional variation of $\partial V/\partial P$ will be investigated in a few well-characterized simple systems.

In figures 6A and 6B are plotted model values of $\partial V/\partial P$ and experimental data for liquids in the systems Na_2O-SiO_2 and CaO-SiO_2, respectively. Note that in both of these systems, the variation in sound speed, volume, thermal expansion and heat capacity is linear. The non-linear behavior in $\partial V/\partial P$ arises solely from the combination of these linear models (eq 5). Agreement between model and experimental values is good in both of these systems, but unfortunately, the experimental data sets are not extensive enough to evaluate the compositional effects. In figures 7A and 7B variation of $\partial V/\partial P$ in the systems Na_2O-Al_2O_3-SiO_2 and CaO-Al_2O_3-SiO_2, respectively, at 1400°C is examined. In figure 7A, the Na_2O-Al_2O_3 interaction term in the sound speed model (eq 28) makes the contours of $\partial V/\partial P$ more parallel to the Na_2O-SiO_2 join but does not substantially alter the geometry of the surface in the vicinity of the experimental data. What the Na_2O-Al_2O_3 interaction term does do is augment the already existing nonlinearity and lower the value of $\partial V/\partial P$ to bring the model into better agreement. In

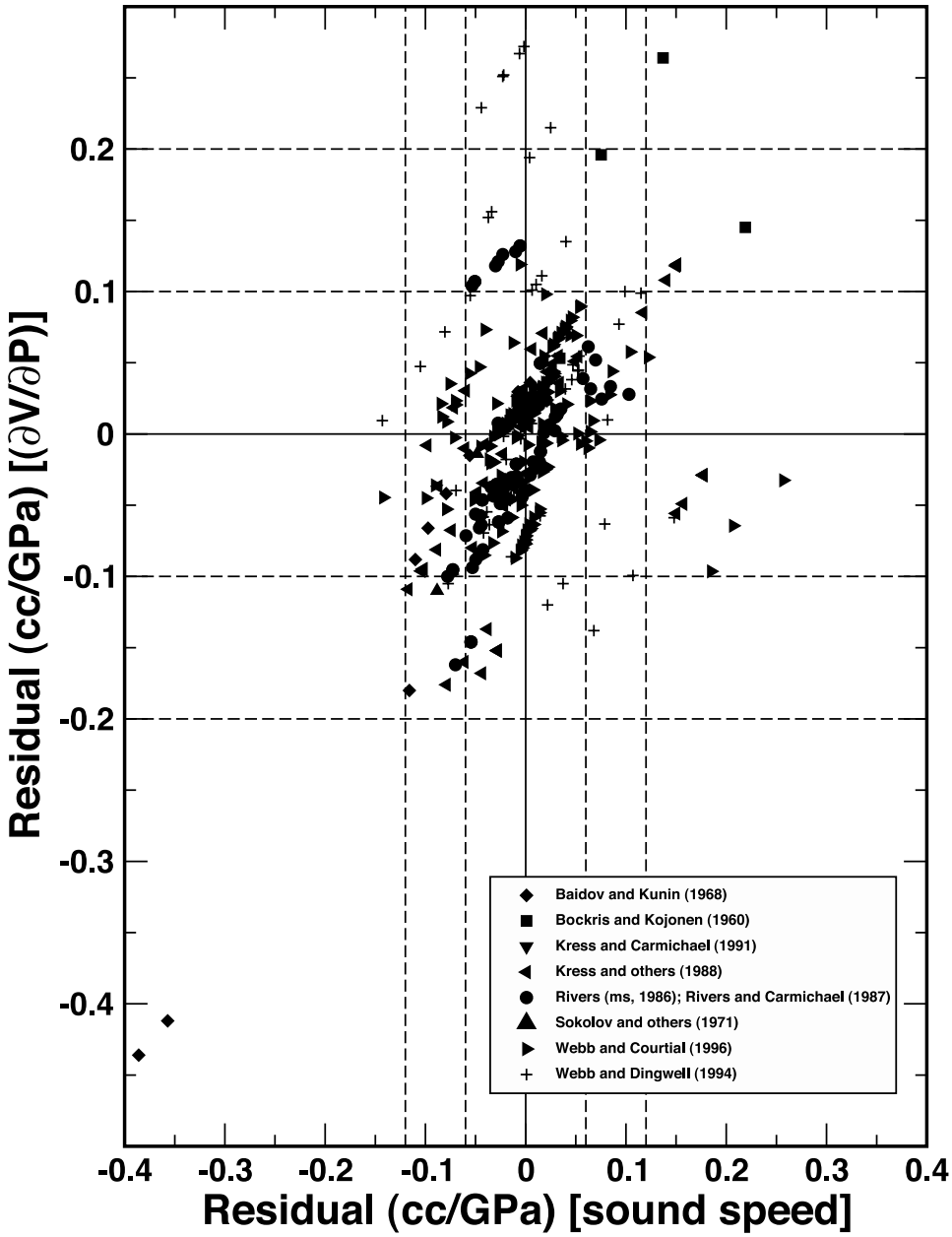

Fig. 5. Residuals of modeled values of $\partial V/\partial P$ calculated from a direct regression of $\partial V/\partial P$ (eq 21) plotted against residuals of modeled values of $\partial V/\partial P$ calculated from the sound speed regression (eqs 19 and 5). The dashed lines correspond to ± 1, ± 2 root mean square deviation. The solid lines are a reference for zero residuals.

the CaO-Al_2O_3-SiO_2 system, the nonlinearity is far less pronounced but clearly evident from the contour spacing on either the CaO-SiO_2 or CaO-Al_2O_3 join. The distribution of data points in this system is consistent with a wider spacing of $\partial V/\partial P$ contours at the

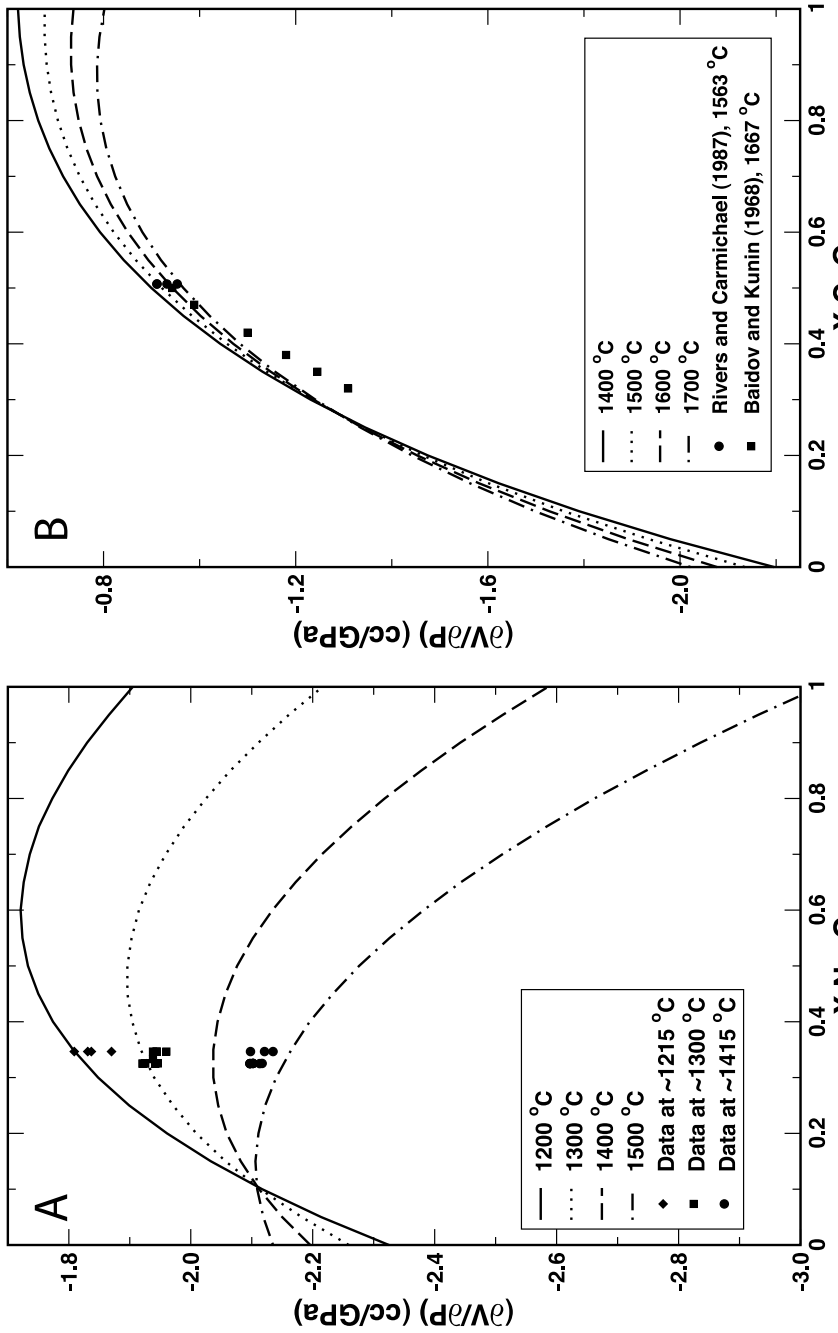

Fig. 6. Calculated variation in $\partial V/\partial P$ as a function of temperature in the systems (A) Na_2O-SiO_2 and (B) CaO-SiO_2, respectively. Data plotted in (A) are from Kress and others (1988).

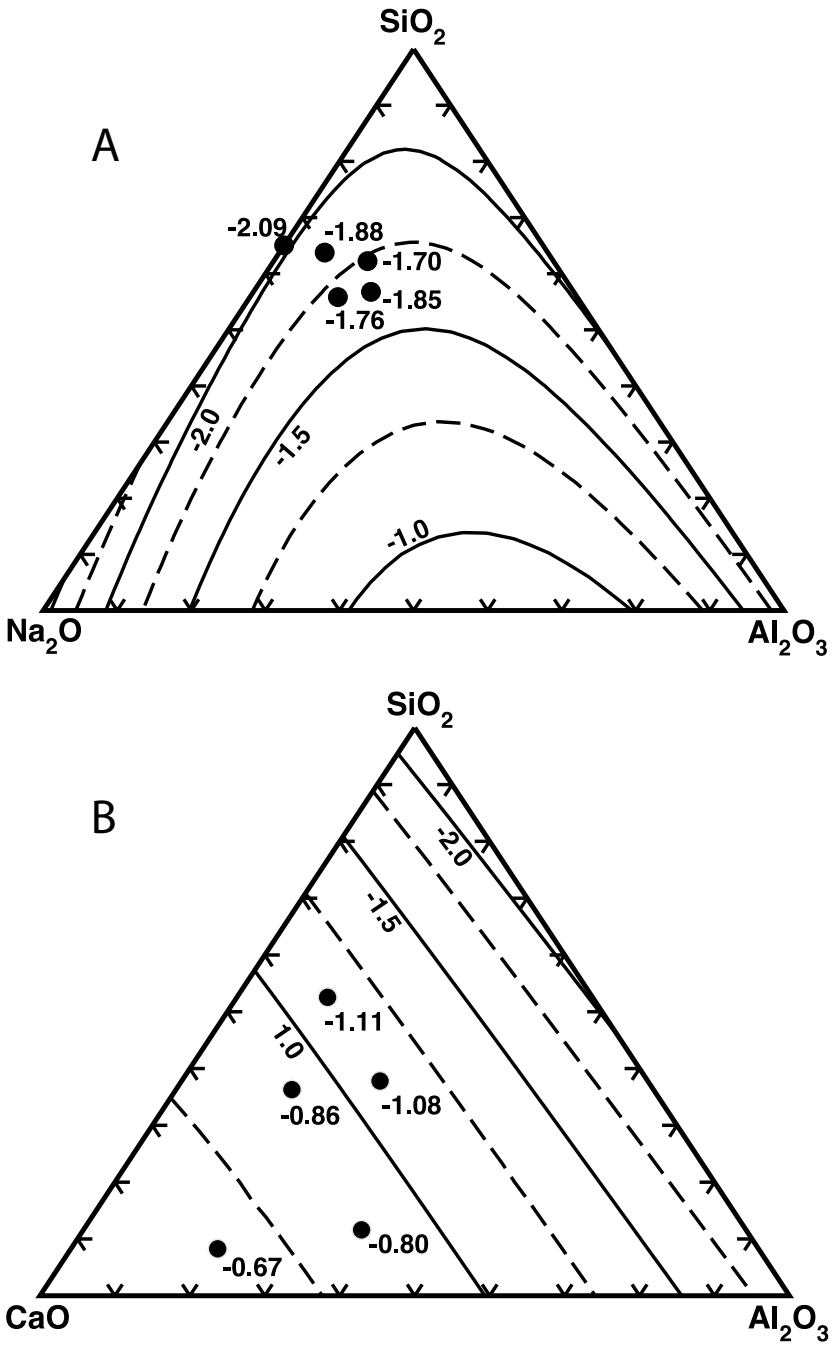

Fig. 7. Calculated variation in $\partial V/\partial P$ at 1400°C in the systems (A) Na_2O-Al_2O_3-SiO_2 and (B) CaO-Al_2O_3-SiO_2, respectively. Contour values are in units of cc/GPa. Compositions are plotted in mole percent. Data plotted in (A) are from Kress and others (1988). Data plotted in (B) are from Webb and Courtial (1996).

high CaO apex. This distribution is probably the reason for the dramatic failure of the linear $\partial V/\partial P$ calibration for this data subset.

AN EXAMPLE CALCULATION

The reference pressure models for silicate liquid volume and sound speed (compressibility) developed in this paper must be carefully applied, especially to Fe-bearing systems. For this reason, an example calculation is particularly useful. In this last section, the volume, density, thermal expansion, sound speed, compressibility and bulk modulus will be estimated from the models calibrated here for a natural liquid with the composition of a mid-ocean ridge basalt. This example is developed in table 9.

In columns A-G and rows 1-14 of table 9 are summarized parameter values for the models derived in this paper and molecular weight and heat capacity coefficients (Lange and Navrotsky, 1992) required to estimate compressibility from the sound speed.

A mid-ocean ridge basalt (MORB) bulk composition is given in column B, rows 18-28 (hereafter B18:28). Before this composition can be processed, temperature must be specified along with the oxygen fugacity of the liquid. For this example a temperature of 1200° C and oxygen fugacity corresponding to the QFM buffer at the same temperature (E17) is chosen. The following procedure is then followed:

- Grams of oxides are converted to moles (B18:27 → C18:27) by dividing the former with the molecular weights (F2:11).
- The moles of oxides, which include iron in oxidized and reduced form, must now be converted to a combination of moles of oxides and moles of Fe-species: FeO, $FeO_{1.3}$, $FeO_{1.5}$. Note that the moles of $FeO_{1.5}$ is twice the moles of the equivalent species Fe_2O_3 ($2m^{melt}_{Fe_2O_3} = m^{melt}_{FeO_{1.5}}$).
  - Equations (21) and (23) are restated in terms of moles of species and solved iteratively along with a mass balance expression:

$$\frac{m^{melt}_{FeO_{1.5}} + 2y m^{melt}_{FeO_{1+y}}}{m^{melt}_{FeO} + (1-2y) m^{melt}_{FeO_{1+y}}} = \frac{K_{D1} f_{O_2}^{1/4} + 2y K_2 K_{D1}^{2y} f_{O_2}^{y/2}}{1 + (1-2y) K_2 K_{D1}^{2y} f_{O_2}^{y/2}} \tag{30}$$

$$\frac{m^{melt}_{FeO_{1+y}}}{(m^{melt}_{FeO})^{1-2y} (m^{melt}_{FeO_{1.5}})^{2y}} = K_2 \tag{31}$$

$$m^{melt}_{FeO} + m^{melt}_{FeO_{1.3}} + m^{melt}_{FeO_{1.5}} = m^{bulk}_{FeO} + 2m^{bulk}_{Fe_2O_3} \tag{32}$$

The solution to this system of three equations and three unknowns is possible because the right-hand-sides of equations (30)-(32) are known from the constants reported in table 1 (column 3) and the bulk composition of the MORB. The bulk composition enters in the value of K_{D1} (eq 22). It is especially important to understand that the summation over components in equation (22), namely the $\sum_i \Delta W_i X_i$ term, requires the mole fractions to be expressed in terms of oxide components with the bulk iron converted entirely to FeO. This procedure is done so that K_{D1} is a constant for a given bulk composition and does not itself depend on speciation of iron. For all oxide components where a ΔW_i is not reported in table 1, assume a value of zero.

- Calculated moles of oxides and Fe-bearing melt species are reported in E18:28 of table 9. For illustrative purposes, these numbers are converted back to grams and reported in D18:28. This step is not necessary for model calculations.
- Mole fractions are calculated from the mole numbers in E18:28 and are listed in F18:27.

TABLE 9

Example calculations

	A	B	C	D	E	F	G
1		V_{1673K} (cc/mol)	$\frac{\partial V}{\partial T}$ (cc/K-mol)	c_{1673K} (m/sec)	$\frac{dc}{dT}$ (m/sec-K)	gfw (gm/mol)	C_P (J/K-mol)
2	**SiO_2**	26.7099	1.00687×10^{-3}	2321.75	0.399342	60.0848	82.6
3	**TiO_2**	23.4478	6.80672×10^{-3}	1693.60	0.811989	79.8988	109.2
4	**Al_2O_3**	37.6165	-6.48602×10^{-4}	2738.35	0.503939	101.9612	170.3
5	**Fe_2O_3**	42.6769	5.53581×10^{-3}	1364.53	0.386082	159.6922	240.9
6	**$FeO_{1.3}$**	16.1393	3.81990×10^{-3}	1955.96	0.104174	76.6462	103.8
7	**FeO**	13.8952	1.53203×10^{-3}	2399.53	-0.107256	71.8464	78.8
8	**MgO**	12.0151	2.88655×10^{-3}	3349.96	0.275638	40.3114	94.2
9	**CaO**	16.6709	3.14295×10^{-3}	3967.42	-0.205261	56.0794	89.8
10	**Na_2O**	29.1169	6.07700×10^{-3}	3080.69	-2.167567	61.9790	97.6
11	**K_2O**	46.4014	1.04319×10^{-2}	1682.35	-2.344056	94.2034	98.5
12	**Na_2O-TiO_2**	20.4756	9.69858×10^{-3}	-1325.21			
13	**K_2O-TiO_2**	27.3874	4.23954×10^{-3}	-994.34			
14	**Na_2O-Al_2O_3**			5800.72			
15							

16		**MORB**		**T = 1200 °C** $\log f_{O_2}$ **= –8.3 (QFM)**		
17		**gm**	**mol**	**gm**	**mol**	**mol fraction**
18	**SiO_2**	48.60	0.808857	48.60	0.808857	0.506663
19	**TiO_2**	1.01	0.012641	1.01	0.012641	0.007918
20	**Al_2O_3**	17.64	0.173007	17.64	0.173007	0.108370
21	**Fe_2O_3**	0.89	0.005573	0.91	0.005677	0.003556
22	**$FeO_{1.3}$**			0.81	0.010615	0.006649
23	**FeO**	7.59	0.105642	6.81	0.094819	0.059394
24	**MgO**	9.10	0.225743	9.10	0.225743	0.141404
25	**CaO**	12.45	0.222007	12.45	0.222007	0.139064
26	**Na_2O**	2.65	0.042756	2.65	0.042756	0.026782
27	**K_2O**	0.03	0.000318	0.03	0.000318	0.000199
28	***Total***	99.96	1.59654	100.01	1.59644	
29						

30		**Extensive**		**Intensive**		**Extensive**	
31		V_{1673K} (cc)	$\frac{\partial V}{\partial T}$ (cc/K)	c_{1673K} (m/sec)	$\frac{dc}{dT}$ (m/sec-K)	gfw (gm)	C_P (J/K)
32	**SiO_2**	21.6045	8.1441×10^{-4}	1176.34	0.202332	48.60	66.81
33	**TiO_2**	0.2964	8.6044×10^{-5}	13.41	0.006430	1.01	1.38
34	**Al_2O_3**	6.5079	-1.1221×10^{-4}	296.76	0.054612	17.64	29.46
35	**Fe_2O_3**	0.2423	3.1429×10^{-5}	4.85	0.001373	0.91	1.37
36	**$FeO_{1.3}$**	0.1713	4.0549×10^{-5}	13.01	0.000693	0.81	1.10
37	**FeO**	1.3175	1.4526×10^{-4}	142.52	-0.006370	6.81	7.47
38	**MgO**	2.7123	6.5162×10^{-4}	473.70	0.038976	9.10	21.26
39	**CaO**	3.7011	6.9776×10^{-4}	551.72	-0.028544	12.45	19.94
40	**Na_2O**	1.2449	2.5983×10^{-4}	82.51	-0.058053	2.65	4.17
41	**K_2O**	0.0148	3.3221×10^{-6}	0.34	-0.000468	0.03	0.03
42	**Na_2O-TiO_2**	0.0069	3.2835×10^{-6}	-0.28			
43	**K_2O-TiO_2**	0.0001	1.0691×10^{-8}	0.00			
44	**Na_2O-Al_2O_3**			16.84			
45	***Total***	37.8200	2.6213×10^{-3}	2771.70	0.210981	100.01	153.00
46	**Total (without Ti-terms)**	37.8130	2.6180×10^{-3}	2771.99			
47							

48	**1200 °C 10^5 Pa**	**Model**	**Model (without Ti-terms)**	**1200 °C 10^5 Pa**	**Model**	**Model (without Ti-terms)**
49	**α (K^{-1})**	6.931×10^{-5}	6.924×10^{-5}	**c (m/sec)**	2729.51	2729.79
50				$\frac{\partial V}{\partial P}$ **(cc/Pa^{-1})**	-1.932×10^{-9}	-1.930×10^{-9}
	V (cc)	37.299	37.293	**β (Pa^{-1})**	5.18×10^{-10}	5.18×10^{-10}
51	**ρ (gm/cc)**	2.68	2.68	***K* (GPa)**	19.3	19.3
52						

- Mole numbers (C18:27) are multiplied by parameter coefficients for reference volume (B2:11), and its temperature derivative (C2:11) to obtain the numbers in B32:41 and C32:41 respectively.
- The cross-composition terms in B42:43 and C42:43 are obtained by multiplying moles of the appropriate two oxides times the parameters reported in B12:13 and C12:13, and then *dividing each result by the total number of moles* (E28).
- Mole fractions (F18:27) are multiplied by parameter coefficients for reference sound speed (D2:11), and its temperature derivative (E2:11) to obtain the numbers in D32:41 and E32:41 respectively.
- The cross-composition terms in D42:44 are obtained by multiplying mole fractions of the appropriate two oxides times the parameters reported in D12:14.
- The gram-formula weight contributions (F32:41) and heat capacity contributions (G32:41) are obtained by multiplying mole numbers (E18:27) by parameter coefficients in F2:11 and G2:11.
- Rows 32 through 44 of table 9 are totaled in columns B through G of row 45. The quantity reported in B45 is the volume of 1.59644 moles (E28) of MORB composition liquid at 1400°C. C45 reports $\frac{\partial V}{\partial T}$ under the same conditions. F45 and G45 report the molecular weight and heat capacity, again for 1.59644 moles of material. These are extensive (mass dependent) thermodynamic quantities. They may be converted to molar or specific quantities by dividing by total moles (1.59644, E28) or total mass (100.01, D28).
- In row 46 of table 9, totals are accumulated neglecting the alkali-metal oxide-titania cross terms. These terms are neglected to illustrate that for natural composition liquids like MORB, such interactions have little consequence on derived model results, and can be readily neglected.
- The thermal coefficient of expansion (B49, C49) is calculated by dividing $\frac{\partial V}{\partial T}$ by the reference temperature volume (B45, B46).
- The volume at 1200°C (B50, C50) is calculated from equation (2). Remember that this quantity is extensive.
- The density (B51, C51) is calculated by dividing the volume into the gram-formula-weight (F45).
- The sound speed (F49, G49) is obtained from the relation $c = c_{1673K} + \frac{dc}{dT}(T - 1673K)$ using values of c_{1673K} and $\frac{dc}{dT}$ from D45:46 and E45. The sound speed is intensive. It only depends on the bulk composition of the liquid, not on the amount of that liquid.
- The quantities $\frac{\partial V}{\partial P}$ (F50, G50) are calculated from the sound speeds using equation (5). Care must be taken to make sure the units cancel. If the temperature is in Kelvins, α in K^{-1} (B49, C49), V_{0,T_r} in *cc* (B50, C50), M in *gm* (F45), c in *m/sec*, and C_P in *J/K*, then equation (5) should be written as

$$\left.\frac{\partial V}{\partial P}\right|_{T,P_r} = -V_{0,T_r}^2\left(\frac{100}{Mc^2} + \frac{T\alpha^2}{10C_P}\right)\left[e^{\alpha(T-T_r)}\right]^2 \times 10^{-9}$$

in order to return a result in *cc/Pa*.

- Compressibility (F51, G51) is calculated from $\frac{\partial V}{\partial T}$ by dividing by the volume and negating the result.
- The bulk modulus (F52, G52) is taken as the inverse of the compressibility, converted to GPa.

An Excel spreadsheet that implements the entire calculation reported in table 9 is available from the authors' website[4].

CONCLUSION

Available data on density determinations of melts and of supercooled silicate liquids at the glass transition temperature, in conjunction with measurements of relaxed sound speeds, provides a means of calibrating equation of state model parameters applicable at 10^5 Pa. The resulting calibration will form a base for extending the EOS to elevated pressures. This extension is the subject of the next two contributions to this series of papers.

ACKNOWLEDGMENTS

Material support for this investigation was generously provided by the National Science Foundation (OCE-9977416 and EAR-9980518) and The University of Chicago.

APPENDIX

Tables A1 and A2 summarize experimental results and model residuals for the data sets utilized in calibration of the volume and sound speed models.

Temperature derivatives of $V_{1,T}$

In order to utilize the calibration of $V_{1,T}$ in thermodynamic calculations involving the EOS developed in Part I, higher order temperature derivatives of equation (5)

$$\left.\frac{\partial V}{\partial P}\right|_{T,P_r} = V_{1,T} = -V_{0,T}^2\left(\frac{1}{Mc^2} + \frac{T\alpha^2}{C_P}\right) \tag{A-1}$$

are required. The first is provided in the text (eq 6) and is reproduced here in slightly different notation for completeness:

$$\frac{\partial V_{1,T}}{\partial T} = 2\alpha V_{1,T} + \frac{2V_{0,T}^2}{Mc^3}\frac{\partial c}{\partial T} - \frac{V_{0,T}^2\alpha^2}{C_P} \tag{A-2}$$

The second derivative is given by

$$\frac{\partial^2 V_{1,T}}{\partial T^2} = 2\alpha\frac{\partial V_{1,T}}{\partial T} + \frac{4\alpha V_{0,T}^2}{Mc^3}\frac{\partial c}{\partial T} - \frac{6V_{0,T}^2}{Mc^4}\left(\frac{\partial c}{\partial T}\right)^2 - \frac{2V_{0,T}^2\alpha^3}{C_P} \tag{A-3}$$

and the third derivative is given by

$$\frac{\partial^3 V_{1,T}}{\partial T^3} = 2\alpha\frac{\partial^2 V_{1,T}}{\partial T^2} + \frac{8\alpha^2 V_{0,T}^2}{Mc^3}\frac{\partial c}{\partial T} - \frac{24\alpha V_{0,T}^2}{Mc^4}\left(\frac{\partial c}{\partial T}\right)^2 + \frac{24V_{0,T}^2}{Mc^5}\left(\frac{\partial c}{\partial T}\right)^3 - \frac{4V_{0,T}^2\alpha^4}{C_P} \tag{A-4}$$

In all four expressions advantage has been taken of the fact that the model sound speed is a linear function of temperature and that both α and C_P are temperature independent quantities in the model.

[4]http://melts.uchicago.edu/EOS/

TABLE A1

Sources of volume data

System	Exp	T (°C)	X SiO_2	V (cc)	Residual	t-value
Bockris and others (1955)						
K_2O-SiO_2	SiO_2 55%	1400	0.550	35.69	-0.12	-0.5
	SiO_2 60%	1400	0.600	34.51	0.08	0.3
	SiO_2 65%	1400	0.650	33.50	0.10	0.5
	SiO_2 70%	1400	0.700	32.60	0.02	0.1
	SiO_2 75%	1400	0.750	31.66	-0.03	-0.1
	SiO_2 80%	1400	0.800	30.63	0.02	0.1
	SiO_2 85%	1400	0.850	29.61	0.05	0.2
	SiO_2 90%	1400	0.900	28.64	0.04	0.2
Na_2O-SiO_2	SiO_2 40%	1400	0.400	28.30	-0.15	-0.7
	SiO_2 42.5%	1400	0.425	28.09	0.00	0.0
	SiO_2 45%	1400	0.450	28.07	-0.04	-0.2
		1400	0.450	28.03	0.00	0.0
		1400	0.450	28.05	-0.02	-0.1
	SiO_2 47.5%	1400	0.475	27.87	0.10	0.5
		1400	0.475	27.95	0.02	0.1
	SiO_2 50%	1400	0.500	27.84	0.07	0.3
	SiO_2 51.3%	1400	0.513	27.82	0.06	0.3
	SiO_2 52.4%	1400	0.524	27.79	0.07	0.3
	SiO_2 52.5%	1400	0.525	27.71	0.14	0.6
		1400	0.525	27.77	0.08	0.4
	SiO_2 53.8%	1400	0.538	27.72	0.10	0.5
	SiO_2 55%	1400	0.550	27.76	0.03	0.1
		1400	0.550	27.74	0.05	0.2
	SiO_2 60%	1400	0.600	27.64	0.03	0.1
	SiO_2 65%	1400	0.650	27.58	-0.03	-0.1
		1400	0.650	27.58	-0.03	-0.1
		1400	0.650	27.58	-0.03	-0.1
	SiO_2 70%	1400	0.700	27.29	0.14	0.6
	SiO_2 75.4%	1400	0.754	27.29	0.01	0.1
	SiO_2 80%	1400	0.800	27.20	-0.01	0.0
	SiO_2 85%	1400	0.850	27.17	-0.10	-0.4
	SiO_2 89%	1400	0.890	27.20	-0.23	-1.0
Courtial and Dingwell (1995)						
CaO-Al_2O_3-SiO_2	Ca 62.00	1500	0.616	23.15	0.01	0.0
		1600	0.616	23.32	0.02	0.1
		1700	0.616	23.49	0.04	0.2
		1800	0.616	23.58	0.13	0.6
	Ca 50.00	1575	0.496	22.15	-0.03	-0.1
		1600	0.496	22.23	-0.06	-0.3
		1650	0.496	22.29	-0.02	-0.1
		1700	0.496	22.45	-0.06	-0.3
		1800	0.496	22.58	0.01	0.0
	Ca 65.09	1292	0.648	24.83	0.03	0.1
		1378	0.648	24.93	0.06	0.3
		1484	0.648	25.08	0.06	0.3

TABLE A1
(continued)

System	Exp	T (°C)	X SiO_2	V (cc)	Residual	t-value
		1561	0.648	25.17	0.08	0.4
		1600	0.648	25.26	0.04	0.2
		1700	0.648	25.39	0.06	0.3
		1800	0.648	25.43	0.16	0.7
	Ca 44.12	1300	0.435	23.38	0.09	0.4
		1400	0.435	23.79	-0.15	-0.7
		1441	0.435	23.72	-0.01	-0.1
		1500	0.435	23.85	-0.04	-0.2
		1512	0.435	23.83	0.00	0.0
		1600	0.435	24.21	-0.22	-1.0
		1700	0.435	24.29	-0.12	-0.6
		1800	0.435	24.53	-0.18	-0.8
	Ca 36.16	1520	0.363	23.89	-0.12	-0.5
		1600	0.363	24.18	-0.27	-1.2
		1700	0.363	24.14	-0.05	-0.2
		1800	0.363	24.35	-0.08	-0.3
	Ca 50.25	1600	0.496	26.90	0.14	0.6
		1625	0.496	27.09	-0.02	-0.1
		1650	0.496	27.12	-0.02	-0.1
		1700	0.496	27.05	0.11	0.5
		1788	0.496	27.26	0.00	0.0
	Ca 87.13	1800	0.866	28.88	-0.40	-1.8
Courtial and Dingwell (1999)						
CaO-MgO-Al_2O_3-SiO_2	CaMg 50.00	1500	0.506	21.24	-0.25	-1.1
		1600	0.506	21.37	-0.18	-0.8
		1700	0.506	21.44	-0.05	-0.2
		1800	0.506	21.63	-0.04	-0.2
	CaMg 40.00	1550	0.396	20.53	-0.37	-1.7
		1600	0.396	20.67	-0.39	-1.7
		1700	0.396	20.78	-0.27	-1.2
	CaMg 44.13	1500	0.438	23.22	-0.36	-1.6
		1600	0.438	23.27	-0.23	-1.0
		1675	0.438	23.23	-0.07	-0.3
		1800	0.438	23.48	-0.11	-0.5
	CaMg 37.26	1650	0.380	25.61	-0.22	-1.0
		1700	0.380	25.67	-0.22	-1.0
		1750	0.380	25.71	-0.19	-0.9
		1800	0.380	25.73	-0.14	-0.6
MgO-Al_2O_3-SiO_2	Mg 60.10	1550	0.614	24.05	-0.10	-0.5
		1600	0.614	24.20	-0.19	-0.9
		1700	0.614	24.17	-0.02	-0.1
		1800	0.614	24.33	-0.04	-0.2
	Mg 38.15	1650	0.388	22.20	-0.09	-0.4
		1700	0.388	22.25	-0.06	-0.2
		1750	0.388	22.38	-0.10	-0.5

TABLE A1
(continued)

System	Exp	T (°C)	X SiO_2	V (cc)	Residual	t-value
		1800	0.388	22.45	-0.09	-0.4
	Mg 50.00	1600	0.512	20.23	-0.18	-0.8
		1650	0.512	20.29	-0.14	-0.6
		1725	0.512	20.33	-0.03	-0.1
		1800	0.512	20.38	0.07	0.3
	Mg 55.22	1575	0.558	26.05	0.07	0.3
		1650	0.558	26.07	0.13	0.6
		1700	0.558	26.09	0.16	0.7
		1750	0.558	26.09	0.21	1.0
		1800	0.558	26.12	0.24	1.1
Courtial and others (1997)						
CaO-MgO-FeO-Fe_2O_3-Al_2O_3-SiO_2	Fe-peridotite	1600	0.397	20.35	0.20	0.9
		1650	0.396	20.55	0.02	0.1
		1700	0.396	20.64	-0.03	-0.2
		1800	0.394	20.72	-0.04	-0.2
	Komatiite	1500	0.438	21.00	-0.22	-1.0
		1550	0.437	21.05	-0.24	-1.1
		1600	0.437	20.97	-0.12	-0.5
		1700	0.401	19.65	0.06	0.2
		1750	0.401	19.66	0.11	0.5
		1800	0.400	19.67	0.17	0.8
	PHN 1611	1650	0.402	19.57	0.08	0.4
		1700	0.435	21.01	-0.06	-0.3
		1750	0.435	21.02	-0.02	-0.1
		1800	0.434	21.10	-0.04	-0.2
Courtial and others (1999)						
Na_2O-CoO-SiO_2	NS2.5Co	990	0.648	25.82	0.04	0.2
		1038	0.648	25.98	0.01	0.0
		1086	0.648	26.05	0.05	0.2
		1136	0.648	26.17	0.05	0.2
		1190	0.648	26.28	0.08	0.3
		947	0.524	23.74	-0.06	-0.3
	NS2.25Co	993	0.524	23.85	-0.07	-0.3
		1087	0.524	24.07	-0.10	-0.5
		1191	0.524	24.31	-0.12	-0.6
	NS2.15Co	992	0.593	24.68	0.11	0.5
		1039	0.593	24.78	0.12	0.5
		1088	0.593	24.90	0.11	0.5
		1135	0.593	25.02	0.09	0.4
		1192	0.593	25.17	0.07	0.3
Na_2O-NiO-SiO_2	NS2.8Ni	1041	0.632	25.49	-0.11	-0.5
		1091	0.632	25.59	-0.08	-0.4
		1141	0.632	25.74	-0.11	-0.5
		1201	0.632	25.81	-0.04	-0.2
	NS2.4NI	1040	0.654	25.66	0.26	1.1

TABLE A1
(continued)

System	Exp	T (°C)	X SiO_2	V (cc)	Residual	t-value
		1091	0.654	25.75	0.30	1.3
		1140	0.654	25.87	0.30	1.3
		1200	0.654	26.03	0.29	1.3
	NS2.12Ni	1040	0.619	25.04	-0.01	0.0
		1090	0.619	25.20	-0.05	-0.2
		1141	0.619	25.38	-0.11	-0.5
		1201	0.619	25.47	-0.05	-0.2
Na_2O-SiO_2		1080	0.685	26.50	0.15	0.7
		1127	0.685	26.56	0.21	0.9
		1174	0.685	26.65	0.24	1.1
		1269	0.685	26.91	0.22	1.0
		1364	0.685	27.26	0.12	0.5
Dingwell and Brearley (1988)						
CaO-FeO-Fe_2O_3-SiO_2	1	1253	0.337	23.77	0.14	0.6
		1366	0.334	23.83	0.05	0.2
		1500	0.329	23.61	0.11	0.5
	2	1260	0.550	24.02	0.40	1.8
		1375	0.544	23.81	0.46	2.1
		1500	0.537	23.70	0.33	1.5
	3	1263	0.120	26.47	0.30	1.4
		1375	0.118	26.29	0.26	1.2
		1500	0.115	25.75	0.32	1.4
	4	1382	0.512	24.59	0.83	3.7
		1476	0.503	24.27	0.67	3.0
		1550	0.496	23.97	0.58	2.6
	5	1400	0.315	25.11	1.00	4.5
		1475	0.310	24.72	0.98	4.4
		1550	0.305	24.36	0.86	3.8
	6	1400	0.386	22.22	-0.03	-0.1
		1475	0.385	22.29	-0.03	-0.1
		1550	0.383	22.36	-0.05	-0.2
	7	1433	0.086	24.20	-1.07	-4.8
		1493	0.086	24.33	-1.18	-5.3
	8	1380	0.583	23.38	0.12	0.5
		1460	0.581	23.31	0.20	0.9
		1554	0.578	23.28	0.23	1.0
	9	1417	0.464	24.95	1.07	4.8
		1501	0.454	24.36	1.00	4.5
		1550	0.449	24.08	0.90	4.0
	10	1505	0.204	26.66	0.74	3.3
		1553	0.200	26.21	0.63	2.8
Dingwell and others (1988)						
Na_2O-FeO-Fe_2O_3-SiO_2	1	1250	0.743	28.22	-0.02	-0.1
		1349	0.738	28.18	-0.06	-0.3
		1451	0.730	28.01	-0.11	-0.5

TABLE A1
(continued)

System	Exp	T (°C)	X SiO_2	V (cc)	Residual	t-value
	2	1298	0.661	28.75	-0.03	-0.1
		1373	0.656	28.50	0.09	0.4
		1439	0.650	28.47	-0.09	-0.4
	3	1300	0.574	28.98	0.23	1.1
		1405	0.567	28.67	0.31	1.4
		1500	0.558	28.34	0.21	1.0
	4	1300	0.527	29.02	0.44	2.0
		1399	0.521	28.80	0.44	2.0
		1500	0.511	28.33	0.47	2.1
	5	1105	0.553	28.63	0.21	0.9
		1301	0.547	28.89	0.11	0.5
		1497	0.535	28.50	0.16	0.7
	6	1002	0.586	27.97	0.02	0.1
		1247	0.582	28.40	0.05	0.2
		1500	0.571	28.35	0.06	0.3
	7	1000	0.599	27.51	-0.05	-0.2
		1251	0.596	28.02	0.00	0.0
		1489	0.590	28.35	-0.09	-0.4
	8	998	0.470	28.44	-0.34	-1.5
		1249	0.467	29.06	-0.34	-1.5
		1485	0.460	29.19	-0.29	-1.3
	9	1001	0.427	29.39	-0.46	-2.1
		1252	0.423	29.76	-0.31	-1.4
		1480	0.413	29.80	-0.50	-2.2
	10	1020	0.399	29.21	0.36	1.6
		1249	0.394	29.78	0.17	0.8
		1479	0.383	29.53	0.04	0.2
	11	1309	0.326	30.76	0.07	0.3
		1403	0.321	30.43	0.10	0.5
		1482	0.315	29.85	0.23	1.0
Na_2O-SiO_2		1100	0.586	26.67	0.12	0.5
		1300	0.586	27.33	0.06	0.3
		1480	0.586	28.00	-0.05	-0.2
Dingwell (1992)						
CaO-TiO_2-SiO_2	1	1500	0.462	21.76	0.21	0.9
		1550	0.462	21.88	0.22	1.0
		1600	0.462	21.98	0.23	1.0
	2	1500	0.429	22.06	0.07	0.3
		1550	0.429	22.17	0.10	0.5
		1600	0.429	22.30	0.11	0.5
	3	1500	0.407	22.23	0.05	0.2
		1550	0.407	22.38	0.06	0.3
		1600	0.407	22.48	0.10	0.5

TABLE A1
(continued)

System	Exp	T (°C)	X SiO_2	V (cc)	Residual	t-value
	4	1400	0.373	22.23	-0.13	-0.6
		1450	0.373	22.36	-0.09	-0.4
		1500	0.373	22.44	-0.02	-0.1
		1550	0.373	22.63	-0.04	-0.2
		1600	0.373	22.74	0.02	0.1
	5	1400	0.332	22.46	-0.19	-0.8
		1450	0.332	22.54	-0.09	-0.4
		1500	0.332	22.65	-0.01	0.0
		1550	0.332	22.81	0.01	0.1
		1600	0.332	22.93	0.08	0.4
	6	1400	0.287	22.44	0.00	0.0
		1450	0.287	22.62	0.02	0.1
		1500	0.287	22.77	0.09	0.4
		1550	0.287	22.82	0.24	1.1
		1600	0.287	22.97	0.30	1.4
Na_2O-TiO_2-SiO_2	1	1000	0.473	26.99	-0.31	-1.4
		1050	0.473	27.16	-0.29	-1.3
		1150	0.473	27.52	-0.27	-1.2
	2	1000	0.441	27.02	-0.27	-1.2
		1050	0.441	27.18	-0.23	-1.0
		1100	0.441	27.34	-0.17	-0.8
		1150	0.441	27.55	-0.17	-0.8
	3	1050	0.402	26.98	0.03	0.1
		1100	0.402	27.24	0.00	0.0
		1150	0.402	27.45	0.02	0.1
	4	1000	0.370	26.81	-0.16	-0.7
		1050	0.370	27.09	-0.19	-0.8
		1100	0.370	27.31	-0.16	-0.7
		1150	0.370	27.52	-0.12	-0.5
	5	1000	0.334	26.78	-0.34	-1.5
		1050	0.334	27.11	-0.41	-1.8
		1100	0.334	27.36	-0.39	-1.8
		1150	0.334	27.67	-0.43	-1.9
Gottsmann and Dingwell (2000)						
CaO-MgO-SiO_2	Di	817	0.511	19.52	0.07	0.3
		890	0.511	19.67	0.06	0.3
		900	0.511	19.69	0.06	0.3
		913	0.511	19.72	0.05	0.2
Gottsmann and Dingwell (2002)						
CaO-MgO-Al_2O_3-SiO_2	An42Di58	804	0.502	21.96	-0.05	-0.2
		940	0.502	22.28	-0.14	-0.6
		973	0.502	22.32	-0.14	-0.6
	An98Di02	872	0.498	26.10	0.02	0.1
		897	0.498	26.14	0.01	0.0
		927	0.498	26.18	0.00	0.0

TABLE A1
(continued)

System	Exp	T (°C)	X SiO_2	V (cc)	Residual	t-value
Hara and others (1988)						
CaO-FeO-Fe_2O_3-SiO_2		1513	0.070	28.93	0.37	1.7
5.3 mol % Ca_2SiO_4						
		1518	0.070	28.85	0.37	1.6
		1545	0.069	28.47	0.31	1.4
		1578	0.068	27.98	0.27	1.2
		1613	0.067	27.44	0.22	1.0
11.1 mol % Ca_2SiO_4		1431	0.129	28.17	0.44	2.0
		1462	0.127	27.96	0.36	1.6
		1499	0.126	27.62	0.32	1.4
		1505	0.125	27.56	0.32	1.4
		1547	0.124	27.25	0.17	0.8
		1596	0.121	26.65	0.19	0.9
17.7 mol % Ca_2SiO_4	Under air	1398	0.175	26.82	0.30	1.3
		1434	0.174	26.67	0.26	1.2
		1470	0.172	26.50	0.21	0.9
		1489	0.172	26.37	0.22	1.0
		1555	0.169	25.96	0.16	0.7
		1601	0.166	25.64	0.11	0.5
	Under CO_2	1396	0.165	24.79	-0.16	-0.7
		1450	0.162	24.45	-0.20	-0.9
		1492	0.160	24.18	-0.24	-1.1
		1504	0.160	24.09	-0.23	-1.0
		1547	0.158	23.81	-0.26	-1.1
		1602	0.156	23.43	-0.25	-1.1
	Under $CO_2/H_2 = 50$	1413	0.151	22.20	-0.65	-2.9
		1465	0.148	21.93	-0.55	-2.4
		1507	0.145	21.68	-0.43	-1.9
		1510	0.142	21.45	-0.39	-1.8
		1549	0.139	21.23	-0.29	-1.3
		1597	0.136	21.03	-0.20	-0.9
Johnson (ms, 1989)						
CaO-K_2O-TiO_2-SiO_2	9	1297	0.407	28.92	-0.36	-1.6
		1300	0.407	28.88	-0.30	-1.4
		1400	0.407	29.26	-0.23	-1.0
		1400	0.407	29.20	-0.17	-0.8
		1500	0.407	29.52	-0.03	-0.1
		1502	0.407	29.56	-0.06	-0.3
	10	1400	0.413	27.49	-0.19	-0.9
		1450	0.413	27.63	-0.13	-0.6
		1500	0.413	27.77	-0.05	-0.2
CaO-K_2O-TiO_2-Al_2O_3-SiO_2	11	1350	0.444	29.86	-0.50	-2.2
		1400	0.444	29.94	-0.42	-1.9

TABLE A1
(continued)

System	Exp	T (°C)	X SiO_2	V (cc)	Residual	t-value
		1400	0.444	30.06	-0.54	-2.4
		1400	0.444	29.75	-0.24	-1.1
		1500	0.444	29.97	-0.15	-0.7
$CaO-Na_2O-TiO_2-SiO_2$	8	1200	0.464	24.96	0.14	0.6
		1300	0.464	25.26	0.21	0.9
		1500	0.464	25.80	0.44	2.0
$CaO-TiO_2-SiO_2$	1	1403	0.402	22.39	0.03	0.1
		1486	0.402	22.64	0.04	0.2
$K_2O-FeO-Fe_2O_3-TiO_2-SiO_2$	12	1100	0.460	27.82	-0.11	-0.5
		1294	0.458	28.08	0.21	0.9
		1497	0.454	28.30	0.47	2.1
$K_2O-TiO_2-SiO_2$	6	1100	0.331	33.58	-0.15	-0.7
		1300	0.331	34.47	0.23	1.0
		1500	0.331	35.34	0.67	3.0
	7	1100	0.420	33.79	-0.17	-0.8
		1300	0.420	34.73	0.05	0.2
		1500	0.420	35.70	0.28	1.3
$MgO-TiO_2-SiO_2$	2	1450	0.382	20.20	-0.07	-0.3
		1538	0.382	20.04	0.35	1.6
	3	1300	0.421	20.73	-0.08	-0.4
		1500	0.421	21.15	0.06	0.2
$Na_2O-TiO_2-SiO_2$	4	1100	0.316	27.20	-0.07	-0.3
		1100	0.316	27.24	-0.10	-0.5
		1300	0.316	28.02	0.24	1.1
		1300	0.316	28.06	0.19	0.9
		1500	0.316	28.82	0.61	2.7
	5	1105	0.613	26.71	0.00	0.0
		1300	0.613	27.29	0.05	0.2
$K_2O-Na_2O-CaO-MgO-FeO-Fe_2O_3-Al_2O_3-TiO_2-SiO_2$	13	1300	0.518	24.77	-0.05	-0.2
		1500	0.515	24.84	0.05	0.2
Knoche and others (1992a)						
$CaO-Al_2O_3-SiO_2$	Anorthite	1572	0.501	26.55	0.39	1.8
		1622	0.501	26.63	0.37	1.7
$CaO-MgO-Al_2O_3-SiO_2$	An 20 Di 80	1422	0.492	23.57	0.15	0.7
		1522	0.503	24.77	0.34	1.5
	An 50 Di 50	1422	0.501	21.72	0.11	0.5
		1522	0.492	23.68	0.20	0.9
	An 70 Di 30	1447	0.503	24.69	0.32	1.4
		1522	0.501	21.82	0.20	0.9
$CaO-MgO-SiO_2$	Diopside	1422	0.511	20.69	0.11	0.5
		1522	0.511	20.81	0.18	0.8
		1622	0.511	20.95	0.25	1.1
Knoche and others (1992b)						
$Na_2O-Al_2O_3-SiO_2$	Albite	1800	0.750	116.06	–0.25	–1.1

TABLE A1
(continued)

System	Exp	T (°C)	X SiO_2	V (cc)	Residual	t-value
Lange and Carmichael (1987)						
Lange (1997)						
$CaO-Al_2O_3-SiO_2$	3	771	0.532	22.08	-0.01	0.0
		1419	0.532	23.17	0.04	0.2
		1504	0.532	23.28	0.08	0.4
		1593	0.532	23.39	0.13	0.6
	4	797	0.367	25.22	0.02	0.1
		1454	0.367	26.07	0.04	0.2
		1555	0.367	26.23	0.01	0.0
		1623	0.367	26.34	-0.01	0.0
	6	793	0.452	22.69	-0.07	-0.3
		1372	0.452	23.67	-0.07	-0.3
		1473	0.452	23.82	-0.05	-0.2
		1574	0.452	23.98	-0.02	-0.1
	8	784	0.607	23.95	-0.10	-0.5
		1254	0.607	24.55	-0.02	-0.1
		1404	0.607	24.73	0.03	0.1
		1554	0.607	24.90	0.08	0.4
$CaO-Al_2O_3-TiO_2-SiO_2$	21	1321	0.485	23.56	0.12	0.5
		1420	0.485	23.82	0.07	0.3
		1522	0.485	24.07	0.04	0.2
$CaO-TiO_2-SiO_2$	23	1440	0.367	22.62	0.04	0.2
		1480	0.367	22.74	0.06	0.3
		1521	0.367	22.86	0.09	0.4
		1561	0.367	22.98	0.12	0.5
$K_2O-Al_2O_3-SiO_2$	18	594	0.658	30.15	0.02	0.1
		1349	0.658	32.70	0.06	0.3
		1450	0.658	32.98	0.15	0.7
		1552	0.658	33.30	0.20	0.9
$K_2O-CaO-SiO_2$	24	697	0.595	24.04	-0.19	-0.9
		1371	0.595	25.54	0.00	0.0
		1421	0.595	25.64	0.03	0.1
		1472	0.595	25.75	0.05	0.2
$K_2O-MgO-CaO-Al_2O_3-SiO_2$	17	743	0.550	23.01	-0.30	-1.3
		1379	0.550	24.03	-0.02	-0.1
		1480	0.550	24.19	0.04	0.2
		1567	0.550	24.31	0.10	0.4
$K_2O-Na_2O-CaO-MgO-FeO-Fe_2O_3-Al_2O_3-TiO_2-SiO_2$	26	1310	0.566	24.95	-0.15	-0.7
		1407	0.564	24.89	-0.04	-0.2
		1486	0.562	24.82	0.06	0.3
	27	1318	0.479	24.68	-0.28	-1.3
		1418	0.477	24.70	-0.23	-1.0
		1504	0.476	24.60	-0.08	-0.4

TABLE A1
(continued)

System	Exp	T (°C)	X SiO_2	V (cc)	Residual	t-value
	28	1389	0.490	24.48	-0.09	-0.4
		1454	0.488	24.33	0.04	0.2
		1513	0.486	24.20	0.15	0.7
K_2O-Na_2O-SiO_2	19	428	0.675	27.18	0.06	0.3
		1148	0.675	29.55	-0.05	-0.2
		1253	0.675	29.88	-0.02	-0.1
		1350	0.675	30.19	-0.02	-0.1
		1452	0.675	30.56	-0.03	-0.2
		1555	0.675	30.89	-0.01	-0.1
MgO-CaO-Al_2O_3-SiO_2	9	805	0.612	22.93	-0.28	-1.3
		1424	0.612	23.48	0.03	0.1
		1497	0.612	23.57	0.04	0.2
		1573	0.612	23.64	0.08	0.3
	10	814	0.561	22.24	-0.13	-0.6
		1422	0.561	22.83	0.16	0.7
		1504	0.561	22.91	0.19	0.8
		1582	0.561	22.98	0.24	1.1
	11	791	0.490	21.62	0.06	0.2
		1505	0.490	22.54	0.19	0.9
		1567	0.490	22.58	0.24	1.1
	12	799	0.511	23.95	0.01	0.1
		1422	0.511	24.65	0.15	0.7
		1498	0.511	24.74	0.16	0.7
		1562	0.511	24.81	0.18	0.8
	13	783	0.467	22.93	-0.04	-0.2
		1421	0.467	23.84	0.02	0.1
		1497	0.467	23.93	0.04	0.2
		1573	0.467	24.03	0.06	0.3
MgO-CaO-SiO_2	14	740	0.498	19.36	-0.12	-0.5
		1449	0.498	20.59	0.04	0.2
		1522	0.498	20.70	0.08	0.3
		1560	0.498	20.76	0.09	0.4
	15	740	0.476	19.43	-0.11	-0.5
		1432	0.476	20.66	0.06	0.3
		1507	0.476	21.32	-0.44	-2.0
		1580	0.476	20.85	0.18	0.8
	16	1432	0.561	21.23	-0.04	-0.2
		1507	0.561	21.32	0.02	0.1
		1582	0.561	21.39	0.09	0.4
Na_2O-CaO-Al_2O_3-SiO_2	2	819	0.534	26.74	-0.04	-0.2
		1522	0.534	27.52	0.05	0.2
		1578	0.534	27.62	0.03	0.1
Na_2O-FeO-Fe_2O_3-SiO_2	25	1366	0.651	29.14	-0.55	-2.5
		1416	0.647	28.89	-0.44	-1.9
		1464	0.643	28.62	-0.33	-1.5

TABLE A1
(continued)

System	Exp	T (°C)	X SiO_2	V (cc)	Residual	t-value
Na_2O-Al_2O_3-TiO_2-SiO_2	22	1319	0.630	28.40	-0.23	-1.0
		1418	0.630	28.55	-0.15	-0.7
		1520	0.630	28.70	-0.07	-0.3
Na_2O-TiO_2-SiO_2	20	1077	0.582	26.52	0.00	0.0
		1172	0.582	26.86	0.00	0.0
		1271	0.582	27.21	0.00	0.0
		1368	0.582	27.50	0.05	0.2
		1470	0.582	27.78	0.15	0.7
Liu and Lange (2001)						
K_2O-TiO_2-SiO_2	2	555	0.501	28.36	0.16	0.7
		1016	0.501	30.93	-0.28	-1.3
		1114	0.501	31.31	-0.19	-0.8
		1207	0.501	31.74	-0.16	-0.7
	3	570	0.650	28.56	0.24	1.1
		1298	0.650	31.54	0.04	0.2
		1389	0.650	31.90	0.04	0.2
		1479	0.650	32.20	0.11	0.5
	6	618	0.602	26.88	0.09	0.4
		1207	0.602	29.51	-0.32	-1.4
		1298	0.602	29.84	-0.29	-1.3
		1389	0.602	30.10	-0.19	-0.8
	7	503	0.450	29.06	0.12	0.6
		1016	0.450	32.03	-0.26	-1.2
		1114	0.450	32.40	-0.11	-0.5
		1207	0.450	32.82	-0.03	-0.1
		1298	0.450	33.20	0.09	0.4
	8	1016	0.350	34.13	-0.09	-0.4
		1114	0.350	34.52	0.13	0.6
		1207	0.350	34.92	0.33	1.5
		1298	0.350	35.36	0.47	2.1
	9	596	0.549	27.65	0.22	1.0
		1114	0.549	30.25	-0.18	-0.8
		1207	0.549	30.61	-0.13	-0.6
		1298	0.549	30.91	-0.02	-0.1
	10	587	0.449	27.35	0.25	1.1
		1161	0.449	30.67	-0.31	-1.4
		1253	0.449	31.04	-0.21	-0.9
		1343	0.449	31.37	-0.08	-0.3
Na_2O-TiO_2-SiO_2	2	577	0.505	23.91	0.50	2.2
		1019	0.505	26.18	-0.04	-0.2
		1119	0.505	26.63	-0.08	-0.4
		1214	0.505	26.94	0.00	0.0
		1305	0.505	27.24	0.08	0.4
	4	497	0.394	23.95	0.35	1.6
		963	0.394	26.37	0.05	0.2
		1064	0.394	26.79	0.11	0.5

TABLE A1
(continued)

System	Exp	T (°C)	X SiO_2	V (cc)	Residual	t-value
		1161	0.394	27.15	0.22	1.0
		1253	0.394	27.44	0.39	1.7
	6	607	0.598	24.35	-0.03	-0.1
		1253	0.598	26.93	-0.42	-1.9
		1343	0.598	27.23	-0.40	-1.8
		1434	0.598	27.43	-0.28	-1.2
		1479	0.598	27.59	-0.27	-1.2
	7	549	0.453	23.95	0.47	2.1
		967	0.453	26.30	-0.12	-0.5
		1069	0.453	26.64	-0.01	-0.1
		1167	0.453	27.02	0.04	0.2
	8	466	0.355	24.06	0.15	0.7
		967	0.355	26.91	-0.31	-1.4
		1069	0.355	27.31	-0.19	-0.9
		1167	0.355	27.68	-0.06	-0.3
		1260	0.355	28.01	0.10	0.4
	9	604	0.555	23.94	0.52	2.3
		1161	0.555	26.60	-0.11	-0.5
		1253	0.555	26.85	-0.01	-0.1
		1343	0.555	27.06	0.12	0.6
		1434	0.555	27.28	0.26	1.2
	10	607	0.452	23.71	0.29	1.3
		1214	0.452	26.65	-0.02	-0.1
		1305	0.452	27.00	0.05	0.2
		1398	0.452	27.32	0.17	0.7
		1498	0.452	27.63	0.33	1.5
Mo and others (1982)						
CaO-FeO-Fe_2O_3-SiO_2	3b	1286	0.365	24.25	-0.07	-0.3
		1321	0.364	24.23	-0.07	-0.3
		1342	0.363	24.17	-0.03	-0.1
		1374	0.362	24.15	-0.04	-0.2
		1395	0.361	24.12	-0.04	-0.2
		1430	0.360	24.01	0.02	0.1
		1449	0.359	23.95	0.05	0.2
		1485	0.357	23.96	-0.03	-0.1
		1497	0.357	23.92	-0.01	-0.1
		1506	0.356	23.92	-0.04	-0.2
		1531	0.355	23.86	-0.03	-0.2
	10	1277	0.384	23.78	-0.19	-0.9
		1305	0.383	23.80	-0.21	-0.9
		1317	0.383	23.77	-0.19	-0.9
		1324	0.383	23.80	-0.21	-1.0
		1351	0.382	23.78	-0.20	-0.9
		1380	0.381	23.78	-0.22	-1.0
		1409	0.380	23.75	-0.20	-0.9
		1435	0.379	23.73	-0.20	-0.9

TABLE A1
(continued)

System	Exp	T (°C)	X SiO_2	V (cc)	Residual	t-value
		1462	0.378	23.70	-0.19	-0.9
		1491	0.377	23.65	-0.18	-0.8
		1520	0.376	23.64	-0.21	-0.9
		1529	0.376	23.62	-0.20	-0.9
K_2O-Na_2O-CaO-MgO-FeO-Fe_2O_3- Al_2O_3-TiO_2-SiO_2	4	1308	0.556	25.20	0.01	0.0
		1323	0.555	25.22	-0.01	0.0
		1365	0.554	25.19	0.02	0.1
		1375	0.554	25.17	0.04	0.2
		1424	0.552	25.17	0.03	0.1
		1432	0.552	25.16	0.04	0.2
		1461	0.551	25.15	0.05	0.2
		1474	0.551	25.17	0.03	0.1
		1493	0.551	25.14	0.06	0.3
		1501	0.550	25.13	0.07	0.3
		1526	0.550	25.05	0.15	0.7
		1539	0.549	25.11	0.09	0.4
	5	1372	0.522	25.05	0.31	1.4
		1390	0.521	25.08	0.26	1.2
		1405	0.520	24.97	0.35	1.6
		1440	0.519	25.08	0.20	0.9
		1440	0.519	25.00	0.28	1.2
		1451	0.519	25.01	0.25	1.1
		1486	0.517	25.00	0.22	1.0
		1495	0.517	24.98	0.22	1.0
		1507	0.516	24.92	0.28	1.2
		1566	0.514	24.94	0.19	0.9
		1574	0.514	24.99	0.13	0.6
	6	1376	0.475	25.47	0.07	0.3
		1383	0.475	25.48	0.03	0.2
		1393	0.474	25.44	0.04	0.2
		1404	0.474	25.47	-0.02	-0.1
		1413	0.473	25.51	-0.09	-0.4
		1431	0.472	25.36	0.00	0.0
		1432	0.472	25.51	-0.15	-0.7
		1440	0.471	25.37	-0.03	-0.1
		1446	0.471	25.49	-0.17	-0.8
		1459	0.470	25.44	-0.16	-0.7
		1473	0.469	25.35	-0.11	-0.5
		1493	0.468	25.54	-0.36	-1.6
		1501	0.468	25.32	-0.16	-0.7
		1509	0.467	25.33	-0.19	-0.9
		1520	0.467	25.51	-0.41	-1.8
		1532	0.466	25.21	-0.13	-0.6
		1543	0.465	25.24	-0.20	-0.9

TABLE A1
(continued)

System	Exp	T (°C)	X SiO_2	V (cc)	Residual	t-value
	9	1417	0.454	22.57	0.09	0.4
		1436	0.453	22.54	0.08	0.4
		1449	0.452	22.59	0.00	0.0
		1478	0.451	22.47	0.07	0.3
		1489	0.450	22.43	0.09	0.4
		1508	0.449	22.38	0.11	0.5
		1529	0.449	22.35	0.11	0.5
		1547	0.448	22.26	0.16	0.7
		1548	0.448	22.42	0.01	0.0
		1568	0.447	22.20	0.19	0.9
Na_2O-FeO-Fe_2O_3-SiO_2	2	1354	0.660	28.73	-0.19	-0.8
		1364	0.659	28.65	-0.13	-0.6
		1391	0.657	28.60	-0.13	-0.6
		1400	0.656	28.57	-0.12	-0.5
		1442	0.653	28.43	-0.11	-0.5
		1448	0.652	28.45	-0.15	-0.7
		1459	0.651	28.45	-0.18	-0.8
		1475	0.650	28.23	-0.03	-0.1
		1490	0.648	28.29	-0.15	-0.7
		1498	0.647	28.25	-0.14	-0.6
		1517	0.645	28.15	-0.12	-0.5
		1524	0.645	28.16	-0.16	-0.7
		1551	0.642	28.06	-0.18	-0.8
		1559	0.641	28.01	-0.17	-0.8
Shiraishi and others (1978)						
FeO-Fe_2O_3-SiO_2	Fayalite	1300	0.340	18.26	-0.01	0.0
		1400	0.340	18.40	-0.01	0.0
Stein and others (1986)						
Lange (1996)						
Na_2O-Al_2O_3-SiO_2	B	560	0.749	26.86	-0.33	-1.5
		1355	0.749	28.04	-0.15	-0.7
		1432	0.749	28.10	-0.07	-0.3
		1509	0.749	28.23	-0.07	-0.3
	2	561	0.681	27.04	-0.13	-0.6
		1356	0.681	28.45	-0.10	-0.4
		1458	0.681	28.61	-0.07	-0.3
		1562	0.681	28.79	-0.05	-0.2
	8	488	0.606	25.77	0.13	0.6
		1199	0.606	27.66	0.00	0.0
		1303	0.606	27.92	0.00	0.0
		1406	0.606	28.17	0.02	0.1
	9	537	0.608	26.88	0.02	0.1
		1199	0.608	28.13	0.14	0.6
		1302	0.608	28.33	0.16	0.7
		1406	0.608	28.64	0.08	0.3

TABLE A1
(continued)

System	Exp	T (°C)	X SiO_2	V (cc)	Residual	t-value
	10	607	0.594	27.60	-0.07	-0.3
		1303	0.594	28.85	0.02	0.1
		1408	0.594	29.05	0.03	0.1
		1511	0.594	29.30	-0.02	-0.1
	12	799	0.600	28.78	-0.22	-1.0
		1509	0.600	29.70	-0.03	-0.1
		1562	0.600	29.82	-0.07	-0.3
	15	547	0.524	27.10	0.07	0.3
		1200	0.524	28.61	0.06	0.3
		1303	0.524	28.85	0.06	0.3
		1406	0.524	29.06	0.10	0.4
Na_2O-SiO_2	A	440	0.606	24.66	0.26	1.2
		1199	0.606	27.03	0.03	0.1
		1199	0.606	27.00	0.06	0.3
		1303	0.606	27.35	0.02	0.1
		1303	0.606	27.40	-0.03	-0.1
Toplis and Richet (2000)						
CaO-MgO-SiO_2	Di	687	0.503	18.91	0.26	1.2
CaO-MgO-Al_2O_3-SiO_2	Di63An37	712	0.498	21.47	0.18	0.8
CaO-Al_2O_3-SiO_2	An	838	0.511	25.86	0.61	2.7
Webb and others (1992)						
Na_2O-SiO_2	$Na_2Si_3O_7$	1500	0.75	27.46	0.08	0.4
		1450	0.75	27.39	0.04	0.2
		1400	0.75	27.29	0.02	0.1
		1350	0.75	27.18	0.02	0.1
		1300	0.75	27.11	–0.02	–0.1
		1250	0.75	26.97	0.00	0.0
		1200	0.75	26.85	0.01	0.0
		1150	0.75	26.56	0.11	0.5
		1100	0.75	25.31	0.08	0.4

TABLE A2

Sources of sound speed data

System	Exp	T (°C)	$\partial V / \partial P$ (cc/Gpa)	Residual (cc/Gpa)	% Residual	c (m/sec)	Residual (m/sec)	% Residual
Bockris and Kojonen (1960)								
Na_2O-SiO_2	BK60-14	1288	-1.93	-3.07E-02	1.59%	2603	-22	-0.86%
K_2O-SiO_2	BK60-31	1359	-3.05	2.19E-01	-7.19%	2256	82	3.65%
	BK60-34	1270	-3.38	7.53E-02	-2.22%	2202	26	1.20%
	BK60-35	1347	-3.63	3.40E-02	-0.94%	2147	11	0.51%
	BK60-40	1315	-3.77	1.37E-01	-3.63%	2168	43	1.97%
Baidov and Kunin (1968)								
CaO-SiO_2	BK68-4	1397	-3.73	-1.16E-01	3.11%	2095	-36	-1.73%
	BK68-5	1397	-4.08	-3.57E-01	8.74%	2016	-103	-5.09%
	BK68-6	1397	-4.29	-3.86E-01	9.01%	1994	-106	-5.30%
	BK68-24	1627	-1.33	-1.10E-01	8.22%	2767	-128	-4.63%
	BK68-25	1627	-1.27	-9.74E-02	7.69%	2818	-122	-4.34%
	BK68-26	1627	-1.2	-7.93E-02	6.63%	2878	-108	-3.74%
	BK68-27	1627	-1.11	-5.58E-02	5.03%	2962	-84	-2.83%
	BK68-28	1627	-0.99	-7.66E-03	0.77%	3108	-13	-0.43%
	BK68-29	1627	-0.94	4.45E-03	-0.47%	3175	8	0.26%
Kress and Carmichael (1991)								
CaO-FeO-Fe_2O_3-Al_2O_3-SiO_2	BFE0012	1260	-1.3	-9.95E-02	7.66%	2605	-112	-4.31%
	BFE0013	1260	-1.29	-9.03E-02	7.01%	2615	-103	-3.92%
	BFE0014	1260	-1.23	-2.93E-02	2.38%	2685	-34	-1.28%
	BFE0022	1353	-1.27	-8.39E-02	6.60%	2645	-97	-3.69%
	BFE0023	1353	-1.26	-7.03E-02	5.58%	2660	-82	-3.08%
	BFE0024	1353	-1.27	-7.00E-02	5.53%	2660	-81	-3.05%
	BFE0025	1353	-1.28	-7.90E-02	6.17%	2650	-91	-3.42%
	BFE022	1432	-1.37	-1.42E-01	10.43%	2606	-154	-5.91%
	BFE023	1432	-1.28	-4.65E-02	3.64%	2705	-53	-1.95%

TABLE A2
(continued)

System	Exp	T (°C)	$\partial V/\partial P$ (cc/Gpa)	Residual (cc/Gpa)	% Residual	c (m/sec)	Residual (m/sec)	% Residual
	BFE031	1433	-1.23	-4.07E-02	3.30%	2720	-48	-1.78%
	BFE032	1433	-1.27	-7.58E-02	5.95%	2680	-88	-3.27%
	BFE033	1434	-1.29	-8.46E-02	6.55%	2670	-96	-3.61%
	BFE034	1434	-1.28	-5.65E-02	4.43%	2700	-65	-2.39%
	BFE041	1530	-1.22	-5.84E-03	0.48%	2780	-7	-0.25%
Na_2O-FeO-Fe_2O_3-SiO_2 (+/-Al_2O_3)	BFE081	1432	-1.88	2.57E-01	-13.67%	2495	161	6.43%
	BFE082	1432	-1.94	1.85E-01	-9.53%	2460	113	4.61%
	BFE083	1432	-1.9	2.07E-01	-10.92%	2490	130	5.23%
	BFE091	1004	-1.67	4.07E-02	-2.43%	2620	34	1.29%
	BFE094	1005	-1.72	-2.47E-02	1.43%	2580	-20	-0.79%
	BFE096	1005	-1.67	2.19E-02	-1.32%	2630	19	0.71%
	BFE097	1005	-1.66	2.81E-02	-1.70%	2640	24	0.91%
	BFE098	1005	-1.67	9.71E-03	-0.58%	2630	8	0.31%
	BFE099	1005	-1.66	9.02E-03	-0.54%	2635	8	0.29%
	BFE0910	1005	-1.67	-7.47E-03	0.45%	2630	-6	-0.24%
	BFE101	1336	-1.97	6.18E-02	-3.14%	2500	42	1.69%
	BFE102	1336	-1.94	5.16E-02	-2.66%	2520	36	1.43%
	BFE103	1336	-1.96	-3.13E-03	0.16%	2510	-2	-0.09%
	BFE104	1336	-1.89	1.64E-02	-0.87%	2555	12	0.47%
	BFE111	943	-1.66	1.50E-02	-0.90%	2605	13	0.48%
	BFE112	944	-1.66	1.97E-03	-0.12%	2605	2	0.06%
	BFE113	943	-1.7	-5.16E-02	3.03%	2575	-43	-1.67%
	BFE114	942	-1.67	-3.66E-02	2.19%	2600	-31	-1.20%
	BFE115	941	-1.66	-4.51E-02	2.72%	2610	-39	-1.50%
	BFE117	940	-1.66	-7.12E-02	4.30%	2620	-63	-2.41%
	BFE122	1224	-1.84	3.51E-02	-1.91%	2570	26	1.03%

TABLE A2
(continued)

System	Exp	T (°C)	$\partial V / \partial P$ (cc/Gpa)	Residual (cc/Gpa)	% Residual	c (m/sec)	Residual (m/sec)	% Residual
	BFE123	1224	-1.88	-1.30E-02	0.69%	2540	-10	-0.38%
	BFE124	1224	-1.83	2.01E-02	-1.10%	2575	15	0.59%
	BFE125	1224	-1.84	-1.65E-02	0.89%	2565	-13	-0.49%
	BFE131	945	-1.62	5.00E-02	-3.09%	2670	43	1.60%
	BFE132	945	-1.62	4.38E-02	-2.71%	2670	38	1.41%
	BFE133	945	-1.61	3.96E-02	-2.45%	2675	34	1.28%
	BFE141	1230	-1.79	1.04E-01	-5.79%	2620	78	2.99%
	BFE142	1230	-1.87	2.18E-02	-1.16%	2560	16	0.62%
	BFE143	1230	-1.87	1.93E-02	-1.03%	2560	14	0.55%
	BFE144	1230	-1.87	1.63E-02	-0.87%	2560	12	0.46%
	BFE145	1230	-1.8	8.59E-02	-4.77%	2615	65	2.48%
	BFE146	1230	-1.82	6.43E-02	-3.53%	2600	48	1.85%
	BFE147	1230	-1.85	3.58E-02	-1.94%	2580	27	1.03%
	BFE151	1035	-1.83	-7.41E-02	4.05%	2530	-56	-2.22%
	BFE152	1034	-1.75	-2.25E-03	0.13%	2590	-2	-0.07%
	BFE153	1034	-1.71	2.87E-02	-1.68%	2620	23	0.88%
	BFE154	1034	-1.7	3.34E-02	-1.96%	2630	27	1.03%
	BFE155	1034	-1.71	2.05E-02	-1.20%	2625	17	0.63%
	BFE156	1032	-1.75	-3.18E-02	1.81%	2590	-25	-0.98%
	BFE162	1320	-1.91	7.27E-02	-3.81%	2555	51	2.00%
	BFE164	1321	-1.84	1.22E-01	-6.61%	2605	88	3.39%
	BFE165	1321	-1.89	6.40E-02	-3.39%	2570	46	1.78%
	BFE166	1320	-1.87	6.66E-02	-3.56%	2580	48	1.86%
Na_2O-CaO-MgO-FeO-TiO_2-Al_2O_3-SiO_2	BFE171	1432	-1.43	1.78E-02	-1.24%	2600	17	0.65%
	BFE172	1432	-1.46	-1.01E-02	0.69%	2580	-9	-0.36%

TABLE A2
(continued)

System	Exp	T (°C)	$\partial V/\partial P$ (cc/Gpa)	Residual (cc/Gpa)	% Residual	c (m/sec)	Residual (m/sec)	% Residual
	BFE173	1432	-1.48	-3.22E-02	2.17%	2565	-30	-1.15%
	BFE174	1432	-1.53	-7.92E-02	5.17%	2530	-71	-2.80%
	BFE181	1529	-1.44	-1.28E-02	0.89%	2615	-12	-0.47%
	BFE182	1529	-1.4	1.96E-02	-1.40%	2660	19	0.72%
	BFE191	1284	-1.41	8.35E-02	-5.93%	2620	78	2.97%
	BFE193	1285	-1.42	5.44E-02	-3.83%	2630	51	1.93%
	BFE194	1285	-1.41	5.95E-02	-4.21%	2650	56	2.12%
	BFE201	1334	-1.55	7.01E-03	-0.45%	2540	6	0.23%
	BFE202	1334	-1.55	-4.89E-03	0.31%	2540	-4	-0.16%
	BFE203	1334	-1.56	-1.43E-02	0.92%	2540	-12	-0.48%
	BFE204	1334	-1.56	-2.44E-02	1.57%	2540	-21	-0.82%
	BFE205	1334	-1.56	-3.31E-02	2.12%	2540	-28	-1.11%
	BFE206	1334	-1.57	-4.19E-02	2.68%	2540	-36	-1.41%
	BFE211	1432	-1.57	-3.51E-02	2.24%	2535	-30	-1.19%
	BFE213	1432	-1.59	-5.14E-02	3.24%	2540	-44	-1.73%
Kress and others (1988)								
Na_2O-SiO_2	NAS A-1	1411	-1.88	-1.90E-02	1.01%	2653	-14	-0.54%
	NAS A-2	1411	-1.88	-1.77E-02	0.94%	2654	-13	-0.50%
	NAS A-3	1411	-1.91	-5.29E-02	2.76%	2628	-39	-1.50%
	NAS A-4	1411	-1.88	-2.30E-02	1.22%	2650	-17	-0.65%
	NAS A-5	1326	-1.79	-4.30E-03	0.24%	2695	-3	-0.13%
	NAS A-6	1327	-1.81	-2.28E-02	1.26%	2680	-18	-0.67%
	NAS A-7	1323	-1.66	2.18E-02	-1.31%	2786	19	0.68%
	NAS A-8	1322	-1.65	3.28E-02	-1.99%	2796	29	1.02%
	NAS A-9	1321	-1.66	2.69E-02	-1.62%	2791	23	0.84%
	NAS A-10	1422	-1.74	3.32E-03	-0.19%	2747	3	0.10%

TABLE A2
(continued)

System	Exp	T (°C)	$\partial V/\partial P$ (cc/Gpa)	Residual (cc/Gpa)	% Residual	c (m/sec)	Residual (m/sec)	% Residual
	NAS A-11	1421	-1.69	4.92E-02	-2.91%	2786	42	1.49%
	NAS A-12	1420	-1.71	3.38E-02	-1.98%	2773	28	1.02%
	NAS A-13	1420	-1.69	5.24E-02	-3.11%	2789	44	1.59%
	NAS A-14	1619	-1.67	1.17E-01	-7.04%	2830	98	3.47%
	NAS A-15	1618	-1.63	1.51E-01	-9.22%	2860	128	4.48%
	NAS A-16	1618	-1.64	1.40E-01	-8.49%	2850	118	4.14%
	NAS A-17	1618	-1.63	1.51E-01	-9.22%	2860	128	4.48%
	NAS A-18	1617	-1.63	1.50E-01	-9.21%	2860	128	4.47%
Na_2O-Al_2O_3-SiO_2	NAS 8-1	1417	-1.64	6.31E-03	-0.38%	2835	6	0.20%
	NAS 8-2	1418	-1.63	1.76E-02	-1.08%	2845	16	0.56%
	NAS 8-3	1410	-2.1	-6.12E-02	2.91%	2520	-40	-1.60%
	NAS 8-4	1410	-2.08	-3.81E-02	1.83%	2535	-25	-1.00%
	NAS 8-5	1407	-2.12	-7.89E-02	3.73%	2510	-52	-2.07%
	NAS 8-6	1310	-1.94	-2.17E-02	1.12%	2594	-16	-0.61%
	NAS 9-1	1310	-1.92	3.70E-04	-0.02%	2610	0	0.01%
	NAS 9-2	1310	-1.93	-6.49E-03	0.34%	2605	-5	-0.18%
	NAS 9-3	1310	-1.93	-6.49E-03	0.34%	2605	-5	-0.18%
	NAS 9-4	1215	-1.86	-4.10E-02	2.21%	2625	-32	-1.21%
	NAS 9-5	1215	-1.82	-7.19E-03	0.39%	2651	-6	-0.21%
	NAS 9-6	1215	-1.82	-2.08E-03	0.11%	2655	-2	-0.06%
	NAS 9-7	1214	-1.8	1.88E-02	-1.04%	2672	15	0.56%
	NAS 10-1	1420	-2.08	-2.81E-02	1.35%	2525	-18	-0.73%
	NAS 10-2	1420	-2.08	-2.81E-02	1.35%	2525	-18	-0.73%
	NAS 10-3	1420	-2.08	-2.81E-02	1.35%	2525	-18	-0.73%
	NAS 10-4	1420	-2.1	-4.36E-02	2.08%	2515	-28	-1.13%
	NAS 10-5	1283	-1.91	-4.62E-03	0.24%	2600	-3	-0.13%
	NAS 15-1	1283	-1.93	-2.54E-02	1.32%	2585	-18	-0.71%

TABLE A2
(continued)

System	Exp	T (°C)	$\partial V/\partial P$ (cc/Gpa)	Residual (cc/Gpa)	% Residual	c (m/sec)	Residual (m/sec)	% Residual
	NAS 15-2	1283	-1.91	-4.62E-03	0.24%	2600	-3	-0.13%
Na_2O-Al_2O_3-SiO_2	NAS B-1	1619	-1.82	1.77E-01	-9.71%	2660	124	4.65%
	NAS B-2	1618	-1.82	1.77E-01	-9.72%	2660	124	4.66%
	NAS B-3	1617	-1.84	1.57E-01	-8.52%	2645	109	4.12%
	NAS B-4	1617	-1.85	1.50E-01	-8.12%	2640	104	3.93%
	NAS B-5	1617	-1.82	1.77E-01	-9.72%	2660	124	4.66%
	NAS K-1	1621	-1.93	-7.40E-02	3.83%	2690	-57	-2.11%
	NAS K-2	1620	-1.96	-1.02E-01	5.20%	2670	-77	-2.89%
	NAS K-3	1619	-1.9	-4.19E-02	2.21%	2715	-33	-1.20%
	NAS K-4	1619	-1.94	-8.86E-02	4.56%	2680	-68	-2.52%
	NAS K-5	1619	-1.9	-4.84E-02	2.54%	2710	-38	-1.39%
	NAS K-6	1619	-1.96	-1.04E-01	5.29%	2669	-79	-2.94%
	NAS K-7	1619	-1.96	-1.02E-01	5.22%	2670	-78	-2.91%
	NAS K-8	1618	-1.97	-1.17E-01	5.92%	2660	-88	-3.31%
	NAS K-9	1518	-1.83	-6.06E-02	3.32%	2740	-50	-1.81%
	NAS K-10	1518	-1.85	-8.72E-02	4.70%	2719	-71	-2.60%
	NAS K-11	1416	-1.78	-9.82E-02	5.52%	2748	-84	-3.07%
	NAS K-12	1416	-1.74	-5.99E-02	3.44%	2780	-52	-1.88%
	NAS K-13	1416	-1.75	-7.17E-02	4.09%	2770	-62	-2.25%
Rivers (ms, 1986)								
Rivers and Carmichael (1987)								
Na_2O-FeO-SiO_2	RIV-3-1	1420	-2.09	-5.45E-02	2.61%	2525	-36	-1.43%
	RIV-3-2	1420	-2.09	-5.45E-02	2.61%	2525	-36	-1.43%
	RIV-3-3	1420	-2.09	-5.45E-02	2.61%	2525	-36	-1.43%
	RIV-3-4	1420	-2.1	-7.01E-02	3.33%	2515	-46	-1.83%
	RIV-3-1	1283	-1.92	-2.91E-02	1.52%	2600	-21	-0.82%
	RIV-3-2	1283	-1.94	-5.00E-02	2.58%	2585	-36	-1.41%

TABLE A2
(continued)

System	Exp	T (°C)	$\partial V/\partial P$ (cc/Gpa)	Residual (cc/Gpa)	% Residual	c (m/sec)	Residual (m/sec)	% Residual
	RIV-3-3	1283	-1.92	-2.91E-02	1.52%	2600	-21	-0.82%
	RIV-5-1	1420	-3.28	1.03E-01	-3.14%	2190	36	1.65%
	RIV-5-1	1280	-2.81	3.30E-01	-11.74%	2335	135	5.80%
Na_2O-MgO-Al_2O_3-SiO_2	RIV-9-1	1640	-1.13	6.24E-03	-0.55%	2860	9	0.30%
	RIV-9-2	1640	-1.13	2.63E-03	-0.23%	2855	4	0.13%
	RIV-9-3	1640	-1.13	6.24E-03	-0.55%	2860	9	0.30%
	RIV-9-4	1640	-1.13	6.24E-03	-0.55%	2860	9	0.30%
CaO-SiO_2	RIV-10-1	1563	-0.95	-2.75E-02	2.90%	3120	-52	-1.65%
	RIV-10-2	1563	-0.93	-6.05E-03	0.65%	3160	-12	-0.37%
	RIV-10-3	1563	-0.91	1.45E-02	-1.61%	3200	28	0.89%
	RIV-10-4	1563	-0.91	1.45E-02	-1.61%	3200	28	0.89%
CaO-MgO-SiO_2	RIV-13-1	1425	-0.94	1.81E-02	-1.92%	3020	31	1.03%
	RIV-13-2	1425	-0.93	2.95E-02	-3.16%	3040	51	1.68%
	RIV-13-3	1425	-0.93	3.51E-02	-3.78%	3050	61	2.00%
	RIV-13-4	1425	-0.94	2.38E-02	-2.54%	3030	41	1.36%
	RIV-13-1	1485	-0.95	2.21E-02	-2.34%	3040	38	1.26%
	RIV-13-3	1485	-0.94	3.34E-02	-3.57%	3060	58	1.90%
CaO-Al_2O_3-SiO_2	RIV-14-1	1560	-1.32	-3.19E-02	2.41%	2850	-36	-1.25%
	RIV-14-2	1560	-1.33	-4.56E-02	3.42%	2835	-51	-1.79%
	RIV-14-3	1560	-1.35	-5.96E-02	4.42%	2820	-66	-2.33%
	RIV-14-4	1560	-1.33	-4.56E-02	3.42%	2835	-51	-1.79%
CaO-MgO-Al_2O_3-SiO_2	RIV-15-1	1400	-1.14	-2.19E-02	1.92%	2885	-29	-1.01%
	RIV-15-2	1400	-1.14	-2.57E-02	2.25%	2880	-34	-1.19%
	RIV-15-3	1400	-1.13	-1.43E-02	1.26%	2895	-19	-0.66%
	RIV-15-4	1400	-1.14	-2.57E-02	2.25%	2880	-34	-1.19%
	RIV-15-1	1300	-1.1	1.47E-02	-1.34%	2910	20	0.69%

TABLE A2
(continued)

System	Exp	T (°C)	$\partial V/\partial P$ (cc/Gpa)	Residual (cc/Gpa)	% Residual	c (m/sec)	Residual (m/sec)	% Residual
	RIV-15-2	1300	-1.1	1.47E-02	-1.34%	2910	20	0.69%
	RIV-15-3	1300	-1.09	2.92E-02	-2.68%	2930	40	1.36%
	RIV-15-4	1300	-1.11	7.40E-03	-0.67%	2900	10	0.34%
Na_2O-CaO-MgO-Al_2O_3-SiO_2	RIV-17-1	1425	-1.39	-1.81E-02	1.30%	2735	-19	-0.68%
	RIV-17-2	1425	-1.38	-3.56E-03	0.26%	2750	-4	-0.13%
	RIV-17-3	1425	-1.38	1.24E-03	-0.09%	2755	1	0.05%
	RIV-17-4	1425	-1.43	-5.31E-02	3.71%	2700	-54	-1.99%
	RIV-17-1	1325	-1.29	8.46E-02	-6.58%	2830	92	3.26%
	RIV-17-2	1325	-1.29	7.58E-02	-5.86%	2820	82	2.92%
	RIV-19-1	1425	-1.33	4.54E-03	-0.34%	2805	5	0.18%
	RIV-19-2	1425	-1.32	1.37E-02	-1.04%	2815	15	0.53%
	RIV-19-3	1425	-1.33	9.13E-03	-0.69%	2810	10	0.35%
FeO-Al_2O_3-SiO_2	RIV-22-1	1420	-1.04	-2.21E-02	2.12%	2345	-26	-1.12%
	RIV-22-2	1420	-1.03	-9.37E-03	0.91%	2360	-11	-0.47%
	RIV-22-3	1420	-1.03	-9.37E-03	0.91%	2360	-11	-0.47%
	RIV-22-4	1420	-1.03	-9.37E-03	0.91%	2360	-11	-0.47%
	RIV-22-1	1325	-0.94	6.97E-02	-7.38%	2450	89	3.62%
	RIV-22-2	1325	-0.98	3.13E-02	-3.19%	2400	39	1.61%
	RIV-22-3	1325	-0.98	3.13E-02	-3.19%	2400	39	1.61%
	RIV-23-3	1380	-0.91	2.02E-02	-2.22%	2400	27	1.13%
	RIV-23-3	1230	-0.85	6.24E-02	-7.32%	2450	88	3.60%
CaO-FeO-Al_2O_3-SiO_2	RIV-24-3	1430	-1.08	-9.25E-03	0.85%	2480	-11	-0.44%
Na_2O-CaO-MgO-SiO_2	RIV-25-3	1450	-1.54	6.48E-02	-4.20%	2735	60	2.20%
	RIV-25-3	1390	-1.51	5.71E-02	-3.77%	2740	54	1.98%
CaO-TiO_2-SiO_2	RIV-26-1	1480	-1.42	-4.33E-02	3.04%	2590	-50	-1.93%
	RIV-26-2	1480	-1.42	-4.33E-02	3.04%	2590	-50	-1.93%
	RIV-26-3	1480	-1.42	-4.33E-02	3.04%	2590	-50	-1.93%

TABLE A2
(continued)

System	Exp	T (°C)	$\partial V/\partial P$ (cc/Gpa)	Residual (cc/Gpa)	% Residual	c (m/sec)	Residual (m/sec)	% Residual
	RIV-26-4	1480	-1.41	-3.44E-02	2.43%	2600	-40	-1.53%
	RIV-26-1	1380	-1.37	-2.10E-02	1.53%	2580	-24	-0.94%
	RIV-26-2	1380	-1.37	-2.54E-02	1.84%	2575	-29	-1.14%
	RIV-26-3	1380	-1.37	-2.10E-02	1.53%	2580	-24	-0.94%
	RIV-26-4	1380	-1.36	-1.23E-02	0.90%	2590	-14	-0.55%
K_2O-Na_2O-CaO-MgO-FeO-TiO_2-Al_2O_3-SiO_2	RIV-27-1	1425	-1.39	-5.36E-02	3.85%	2695	-58	-2.15%
	RIV-27-2	1425	-1.39	-5.07E-02	3.65%	2698	-55	-2.04%
	RIV-27-3	1425	-1.39	-5.07E-02	3.65%	2698	-55	-2.04%
	RIV-27-1	1335	-1.35	-3.01E-02	2.24%	2712	-33	-1.23%
	RIV-27-2	1335	-1.34	-2.28E-02	1.70%	2720	-25	-0.93%
	RIV-27-3	1335	-1.34	-2.74E-02	2.04%	2715	-30	-1.12%
	RIV-27-1	1230	-1.3	-1.01E-02	0.78%	2725	-11	-0.42%
	RIV-27-2	1230	-1.3	-5.65E-03	0.44%	2730	-6	-0.24%
	RIV-27-3	1230	-1.3	-5.65E-03	0.44%	2730	-6	-0.24%
	RIV-28-1	1435	-1.39	-7.78E-02	5.60%	2600	-79	-3.05%
	RIV-28-2	1435	-1.38	-7.27E-02	5.25%	2605	-74	-2.85%
	RIV-28-3	1435	-1.38	-7.27E-02	5.25%	2605	-74	-2.85%
	RIV-28-1	1335	-1.36	-4.98E-02	3.66%	2608	-51	-1.96%
	RIV-28-2	1335	-1.35	-4.28E-02	3.16%	2615	-44	-1.68%
	RIV-28-3	1335	-1.36	-4.58E-02	3.38%	2612	-47	-1.80%
	RIV-28-4	1335	-1.36	-4.58E-02	3.38%	2612	-47	-1.80%
Na_2O-CaO-MgO-FeO-Al_2O_3-SiO_2	RIV-29-1	1530	-1.37	-4.62E-02	3.38%	2700	-49	-1.81%
	RIV-29-2	1530	-1.36	-4.43E-02	3.25%	2702	-47	-1.73%
	RIV-29-3	1530	-1.36	-4.43E-02	3.25%	2702	-47	-1.73%

TABLE A2
(continued)

System	Exp	T (°C)	$\partial V / \partial P$ (cc/Gpa)	Residual (cc/Gpa)	% Residual	c (m/sec)	Residual (m/sec)	% Residual
	RIV-29-1	1430	-1.34	-2.70E-02	2.01%	2700	-29	-1.06%
	RIV-29-2	1430	-1.34	-2.70E-02	2.01%	2700	-29	-1.06%
	RIV-29-3	1430	-1.34	-2.70E-02	2.01%	2700	-29	-1.06%
Sokolov and others (1971)								
CaO-Al_2O_3-SiO_2	Sea71-1	1727	-1.45	-8.84E-02	6.10%	2840	-91	-3.21%
	Sea71-5	1727	-1.22	-4.85E-02	3.98%	2960	-62	-2.09%
Webb and Courtial (1996)								
CaO-Al_2O_3-SiO_2	WC96-1	1350	-1.1	2.37E-02	-2.17%	2977	33	1.11%
	WC96-2	1350	-1.1	2.16E-02	-1.97%	2974	30	1.01%
	WC96-3	1350	-1.09	2.80E-02	-2.56%	2983	39	1.31%
	WC96-4	1375	-1.1	1.95E-02	-1.77%	2976	27	0.91%
	WC96-5	1375	-1.1	1.66E-02	-1.51%	2972	23	0.77%
	WC96-6	1375	-1.12	-7.21E-04	0.06%	2948	-1	-0.03%
	WC96-7	1375	-1.1	1.59E-02	-1.44%	2971	22	0.74%
	WC96-8	1375	-1.09	2.73E-02	-2.50%	2987	38	1.27%
	WC96-9	1375	-1.11	6.56E-03	-0.59%	2958	9	0.30%
	WC96-10	1400	-1.12	2.23E-03	-0.20%	2957	3	0.10%
	WC96-11	1400	-1.12	3.68E-03	-0.33%	2959	5	0.17%
	WC96-12	1400	-1.12	2.95E-03	-0.26%	2958	4	0.14%
	WC96-13	1400	-1.12	4.13E-05	0.00%	2954	0	0.00%
	WC96-14	1400	-1.13	-7.29E-03	0.65%	2944	-10	-0.34%
	WC96-15	1400	-1.11	6.58E-03	-0.59%	2963	9	0.31%
	WC96-16	1425	-1.12	-1.39E-03	0.12%	2957	-2	-0.06%
	WC96-17	1425	-1.11	7.32E-03	-0.66%	2969	10	0.34%
	WC96-18	1425	-1.12	2.98E-03	-0.27%	2963	4	0.14%
	WC96-19	1450	-1.13	-5.73E-03	0.51%	2956	-8	-0.27%

TABLE A2
(continued)

System	Exp	T (°C)	$\partial V/\partial P$ (cc/Gpa)	Residual (cc/Gpa)	% Residual	c (m/sec)	Residual (m/sec)	% Residual
	WC96-20	1450	-1.12	3.01E-03	-0.27%	2968	4	0.14%
	WC96-21	1450	-1.12	3.01E-03	-0.27%	2968	4	0.14%
	WC96-22	1450	-1.14	-1.90E-02	1.67%	2938	-26	-0.88%
	WC96-23	1450	-1.13	-9.41E-03	0.83%	2951	-13	-0.44%
	WC96-24	1450	-1.13	-7.94E-03	0.70%	2953	-11	-0.37%
	WC96-25	1450	-1.13	-1.24E-02	1.09%	2947	-17	-0.57%
	WC96-26	1475	-1.13	-3.50E-03	0.31%	2964	-5	-0.16%
	WC96-27	1475	-1.14	-1.38E-02	1.21%	2950	-19	-0.64%
	WC96-28	1475	-1.13	-8.62E-03	0.76%	2957	-12	-0.40%
	WC96-29	1500	-1.14	-1.97E-02	1.72%	2947	-27	-0.91%
	WC96-30	1500	-1.14	-1.30E-02	1.14%	2956	-18	-0.60%
	WC96-31	1500	-1.16	-3.55E-02	3.06%	2926	-48	-1.63%
	WC96-32	1500	-1.14	-1.45E-02	1.27%	2954	-20	-0.67%
	WC96-33	1500	-1.13	-4.19E-03	0.37%	2968	-6	-0.19%
	WC96-34	1500	-1.13	-7.84E-03	0.69%	2963	-11	-0.36%
	WC96-35	1525	-1.14	-1.59E-02	1.39%	2957	-22	-0.73%
	WC96-36	1550	-1.15	-2.92E-02	2.53%	2944	-40	-1.35%
	WC96-37	1475	-0.87	3.52E-02	-4.03%	3257	68	2.09%
	WC96-38	1475	-0.86	5.40E-02	-6.31%	3295	106	3.21%
	WC96-39	1475	-0.86	4.62E-02	-5.35%	3279	90	2.74%
	WC96-40	1525	-0.88	3.52E-02	-4.00%	3263	68	2.08%
	WC96-41	1525	-0.88	3.92E-02	-4.48%	3271	76	2.32%
	WC96-42	1525	-0.86	5.35E-02	-6.21%	3300	105	3.17%
	WC96-43	1550	-0.89	3.16E-02	-3.57%	3259	61	1.86%
	WC96-44	1550	-0.88	3.92E-02	-4.46%	3274	76	2.31%
	WC96-45	1550	-0.87	4.42E-02	-5.06%	3284	86	2.61%

TABLE A2
(continued)

System	Exp	T (°C)	$\partial V / \partial P$ (cc/Gpa)	Residual (cc/Gpa)	% Residual	c (m/sec)	Residual (m/sec)	% Residual
	WC96-46	1575	-0.89	2.75E-02	-3.09%	3254	53	1.61%
	WC96-47	1575	-0.89	3.11E-02	-3.50%	3261	60	1.83%
	WC96-48	1575	-0.88	3.82E-02	-4.33%	3275	74	2.25%
	WC96-49	1600	-0.9	2.60E-02	-2.90%	3254	49	1.52%
	WC96-50	1600	-0.9	2.65E-02	-2.96%	3255	50	1.55%
	WC96-51	1600	-0.89	3.26E-02	-3.66%	3267	62	1.91%
	WC96-52	1450	-0.64	2.79E-03	-0.44%	3599	9	0.25%
	WC96-53	1450	-0.63	7.71E-03	-1.22%	3615	25	0.69%
	WC96-54	1450	-0.63	1.35E-02	-2.14%	3634	44	1.21%
	WC96-55	1475	-0.64	3.87E-03	-0.60%	3602	12	0.34%
	WC96-56	1475	-0.64	1.06E-03	-0.16%	3593	3	0.09%
	WC96-57	1475	-0.63	1.34E-02	-2.11%	3633	43	1.19%
	WC96-58	1500	-0.65	-5.92E-05	0.01%	3589	0	-0.01%
	WC96-59	1500	-0.65	-6.90E-04	0.11%	3587	-2	-0.06%
	WC96-60	1500	-0.65	3.39E-03	-0.52%	3600	11	0.30%
	WC96-61	1500	-0.65	4.95E-03	-0.77%	3605	16	0.44%
	WC96-62	1500	-0.64	7.74E-03	-1.20%	3614	25	0.69%
	WC96-63	1525	-0.66	-4.39E-03	0.67%	3575	-14	-0.39%
	WC96-64	1525	-0.66	-5.63E-04	0.09%	3587	-2	-0.05%
	WC96-65	1525	-0.66	-5.63E-04	0.09%	3587	-2	-0.05%
	WC96-66	1525	-0.66	-2.15E-03	0.33%	3582	-7	-0.19%
	WC96-67	1550	-0.67	-1.08E-02	1.61%	3555	-33	-0.94%
	WC96-68	1550	-0.67	-5.25E-03	0.79%	3572	-16	-0.46%
	WC96-69	1550	-0.66	-7.54E-04	0.11%	3586	-2	-0.07%
	WC96-70	1550	-0.66	-7.54E-04	0.11%	3586	-2	-0.07%
	WC96-71	1550	-0.67	-5.90E-03	0.89%	3570	-18	-0.51%

TABLE A2
(continued)

System	Exp	T (°C)	$\partial V/\partial P$ (cc/Gpa)	Residual (cc/Gpa)	% Residual	c (m/sec)	Residual (m/sec)	% Residual
	WC96-72	1550	-0.66	-3.64E-03	0.55%	3577	-11	-0.32%
	WC96-73	1525	-0.83	1.84E-02	-2.23%	3375	39	1.14%
	WC96-74	1525	-0.84	1.13E-02	-1.36%	3360	24	0.70%
	WC96-75	1525	-0.84	1.04E-02	-1.24%	3358	22	0.64%
	WC96-76	1525	-0.83	1.42E-02	-1.71%	3366	30	0.88%
	WC96-77	1550	-0.83	1.36E-02	-1.63%	3368	28	0.84%
	WC96-78	1550	-0.84	7.42E-03	-0.88%	3355	15	0.46%
	WC96-79	1550	-0.84	7.90E-03	-0.94%	3356	16	0.49%
	WC96-80	1550	-0.84	1.22E-02	-1.46%	3365	25	0.75%
	WC96-81	1575	-0.85	1.52E-03	-0.18%	3346	3	0.09%
	WC96-82	1575	-0.85	2.49E-03	-0.29%	3348	5	0.15%
	WC96-83	1575	-0.85	-1.89E-03	0.22%	3339	-4	-0.12%
	WC96-84	1575	-0.86	-8.28E-03	0.97%	3326	-17	-0.51%
	WC96-85	1575	-0.86	-9.76E-03	1.14%	3323	-20	-0.60%
	WC96-86	1400	-1.08	1.17E-02	-1.08%	3037	17	0.55%
	WC96-87	1400	-1.08	1.58E-02	-1.47%	3043	23	0.75%
	WC96-88	1400	-1.08	8.23E-03	-0.76%	3032	12	0.39%
	WC96-89	1425	-1.09	1.03E-03	-0.09%	3027	1	0.05%
	WC96-90	1425	-1.09	1.03E-03	-0.09%	3027	1	0.05%
	WC96-91	1425	-1.09	1.73E-03	-0.16%	3028	2	0.08%
	WC96-92	1425	-1.09	-3.89E-03	0.36%	3020	-6	-0.18%
	WC96-93	1425	-1.09	3.83E-03	-0.35%	3031	5	0.18%
	WC96-94	1450	-1.09	1.54E-03	-0.14%	3033	2	0.07%
	WC96-95	1450	-1.09	-2.67E-03	0.24%	3027	-4	-0.13%
	WC96-96	1450	-1.09	2.93E-03	-0.27%	3035	4	0.14%
	WC96-97	1475	-1.09	-4.26E-03	0.39%	3030	-6	-0.20%

TABLE A2
(continued)

System	Exp	T (°C)	$\partial V / \partial P$ (cc/Gpa)	Residual (cc/Gpa)	% Residual	c (m/sec)	Residual (m/sec)	% Residual
	WC96-98	1475	-1.09	-2.86E-03	0.26%	3032	-4	-0.13%
	WC96-99	1475	-1.09	-5.67E-05	0.01%	3036	0	0.00%
	WC96-100	1500	-1.1	-7.25E-03	0.66%	3031	-10	-0.34%
	WC96-101	1500	-1.1	-1.29E-02	1.17%	3023	-18	-0.61%
	WC96-102	1500	-1.09	1.14E-03	-0.11%	3043	2	0.05%
	WC96-103	1500	-1.1	-1.58E-02	1.43%	3019	-22	-0.74%
	WC96-104	1500	-1.1	-1.08E-02	0.98%	3026	-15	-0.51%
	WC96-105	1525	-1.09	-6.03E-03	0.55%	3038	-9	-0.28%
	WC96-106	1525	-1.11	-2.23E-02	2.01%	3015	-32	-1.05%
	WC96-107	1525	-1.1	-1.52E-02	1.38%	3025	-22	-0.72%
	WC96-108	1525	-1.09	-1.14E-03	0.10%	3045	-2	-0.05%
	WC96-109	1525	-1.1	-1.24E-02	1.12%	3029	-18	-0.58%
	WC96-110	1550	-1.1	-1.39E-02	1.26%	3032	-20	-0.66%
	WC96-111	1550	-1.11	-2.68E-02	2.40%	3014	-38	-1.26%
	WC96-112	1550	-1.1	-1.54E-02	1.39%	3030	-22	-0.72%
Webb and Dingwell (1994)								
Na_2O-TiO_2-SiO_2	WD94-14	1025	-3.88	-3.62E-02	1.53%	2273	-21	-0.91%
	WD94-15	1025	-3.93	-1.18E-02	0.50%	2287	-7	-0.30%
	WD94-16	1025	-4.2	-4.20E-02	1.78%	2269	-24	-1.06%
	WD94-17	1025	-4.2	-3.75E-05	0.00%	2293	0	0.00%
	WD94-18	1025	-4.04	-7.73E-02	3.22%	2250	-44	-1.94%
	WD94-19	1075	-4.06	-1.43E-02	0.59%	2274	-8	-0.35%
	WD94-20	1075	-4.41	1.44E-02	-0.60%	2290	8	0.35%
	WD94-21	1075	-4.37	8.17E-02	-3.52%	2329	47	2.03%
	WD94-22	1150	-4.45	2.18E-02	-0.87%	2276	12	0.52%
	WD94-23	1150	-1.76	3.73E-02	-1.50%	2284	20	0.88%

TABLE A2
(continued)

System	Exp	T (°C)	$\partial V/\partial P$ (cc/Gpa)	Residual (cc/Gpa)	% Residual	c (m/sec)	Residual (m/sec)	% Residual
	WD94-24	1150	-1.78	7.89E-02	-3.22%	2307	43	1.87%
K_2O-TiO_2-SiO_2	WD94-25	950	-1.76	-8.06E-02	2.06%	2123	-26	-1.22%
	WD94-26	950	-1.74	-1.43E-01	3.60%	2103	-45	-2.14%
	WD94-27	950	-1.74	-5.53E-02	1.43%	2131	-18	-0.83%
	WD94-28	950	-1.88	-1.05E-01	2.67%	2115	-33	-1.58%
	WD94-29	1050	-1.86	-4.23E-02	1.01%	2093	-12	-0.59%
	WD94-30	1050	-1.92	-3.88E-02	0.93%	2094	-11	-0.54%
	WD94-31	1050	-1.91	1.15E-01	-2.84%	2140	35	1.62%
	WD94-32	1050	-2.02	9.30E-02	-2.29%	2134	28	1.31%
	WD94-33	1150	-2	1.07E-01	-2.43%	2092	29	1.40%
	WD94-34	1150	-2.03	1.48E-01	-3.38%	2103	41	1.93%
	WD94-35	1150	-2.03	6.80E-02	-1.53%	2081	18	0.89%
Na_2O-TiO_2-SiO_2	WD94-36	1100	-1.28	-2.29E-02	1.30%	2745	-20	-0.74%
	WD94-37	1100	-1.28	-4.42E-02	2.48%	2726	-39	-1.44%
	WD94-38	1100	-1.27	-2.20E-02	1.25%	2745	-20	-0.71%
	WD94-39	1100	-1.27	-1.69E-03	0.10%	2763	-2	-0.06%
	WD94-40	1100	-1.33	-6.13E-03	0.35%	2759	-6	-0.20%
	WD94-41	1200	-1.29	3.91E-03	-0.21%	2701	3	0.12%
	WD94-42	1200	-1.34	2.49E-02	-1.34%	2719	21	0.76%
	WD94-43	1200	-1.36	-3.73E-02	1.95%	2668	-30	-1.12%
	WD94-44	1200	-1.28	-3.39E-02	1.77%	2671	-27	-1.02%
	WD94-45	1300	-1.32	1.61E-02	-0.80%	2643	12	0.45%
	WD94-46	1300	-1.24	4.01E-02	-2.01%	2661	30	1.13%
	WD94-47	1300	-1.35	1.04E-02	-0.52%	2639	8	0.29%
	WD94-48	1300	-1.34	6.40E-03	-0.32%	2636	5	0.18%
CaO-TiO_2-SiO_2	WD94-49	1400	-1.33	4.59E-02	-3.60%	2709	58	2.13%

TABLE A2
(continued)

System	Exp	T (°C)	$\partial V / \partial P$ (cc/Gpa)	Residual (cc/Gpa)	% Residual	c (m/sec)	Residual (m/sec)	% Residual
	WD94-50	1400	-1.35	3.95E-02	-3.08%	2700	49	1.83%
	WD94-51	1400	-1.39	5.22E-02	-4.11%	2717	66	2.43%
	WD94-52	1400	-1.37	5.27E-02	-4.15%	2718	67	2.45%
	WD94-53	1450	-1.37	5.83E-03	-0.44%	2675	7	0.27%
	WD94-54	1450	-1.38	4.71E-02	-3.65%	2727	59	2.18%
	WD94-55	1450	-1.4	-4.88E-03	0.36%	2662	-6	-0.22%
	WD94-56	1450	-1.45	-1.94E-02	1.43%	2644	-23	-0.89%
	WD94-57	1450	-1.37	5.32E-02	-4.14%	2735	67	2.47%
	WD94-58	1450	-1.42	2.12E-02	-1.61%	2694	26	0.97%
	WD94-59	1450	-5.18	9.90E-02	-7.99%	2798	130	4.64%
	WD94-60	1500	-5.12	-2.11E-03	0.16%	2682	-3	-0.10%
	WD94-61	1500	-4.48	1.26E-02	-0.94%	2700	16	0.57%
	WD94-62	1500	-4.43	1.79E-02	-1.34%	2707	22	0.82%
	WD94-63	1500	-1.75	-1.46E-03	0.11%	2683	-2	-0.07%
	WD94-64	1550	-1.97	-2.21E-02	1.59%	2675	-27	-1.00%
	WD94-65	1550	-1.79	-3.61E-03	0.26%	2697	-4	-0.16%
	WD94-66	1550	-3.24	2.50E-03	-0.18%	2705	3	0.11%
	WD94-67	1550	-1.36	-9.11E-03	0.66%	2691	-11	-0.41%
	WD94-68	1600	-1.33	-2.04E-02	1.45%	2694	-25	-0.92%
	WD94-69	1600	-1.3	-6.95E-02	4.78%	2637	-82	-3.10%
	WD94-70	1600	-1.94	1.77E-02	-1.29%	2741	22	0.80%
	WD94-71	1600	-1.87	-3.11E-02	2.19%	2681	-37	-1.40%

References

Baidov, V. V., and Kunin, L. L., 1968, Speed of ultrasound and compressibility of molten silica: Soviet Physics Doklady, v. 1, p. 64–65.

Bevington, P. R., 1969, Data reduction and error analysis for the physical sciences: New York, McGraw-Hill Book Company, 336 p.

Bockris, J. O., and Kojonen, E., 1960, The compressibilities of certain molten silicates and borates: Journal of the American Chemical Society, v. 82, p. 4493–4497.

Bockris, J. O'M., Tomlinson, J. W., and White, J. L., 1955, The structure of the liquid silicates: Partial molar volumes and expansivities: Faraday Society Transactions, v. 52, p. 299–310.

Bottinga, Y., and Weill, D., 1970, Densities of liquid silicate systems calculated from partial molar volumes of oxide components: American Journal of Science, v. 269, p. 169–182.

Bottinga, Y., Weill, D., and Richet, P., 1982, Density calculations for silicate liquids. I. Revised method for aluminosilicate compositions: Geochimica et Cosmochimica Acta, v. 46, p. 909–919.

——— 1984, Density calculations for silicate liquids. I. Reply to a critical comment by Ghiorso and Carmichael: Geochimica et Cosmochimica Acta, v. 48, p. 409–414.

Courtial, P., and Dingwell, D. B., 1995, Nonlinear composition dependence of molar volume of melts in the CaO-Al_2O_3-SiO_2 system: Geochimica et Cosmochimica Acta, v. 59, p. 3685–3695.

——— 1999, Densities of melts in the CaO-MgO-Al_2O_3-SiO_2 system: American Mineralogist, v. 84, p. 465–476.

Courtial, P., Ohtani, E., and Dingwell, D. B., 1997, High-temperature densities of some mantle melts: Geochimica et Cosmochimica Acta, v. 61, p. 3111–3119.

Courtial, P., Gottsmann, J., Holzheid, A., and Dingwell, D. B., 1999, Partial molar volumes of NiO and CoO liquids: implications for the pressure dependence of metal-silicate partitioning: Earth and Planetary Science Letters, v. 171, p. 171–183.

Dingwell, D. B., 1992, Density of some titanium-bearing silicate liquids and the compositional dependence of the partial molar volume of TiO_2: Geochimica et Cosmochimica Acta, v. 56, p. 3403–3407.

Dingwell, D. B., and Brearley, M., 1988, Melt densities in the CaO-FeO-Fe_2O_3-SiO_2 system and the compositional dependence of the partial molar volume of ferric iron in silicate melts: Geochimica et Cosmochimica Acta, v. 52, p. 2815–2825.

Dingwell, D. B., and Gottsmann, J., 2002, Reply to: Comment on: Supercooled diopside melt: confirmation of temperature-dependent expansivity using container-based dilatometry by J. Gottsmann and D. B. Dingwell: Contributions to Mineralogy and Petrology, v. 142, p. 759–762.

Dingwell, D. B., Brearley, M., and Dickinson, J. E., Jr., 1988, Melt densities in the Na_2O-FeO-Fe_2O_3-SiO_2 system and the partial molar volume of tetrahedrally-coordinated ferric iron in silicate melts: Geochimica et Cosmochimica Acta, v. 52, p. 2467–2475.

Ghiorso, M. S., 2004a, An Equation of State for Silicate Melts. I. Formulation of a General Model: American Journal of Science, v. 304, p. 637–678.

——— 2004b, An Equation of State for Silicate Melts. III. Analysis of stoichiometric liquids at elevated pressure: shock compression data, molecular dynamics simulations and mineral fusion curves: American Journal of Science, v. 304, p. 752–810.

——— 2004c, An Equation of State for Silicate Melts. IV. Calibration of a multicomponent mixing model to 40 GPa: American Journal of Science, v. 304, p. 811–838.

Ghiorso, M. S., and Carmichael, I. S. E., 1984, Comment on "Density calculations for silicate liquids. I. Revised method for aluminosilicate compositions" by Bottinga, Weill and Richet: Geochimica et Cosmochimica Acta, v. 48, p. 401–408.

Gottsmann, J., and Dingwell, D. B., 2000, Supercooled diopside melt: confirmation of temperature-dependent expansivity using container-based dilatometry: Contributions to Mineralogy and Petrology, v. 139, p. 127–135.

——— 2002, Thermal expansivities of supercooled haplobasaltic liquids: Geochimica et Coscomchimica Acta, v. 66, p. 2231–2238.

Hara, S., Irie, K., Gaskell, D. R., and Ogino, K., 1988, Densities of melts in the FeO-Fe_2O_3-CaO and FeO-Fe_2O_3-$2CaO{\cdot}SiO_2$ systems: Transactions of the Japan Institute of Metals, v. 29, p. 977–989.

Johnson, T. M., ms, 1989, The densities of titanium-rich silicate liquids: Non-ideal mixing and structural implications: M. S. Thesis in Geology, University of California Berkeley, 18 p.

Knoche, R., Dingwell, D. B., and Webb, S. L., 1992a, Temperature-dependent thermal expansivities of silicate melts: The system anorthite-diopside: Geochimica et Cosmochimica Acta, v. 56, p. 689–699.

——— 1992b, Non-linear temperature dependence of liquid volumes in the system albite-anorthite-diopside: Contributions to Mineralogy and Petrology, v. 111, p. 61–73.

Knoche, R., Dingwell, D. B., Seifert, F. A., and Webb, S. L., 1994, Non-linear properties of supercooled liquids in the system Na_2O-SiO_2: Chemical Geology, v. 116, p. 1–16.

Knoche, R., Dingwell, D. B., and Webb, S. L., 1995, Melt densities for leucogranites and granitic pegmatites: Partial molar volumes for SiO_2, Al_2O_3, Na_2O, Li_2O, Rb_2O, Cs_2O, MgO, CaO, SrO, BaO, B_2O_3, P_2O_5, F_2O_{-1}, TiO_2, Nb_2O_5, Ta_2O_5 and WO_3: Geochimica et Cosmochimica Acta, v. 59, p. 4445–4452.

Kress, V. C., and Carmichael, I. S. E., 1989, The lime-iron-silicate melt system: Redox and volume systematics: Geochimica et Cosmochimica Acta, v. 53, p. 2883–2892.

——— 1991, The compressibility of silicate liquids containing Fe_2O_3 and the effect of composition, temperature, oxygen fugacity and pressure on their redox states: Contributions to Mineralogy and Petrology, v. 108, p. 82–92.

Kress, V. C., Williams, Q., and Carmichael, I. S. E., 1988, Ultrasonic investigation of melts in the system Na_2O-Al_2O_3-SiO_2: Geochimica et Cosmochimica Acta, v. 52, p. 283–293.

Lange, R. A., 1996, Temperature independent thermal expansivities of sodium aluminosilicate melts between 713 and 1835 K: Geochimica et Cosmochimica Acta, v. 60, p. 4989–4996, Correction: v. 61, p. 3275–3276.

——— 1997, A revised model for the density and thermal expansivity of K_2O-Na_2O-CaO-MgO-Al_2O_3-SiO_2 liquids from 700 to 1900 K: extension to crustal magmatic temperatures: Contributions to Mineralogy and Petrology, v. 130, p. 1–11.

——— 2002, Comment on: Supercooled diopside melt: confirmation of temperature-dependent expansivity using container-based dilatometry by J. Gottsmann and D. B. Dingwell: Contributions to Mineralogy and Petrology, v. 142, p. 753–758.

Lange, R. A., and Carmichael, I. S. E., 1987, Densities of Na_2O-K_2O-CaO-MgO-FeO-Fe_2O_3-Al_2O_3-TiO_2-SiO_2 liquids: New measurements and derived partial molar properties: Geochimica et Cosmochimica Acta, v. 51, p. 2931–2946.

——— 1989, Ferric-ferrous equilibria in Na_2O-FeO-Fe_2O_3-SiO_2 melts: effects of analytical techniques on derived partial molar properties: Geochimica et Cosmochimica Acta, v. 53, p. 2195–2204.

——— 1990, Thermodynamic properties of silicate liquids with emphasis on density, thermal expansion and compressibility *in* Modern Methods of Igneous Petrology: Understanding Magmatic Processes: Reviews in Mineralogy, v. 24, p. 25–64.

Lange, R. A., and Navrotsky A., 1992, Heat capacities of Fe_2O_3-bearing silicate liquids: Contributions to Mineralogy and Petrology, v. 110, p. 311–320.

Liu, Q., and Lange, R. A., 2001, The partial molar volume and thermal expansivity of TiO_2 in alkali silicate melts: Systematic variation with Ti coordination: Geochimica et Cosmochimica Acta, v. 65, p. 2379–2393

Mo, X., Carmichael, I. S. E., Rivers M., and Stebbins J., 1982, The partial molar volume of Fe_2O_3 in multicomponent silicate liquids and the pressure dependence of oxygen fugacity in magmas: Mineralogical Magazine, v. 45, p. 237–245.

Press, W. H., Teukolsky, S. A., Vetterling, W. T., and Flannery, B. P., 1992, Numerical Recipes in C: New York, Cambridge University Press, 994 p.

Rivers, M. L., ms, 1986, Ultrasonic Studies of Silicate Melts: Ph. D. Thesis, University of California Berkeley, 215 p.

Rivers, M. L., and Carmichael, I. S. E., 1987, Ultrasonic studies of silicate melts: Journal of Geophysical Research, v. 92, p. 9247–9270.

Shiraishi, Y., Ikeda, K., Tamura, A., and Saitô, T., 1978, On the viscosity and density of the molten FeO-SiO_2 system: Transactions of the Japanese Institute of Metallurgy, v. 19, p. 264–274.

Sokolov, L. N., Baidov, V. V., Kunin, L.L., and Dymov, V. V., 1971, Surface and volume characteristics of the calcium oxide-alumina-silica system: Sbornik trudov Tsentralno Nauchno-issledovatel'skii institut chernoi metallurgii, v. 74, p. 53–61.

Stein, D. J., Stebbins, J. F., Carmichael, I. S. E., 1986, Density of molten sodium aluminosilicates: Journal of the American Ceramics Society, v. 69, p. 396–399.

Toplis, M. J., and Richet, P., 2000, Equilibrium density and expansivity of silicate melts in the glass transition range: Contributions to Mineralogy and Petrology, v. 139, p. 672–683.

Webb, S., and Courtial, P., 1996, Compressibility of melts in the CaO-Al_2O_3-SiO_2 system: Geochimica et Cosmochimica Acta, v. 60, p. 75–86.

Webb, S. L., and Dingwell, D. B., 1994, Compressibility of titanosilicate melts: Contributions to Mineralogy and Petrology, v. 118, p. 157–168.

Webb, S. L., Knoche, R., and Dingwell, D. B., 1992, Determination of silicate liquid thermal expansivity using dilatometry and calorimetry: European Journal of Mineralogy, v. 4, p. 95–104.